Synthesis and characterizations of high permittivity ultraviolet cured soft elastomeric networks and composites applicable as dielectric electroactive polymer

Goswami, Kaustav

Publication date:
2014

Document Version
Publisher's PDF, also known as Version of record

Synthesis and characterizations of high permittivity ultraviolet cured soft elastomeric networks and composites applicable as dielectric electroactive polymer

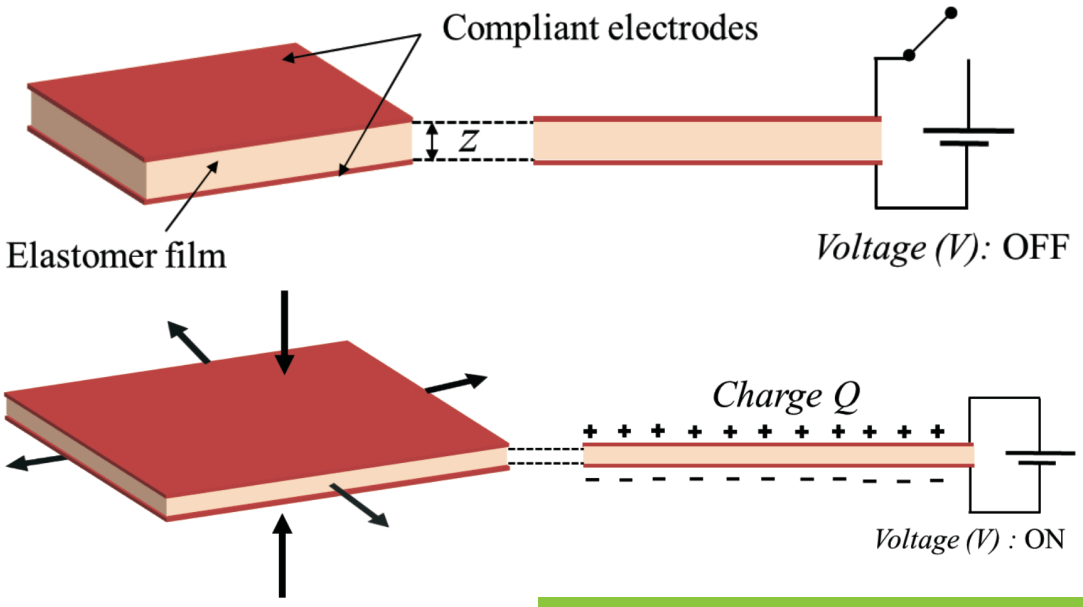

Kaustav Goswami
Ph.D. Thesis
July 2014

DTU Chemical Engineering
Department of Chemical and Biochemical Engineering

Synthesis and characterizations of high permittivity ultraviolet cured soft elastomeric networks and composites applicable as dielectric electroactive polymer

PhD Thesis

Kaustav Goswami

Department of Chemical and Biochemical Engineering

Technical University of Denmark DTU

July 2014

Address: The Danish Polymer Centre
Department of Chemical and Biochemical Engineering
Technical University of Denmark
Building 227
DK-2800 Kgs. Lyngby
Denmark
Phone: +45 4525 6801
Web: www.dpc.kt.dtu.dk

Print: J&R Frydenberg A/S
København
November 2014

ISBN: 978-87-93054-47-9

Preface

This Ph.D. thesis was written as a partial fulfillment of the requirements for obtaining the Ph.D. degree at the Technical University of Denmark (DTU). The Ph.D. project was carried out at the Danish Polymer Center (DPC), Department of Chemical and Biochemical Engineering, Technical University of Denmark during the period from the 1st of August 2011 to the 31st of July 2014. The project was partly financed by InnovationsFonden.

I want to acknowledge the persons that made possible the accomplishment of the work presented in this thesis. First of all I would like to thank Anne Ladegaard Skov for giving me the opportunity to do a PhD project in her group. She has been a great supervisor offering endless support, patience and guidance throughout the past three years. I am thankful to Anders Egede Daugaard for his valuable ideas and support all throughout the project. Thanks to Giuseppe Gallone for allowing me to conduct some part of the research in his group. A special thanks to Fabia Galantini for her enduring efforts and scientific discussions during my stay in Pisa. I would like to thank all the members of the Danish Polymer Centre for a lot of assistance and helpful discussions. Thanks to Ole Hassager, Søren Hvilsted, Peter Szabo and Katja Jankova for their help whenever needed. I am very thankful to Kim Chi Szabo for helping with the lab stuffs, to Irakli Javakhishvili for good time spent over various discussions ranging from scientific to philosophical and to Piotr Stanislaw Mazurek for being a great companion during our experiments together. Special thanks go to Anca Gabriela Bejenariu for her invaluable support during my initial days in the department. I am really thankful to my great colleagues Sindhu Vudayagiri, Frederikke Bahrt Madsen, Liyun Yu, Qian Huang, Suzan Sager Hassouneh, Shamsul Bin Zakaria, Baoguang Ma, Jon Trifol Guzman, Ludovica Hengeller, Nicolas Javier Alvarez, Malgorzata Kostrzewska, Hiep Dinh Nguyen, Aliff Hisyam A Razak and Aamir Shabbir for providing a friendly atmosphere at work.

Thanks to my parents Gautam Goswami and Bharati Goswami for their endless support and encouragement. A special thank goes to my wife Sanjukta Bose for being with me for the past 10 years in every joys and woes that life has offered. Thanks to all my friends in Denmark outside DTU specially Saswati Chakladar and Krishnendu Mukherjee for giving a feeling of home away from home.

Finally a note of thanks to InnovationsFonden for partly funding the project, European Scientific Network for Artificial Muscles (ESNAM) and our collaborators in Danfoss Polypower A/S.

Kaustav Goswami

July 31, 2014

DPC, Department of Chemical and Biochemical Engineering

Technical University of Denmark

Abstract

The objective of this thesis was preparation and characterizations of high permittivity ultraviolet (UV) cured elastomeric networks and composites applicable as dielectric electroactive polymers (DEAPs). At present, none of the commercially available elastomers such as acrylics, poly (dimethyl siloxane) (PDMS) and polyurethanes are designed with the requirements specific for DEAPs. Thus there is a need to develop elastomers with low elastic modulus, low viscous and dielectric losses and high relative permittivity.

Interpenetrating networks and fumed silica reinforced composites of poly (propylene oxide) (PPO) were prepared which showed marked improvements in properties compared to the acrylic elastomers. But difficulties in curing by industrial processes and handling of these elastomers posed as limitations. So the focus was on optimizing UV induced thiol-ene reactions for curing commercially available PDMS.

UV curing of PDMS was successfully established which eliminated the major drawbacks of widely used platinum catalyzed addition curing of PDMS. An advanced sequential curing used to form the PDMS networks showed low elastic modulus and low viscous losses than the former-developed processes due to better control over the heterogeneity of the networks.

The sequential curing approach was successfully used to incorporate conductive multiwalled carbon nanotubes (MWCNTs) in higher concentrations than usual without making the elastomers conductive. The PDMS-MWCNT composites also showed high relative permittivity, low elastic modulus and low viscous and dielectric losses.

Thus the elastomers developed in this project show promising properties to be considered as potential DEAPs.

Dansk Résumé

Formålet med denne afhandling er at fremstille og karakterisere høj-permittivitets, ultra-violet hærdede elastomerer og kompositter til brug i dielektrisk elektroaktive polymerer (DEAP). På nuværende tidspunkt er der ingen af de kommercielt tilgængelige elastomerer, såsom akryl, polydimethylsiloxan (PDMS) og polyuretan, der er designede med henblik på at opfylde de specifikke krav for DEAP materialer. Derfor er der et behov for at udvikle elastomerer med eksempelvist lavt elastisk modul, lave viskøse og dielektriske tab og høj dielektrisk permittivitet.

Interpenetrerende netværk og silica-forstærkede kompositter af polypropyleneoxid (PPO) blev fremstillet, og de fremviste væsentlige forbedringer i egenskaber i forhold til akrylat elastomererne. Dog vurderedes den meget langsomme hærdetid at være et problem for kommerciel produktion af disse elastomerer. Derfor blev fokus flyttet mod optimeringen af UV-inducerede thiolene reaktioner for hærdning af kommerciel PDMS.

UV-hærdning af PDMS blev etableret med godt resultat, og det blev vist, at metoden var et godt alternativ til den traditionelle platinum katalyserede additionshærdning af PDMS. En avanceret sekventiel hærdning forårsagede PDMS elastomerer med lavt elastisk modul og lave viskøse tab i forhold til systemet baseret på PPO på grund af den øgede kontrol over heterogeniteten.

Den sekventielle hærdeteknik viste sig succesfuld i introduktion af ledende multiwalled carbon nanotubes (MWCNT) i højere koncentrationer end den traditionelle perkolerings-grænse uden at gøre elastomeren leddende. PDMS-MWCNT kompositterne havde højere permittivitet, lave viskøse og dielektriske tab samt et lavt elastisk modul.

Dermed er forskellige typer af elastomerer udviklet, som alle kan være mulige kandidater for fremtidens DEAP elastomer.

Contents

List of Figures

List of Tables

List of Abbreviations

AC	Alternating current
ATR-FTIR	Attenuated total reflectance- Fourier Transform Infrared Spectroscopy
BET	Brunauer, Emmett and Teller
$CDCl_3$	Deuterated chloroform
CPO	Copper-phthalocyanine oligomer
DBS	Dielectric breakdown strength
DEAP	Dielectric electroactive polymer
DMPA	2, 2-dimethyl-2- phenylacetophenone
DRS	Dielectric relaxation spectroscopy
DSC	Differential scanning calorimetry
EAP	Electroactive polymer
HDDA	1,6-hexandiol diacrylate
HMDS	Hexamethyldisilazane
IPN	Interpenetrating network
LCR	Inductance-Capacitance-Resistance
LVE	Linear viscoelastic
MWCNT	Multiwalled carbon nanotube
NMP	N-methyl pyrrolidone
NMR	Nuclear magnetic resonance

PANI	Polyaniline
PDI	Polydispersity index
PDMS	Poly (dimethyl siloxane)
PEDOT	Poly (3,4-ethylenedioxythiophene)
phr	Parts per hundred rubber
PPG/PPO	Poly (propylene glycol)/Poly (propylene oxide)
PS	Polystyrene
PTFE	Poly (tetrafluoro ethylene)
PU	Polyurethane
SEC	Size exclusion chromatography
SPE	Solid polymer electrolyte
TGA	Thermogravimetric analysis
THF	Tetrahydrofuran
TiO_2	Titanium dioxide
TMPTMA	Trimethylolpropane trimethacrylate
UV	Ultraviolet
wt%	Weight percent

List of symbols

$\bar{M}_n$	Number average molecular weight
f	Frequency
F_{om}	Figure of merit
G	Elastic modulus
G'	Storage modulus
G''	Loss modulus
M_e	Entanglement molecular weight
r	Stoichiometric imbalance
r_c	Critical stoichiometric imbalance
s	Actuation strain
T_g	Glass transition temperature
Y	Young's modulus
z	Thickness
ε'	Storage permittivity
ε''	Loss permittivity
ε_r	Relative permittivity
λ	Wavelength
σ'	Real part of AC conductivity

Chapter 1

Introduction

In early 1990s, electro active polymers (EAPs) emerged as a class of "smart materials" that exhibit change in shape or size in response to electrical stimulation. Within the EAPs, Dielectric Electro Active Polymers (DEAPs) gained special interest in the field of electro-mechanical transduction technology due to their ability to show large strains, frequency responses of the order of milliseconds and work densities higher than human muscles[1,2]. DEAPs show flexibilities, reversible contraction and expansion in area similar to human muscles and thus termed as functional surrogates to natural muscles or "artificial muscles"[3]. DEAP transducers that convert electrical energy to mechanical energy are called actuators. In addition to actuator mode, DEAPs can also be used as generators[4,5] and sensors[6,7] where mechanical energy is converted into electrical energy. For commercial applications, a single DEAP film is usually never used. DEAP actuators require multilayer stacked configuration of DEAP films such as those used in tensile force transmission devices [8–10] and tactile displays with high structural compliance[11,12]. The stacked actuator configuration has been further developed and commercialized by Bayer Materials Science in high definition haptic feedback devices in 2011[13]. Performances of DEAP actuators are governed by low elastic modulus, high relative permittivity and high dielectric breakdown strength (DBS) of the elastomers used. Whereas, low viscous losses, high tear strength, high maximum elongation, low stress softening, low hysteresis, insignificant specific conductivity and low dielectric losses of the elastomers increase actuation and influence lifetime of DEAP actuators[14]. At present, among commercially available elastomers, poly (dimethyl siloxane) (PDMS), acrylics in the form of VHB tapes and polyurethane (PU) show the best actuation performances. However, these materials are not tailored with the requirements specific for

DEAP actuators and they suffer from one or more drawbacks like low relative permittivity, long response times, high dielectric losses or high elastic modulus.

Therefore, it is crucial and interesting to engineer new materials with properties specific for application as DEAP actuators. The existing need for novel engineered materials applicable as DEAP actuators thus forms the basis of the work conducted in this thesis. Since it is difficult to optimize all the material requirements for DEAP actuators simultaneously, this thesis mainly focuses on developing elastomeric materials possessing low elastic modulus, low viscous and dielectric losses and high relative permittivity.

1.1 Objective

The overall objective of this project was preparation and characterizations of high permittivity ultra violet (UV) cured soft elastomeric networks and composites applicable as DEAP actuators. The materials should combine the advantages such as low elastic modulus, low viscous and dielectric losses like PDMS with enhanced relative permittivity like acrylics and PU elastomers. As will be motivated in section 1.4, UV induced thiol-ene crosslinking was chosen in this project as a method of obtaining soft elastomeric materials applicable as DEAP actuators.

This chapter aims at providing the background and motivations for the work presented in this thesis. Section 1.2 introduces the working principle of DEAP actuation, while section 1.3 provides a thorough study on the property requirements of elastomers suitable for DEAP actuators. Section 1.4 focuses on the advantages and the disadvantages of currently used materials as actuators along with the preparation of elastomeric networks. Different techniques followed towards engineering new materials with properties specific for application as DEAP actuators are presented in section 1.5. Section1.6 holds a discussion on the motivations that drove the different approaches undertaken in this project and finally based on the motivations, section 1.7 presents the overall thesis outline.

1.2 Working principle of DEAP actuators

The basic structure of a DEAP actuator shown in Figure 1.1 is equivalent to a parallel plate capacitor[15].

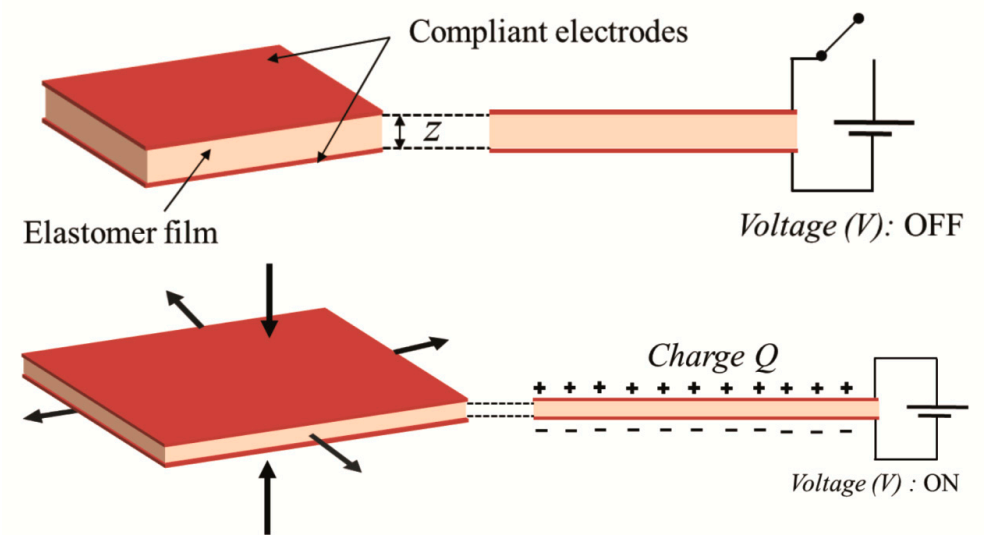

Figure 1.1: Basic structure of a DE actuator

The dielectric medium consists of incompressible, yet highly deformable thin elastomeric material, sandwiched between two compliant electrodes. As for any capacitor, when an electric field is applied to the electrodes, positive charges appear on one electrode, and negative charges on the other. This gives rise to Coulomb forces between opposite charges, generating a stress, known as the Maxwell stress. The Maxwell stress forces the opposite electrodes to move closer, thereby squeezing the elastomer in between. As the elastomer is squeezed, it elongates in planar directions and consequently the area of the electrodes is increased. The increase in electrode area causes a decrease in charge density on the electrodes and this decrease in charge density is the driving force for actuation[3].

The equation governing the actuation of DEAPs is given as [15],

$$p = \varepsilon_0 \varepsilon_r E^2 = \varepsilon_0 \varepsilon_r \left(\frac{V}{z} \right)^2 \tag{1.1}$$

Where p is the Maxwell stress acting on the elastomer due to applied electric field E, ε_0 and ε_r are the permittivities of the free space and the elastomer, respectively. V is the voltage applied across the elastomer of thickness z. At equilibrium, the Maxwell stress equals the internal stress in the material so that the strain (s) i.e. actuation strain is produced on the elastomer which can be written as,

$$s = \frac{\varepsilon_0 \varepsilon_r}{Y} \left(\frac{V}{z} \right)^2 \tag{1.2}$$

Where Y is the Young's modulus of the elastomer. The strain produced by the elastomer at a voltage V can be experimentally determined by knowing ε_r, Y and z of the elastomer.

One downside of the currently used DEAP actuator materials is the high voltage required for actuation, which adds cost to the transducer devices due to expensive electronic components. Thus to lower the required voltage for a given strain of DEAP, it can be seen from equation(1.2), that either the relative permittivity of the elastomer (ε_r) can be increased, the film thickness (z) can be decreased or the Young's modulus (Y) can be reduced. The equation however does not account for the effects of viscous losses, tear strength, maximum elongation, plastic deformation, low hysteresis, specific conductivity, dielectric losses and dielectric breakdown strength of the elastomer on the performances of DEAP actuators.

1.3 Material requirements

Elastomers are crosslinked networks of polymer chains above the glass transition temperature (T_g), which show large deformations when subjected to mechanical load and recover the original shape when the load is removed. The property requirements of elastomeric materials for best actuation performances has been discussed in section 1.1. It can be seen from equation(1.2), that low elastic modulus, high relative permittivity and low thickness of elastomer films reduce the operating voltage

of DEAP actuators for a given strain. In this section, effects of other material properties such as viscous losses, tear strength, maximum elongation, hysteresis, stress softening (also known as plastic deformation or Mullins effect) [16,17], specific conductivity (which governs amount of leakage current flowing through the elastomer), dielectric losses and dielectric breakdown strength of elastomers are discussed. Viscoelastic properties in the small strain region of elastomers as a function of time are usually determined in terms of the storage modulus $G'(f)$ and the loss modulus $G''(f)$, where f is the frequency of the applied stress in oscillatory shear experiments. Young's modulus of elastomers can be directly determined from the shear modulus by the following relation, $Y=3G'(f\rightarrow 0) = 3G$ where G is the elastic modulus of the elastomer. The viscous losses of elastomers are defined by the loss function (Tan delta) which is a ratio of the loss modulus and the storage modulus i.e., Tan delta $(f) = G''(f)/G'(f)$. When Tan delta <1, the elastic part of the material predominates while the viscous part predominates when Tan delta >1 at a given frequency. Thus, to have higher elastic properties for better actuation performances, lower viscous losses of elastomers are desirable. Tear strength of elastomers used as DEAP actuators should be preferably high for easy handling of thin films. Stress softening is characterized by a decrease in elastic modulus with strain. Hence, it is preferable that elastomers as DEAPs do not show any strain softening effect. Hysteresis is characterized by the difference in the loading and unloading paths and it is related to the viscous losses of the material. Consequently, to lower the hysteresis effects, low viscous losses of elastomers are desired. Dielectric losses of materials are determined by Tan delta $(f) = \varepsilon''(f)/\varepsilon'(f)$ where $\varepsilon'(f)$ and $\varepsilon''(f)$ are the storage and loss permittivities of materials, respectively as function of applied frequencies f. In general, increase in the concentrations of polarizable groups in the elastomer raises the dielectric permittivity at a cost of increased dielectric loss and leakage current flowing across the material. Thus, dielectric losses and leakage current should be low in order to maintain non-conductivity of elastomers, which is a pre-requisite for DEAP actuators. The upper limit of voltage

that can be used safely for actuation is governed by the dielectric breakdown strength of materials. Therefore, it is necessary to have high breakdown strength of elastomers in order to prevent electrical breakdown, which leads to failure of DEAP actuators. Sommer-Larsen and Larsen[18] showed that it is possible to combine dielectric permittivity, breakdown strength and Young's modulus of elastomers into a single parameter F_{OM} to measure static performances of elastomers as DEAP actuators. F_{OM} of DEAP actuator is expressed as,

$$F_{OM} = \frac{3\varepsilon_r \varepsilon_0 E_{BD}^{\ 2}}{Y} \tag{1.3}$$

where E_{BD} is the electrical field at which electrical breakdown of the DEAP occurs. Though F_{OM} is widely regarded as an optimizing parameter to evaluate performances of DEAP materials, it does not account for other optimizing parameters mentioned earlier in this section.

However, no such elastomeric material exists so far which holds all the positive attributes of DEAP actuator material since optimization of one property most of the time affect another in a negative way. For example, addition of reinforcing fillers to improve mechanical properties of elastomers such as tear strength and maximum elongation also increases the elastic modulus, thereby reducing the strain produced at an applied voltage. Therefore, the challenge for development of novel DEAP material will require careful balance between increasing relative permittivity and decreasing elastic modulus, viscous and dielectric losses of elastomeric materials for better actuation performances. It can be seen from equation(1.2) that the operating voltage of DEAP actuators can be reduced by decreasing the elastomer film thickness. For large scale processing, an elastomer film thickness of 40 μm is currently the threshold value [19] so thickness of elastomer film is not considered as a possible optimization parameter in this study.

1.4 Choice of materials applied as DEAP actuators

For developing DEAP actuators, it is essential to know the advantages, disadvantages and preparation procedures of the applied elastomeric materials. Commercially available elastomers that show best actuation performances include acrylics[20–24], silicone elastomers[7,14,25–29] and PU elastomers[30,31] among several other elastomeric materials such as acrylonitrile butadiene rubber[32], fluorinated[33] and styrenic copolymers[34,35].

One of the first materials used as DEAP transducers include acrylics in the form of VHB tapes from 3M due to their exhibited high strains, high relative permittivity and high Maxwell stresses. However, VHB tapes are only available in fixed thicknesses thus pre-straining is mandatory to achieve the desired thickness[7]. Breakdown strength[20,23,36–38] and frequency responses[39] of VHB could be increased manifold by applying pre-strain in planar direction along with a reduction in applied voltage due to the reduced thickness of the pre-strained film. However, pre-straining of VHB not only requires firm structures for maintaining the strained state of the film, which add cost and weight to the DEAP actuator but also reduces its lifetime due to stress concentration at the interface between the film and the support structure[2,40]. However, formation of interpenetrating networks (IPNs) were reported to maintain the performance benefits of VHB without the requirement of mechanical pre-straining due to the stabilized morphology of the formed networks[36,40–42]. The need for pre-strain, long response times and sensitivity to humidity limit the applications of acrylics as DEAP actuators[43].

PU elastomers exhibit high relative permittivity like the acrylics due to the presence of polarizable groups on the polymer backbone. However, PU elastomers also possess high elastic modulus which in turn increases the operating voltage to achieve a particular strain as seen from equation(1.2).

Additionally, due to their sensitivity towards humidity, PU elastomers suffer from high dielectric losses and low breakdown strength than silicone elastomers[30,31].

Silicone elastomers on the other hand neither require pre-strain like VHB nor suffer from high dielectric losses like PU elastomers, which make them excellent DEAP materials. Pre-straining in silicone elastomers is not mandatory as in VHB but still favorable, since the films reduce in thickness and elastic modulus decreases after applying pre-strain[7]. Additionally, silicone elastomers based DEAP transducers show very fast response times due to low viscous losses and exhibit higher lifetime than acrylics and PUs[43]. In spite of the mentioned advantages, silicone elastomers exhibit low relative permittivity which in turn reduces the performances of silicone based DEAP actuators when compared to commonly used acrylics and PU elastomers. Consequently, there is scope for developing new elastomeric materials for DEAPs, which combine the advantages such as low elastic modulus, low viscous and dielectric losses like silicones with enhanced relative permittivity like acrylics and PU elastomers.

Linear PDMS chains having vinyl end groups are crosslinked by addition curing reactions involving a hydride crosslinker containing three or more reactive groups per chain in presence of platinum catalyst to form the networks. Stoichiometric imbalance (r) of the network is defined as the ratio of the molar concentrations of functional groups present in the crosslinker and the vinyl groups in PDMS i.e. $r = [\text{hydride}]/[\text{vinyl}] = f[\text{crosslinker}]/2[\text{PDMS}]$ where f is the average functionality of the crosslinker used and [crosslinker] and [PDMS] are the molar concentrations of the crosslinker and PDMS, respectively. Due to fast curing times, addition curing is the most common curing method to obtain PDMS networks used as DEAPs. Unlike addition curing of vinyl terminated silicones, condensation reactions used for crosslinking hydroxyl terminated silicones suffer from long reaction time, generation of by-products and possibilities of side reactions, which may affect the elastomer

properties. Therefore, majority of vinyl terminated silicones as DEAPs that are cured at low temperatures use platinum catalyzed addition reactions. Nevertheless, expensive catalyst requirement and catalyst poisoning are identified weaknesses of platinum catalyzed addition curing reactions[44]. As an alternative approach, UV induced thiol-ene reactions not only overcome the drawbacks of platinum catalyzed addition curing but also offers added advantages of executing rapid reactions at ambient temperature, insensitivity towards oxygen inhibition and being environmental friendly due to minimum solvent requirements[45,46]. UV induced thiol-ene crosslinking reactions are carried out by free radical addition reactions of polymers containing vinyl end groups in presence of a photo initiator[46,47]. Hence, in this thesis UV induced thiol-ene curing chemistry has been demonstrated as a possible curing method to obtain soft elastomer networks as applicable to DEAP actuators.

1.5 Different approaches applicable towards the development of elastomers as DEAP actuator

The purpose of the choice of material discussed in the previous section and the choice of methods presented in this section is not only to get an overview of the different approaches applicable towards the development of novel elastomeric materials applicable as DEAP actuators but also to get motivations for different techniques applied for the accomplishment of this project. Different approaches that are currently applicable for increasing the relative permittivity of elastomers are shown in Scheme 1.1.

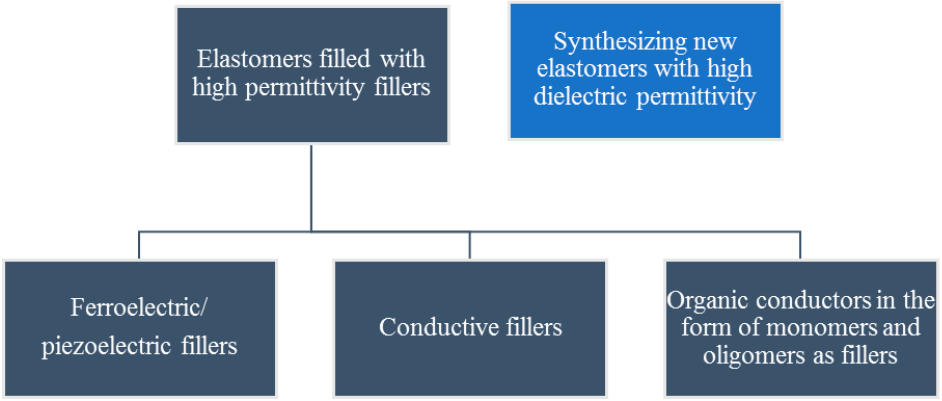

Scheme 1.1: Different approaches applicable towards increasing relative permittivity of elastomers

Ferroelectric and piezoelectric ceramic powders mixed in elastomer matrices show significant improvement in relative permittivity as predicted by mixing rules of high and low relative permittivity materials[48,49]. Gallone *et al.*[50] showed that a four-fold increase in the relative permittivity of the silicone matrix was obtained by incorporating 30% lead magnesium niobate–lead titanate filler yet retaining good stretchability of the composites. Studies reported by Carpi *et al.*[51], Szabo *et al.*[52] and Yu *et al.* [53] on titanium dioxide (TiO_2) filled silicone matrix showed improvements in relative permittivity of the matrix with increasing content of TiO_2. However, addition of ferroelectric/piezoelectric fillers increase dielectric losses of DEAPs which affect its actuation performances negatively. Some studies[54,55] revealed that silicone elastomers filled with ferroelectric fillers showed preferential alignment of intrinsic polar groups in presence of external electric field. This preferential alignment increased global polarizability of the composites that resulted in an increase in relative permittivity. However, it is worth mentioning that increased polarizability of these composites can only occur in the direction of the applied electric field thereby exhibiting a marked anisotropy in the material properties[54,55].

Incorporation of conductive or semi-conductive fillers in very low concentrations in elastomer matrices increases relative permittivity of the host matrices[56–58]. However, when the filler content exceeds a certain threshold, known as the percolation threshold, such composites exhibit conductivity, which leads to the premature failure of the composites. Percolation threshold can be visualized as the concentration of the filler when conductive paths are formed leading to electrical conduction across the volume of the sample. Among several conductive and semi-conductive fillers, carbon nanotubes due to their outstanding electrical and mechanical properties[59,60] are most commonly used. PU matrix filled with covalently modified multiwalled carbon nanotubes (MWCNTs) [61] and graphite filler[62] below the percolation threshold showed better actuation performances than pure PU at the cost of higher dielectric losses and lower breakdown strength.

On the other hand using organic conductors in the form of monomers or oligomers as high permittivity fillers have shown to increase actuation performances and mechanical stability of DEAP actuators due to enhanced compatibility between the fillers and matrices. Extensive work by Zhang *et al.*[63] on copper-phthalocyanine oligomer (CPO) filled silicone elastomers showed that on increasing the relative permittivity of the composites from 3.27 to 11.82 at 40% CPO loading, the electric field required to produce 10% strain reduced from 32 V/μm to 25 V/μm following equation(1.2). Incorporation of polyaniline (PANI) in blends with PU[64] and in encapsulated form in PDMS[65] had also shown to enhance the permittivity of the host matrices.

Alternative approaches of increasing relative permittivity of elastomers without affecting the mechanical properties can be achieved by synthetic approaches like copolymerization[66], grafting polar groups on the elastomer back bone[67,68] or using new elastomer matrices with high relative permittivity[32]. However, grafting approach involves tedious efforts for preparation of these specialty polymers.

In order to improve mechanical stabilities such as, tear strength and maximum elongations of elastomers, reinforcing fillers are mostly used which also increases the elastic modulus of elastomers. Therefore, it is difficult to reduce elastic modulus without affecting tear strength, maximum elongation and viscous losses. Attempts had been made to reduce elastic modulus of elastomers by either using high molecular weight polymers which is limited by polymer chain entanglements or changing the stoichiometry of network formations which is accompanied by increase in viscous losses[28,29,69]. On the other hand heterogeneous bimodal networks formed by advanced mixing sequence showed reduction in elastic modulus of unfilled PDMS without increasing viscous losses due to low chances of network irregularities as a result of efficient crosslinking between short and relatively long chemically identical polymer chains which form the bimodal networks[69–71].

1.6 Motivation

From the discussions about different aspects of the choice of materials in section 1.4 and different approaches applicable towards the development of elastomers as DEAP actuators in section 1.5 interesting possibilities were identified in terms of material selection, preparation of elastomeric networks and approaches towards achieving low elastic modulus, low viscous and dielectric losses and high relative permittivity of elastomeric materials as applicable to DEAP actuators. These identified possibilities served as an inspiration for the experimental works undertaken to fulfil the objectives of this project.

From section 1.4, it is now known that IPN formation can be successfully used as a promising method for DEAP optimization for better actuation performances. So far IPNs as DEAP actuators were mainly focused on VHB acrylics where, IPN formation was used as a method for pre-straining without the need for external rigid structures[36,40,41]. As mentioned in section 1.4 pre-straining reduces lifetime of DEAP actuators due to stress concentrations. So there is a need to find ways for

eliminating the requirement of pre-straining as the basis for DEAP actuation. Additionally, lack of literatures available on non-acrylic based IPNs as DEAP actuators gave encouragement to choose a novel, non-acrylic based, low elastic modulus material, poly (propylene glycol) (PPG) also known as poly (propylene oxide) (PPO), as a potential DEAP candidate. As a suitable alternative to commonly used VHB and PDMS elastomers, IPNs prepared from PPGs were expected to exhibit enhanced mechanical properties due to morphological stability offered by the interpenetrating networks thereby excluding the need for pre-straining.

While performing the previous study on IPNs, it was judged that the IPNs were difficult to cure industrially due to long curing time. On the other hand, homo networks obtained from vinyl terminated PPG (also known as PPO) exhibited rapid curing via UV induced thiol-ene reactions. Moreover, PPO homo networks exhibited high relative permittivity, low viscous and dielectric losses but were mechanically too weak for easy handling of thin films. Therefore, filler reinforcement was necessary for improving the mechanical properties of PPO homo networks in terms of elastic modulus and viscous losses. VHB acrylics being one of the first materials to be used as DEAPs, were chosen as the benchmark for comparing the elastic modulus, viscous and dielectric losses, relative permittivity and actuation properties of treated fumed silica reinforced PPO networks. Stickiness was identified as the downside of PPO composites for handling thin films. Increase in fumed silica loading showed reduction in stickiness of the PPO films, however at high filler concentrations films became stiff and showed reduced actuation strains at a particular voltage. Further optimizations on reduction of stickiness was not performed as it was beyond the scope of the study.

Hence at this point, a decision was made to shift the focus from PPO to PDMS which is a widely used elastomer for DEAP actuators due to its excellent properties namely high flexibility, high breakdown strength and fast response time. Literature studies revealed that preparation of silicone elastomers as

DEAPs by formation of heterogeneous bimodal networks was a possible approach towards achieving reduced elastic modulus without increasing viscous losses due to low chances of network irregularities[69]. Encouraged by the idea of stepwise (sequential) network formation, the same approach was employed for preparing UV curable PDMS networks in a fast and efficient way thereby overcoming the drawbacks of platinum catalyzed addition curing of vinyl terminated PDMS.

As mentioned in section 1.4 that the major drawback of PDMS as DEAPs is the low relative permittivity in comparison to acrylics and PUs. Therefore, extensive work had already been reported on increasing the relative permittivity of PDMS for reducing the operating voltage of DEAP actuators[50–53]. Incorporation of MWCNTs in PDMS matrices was found to be an attractive method for increasing relative permittivity without increasing elastic modulus of PDMS[56,57]. However, due to the low percolation threshold of PDMS-MWCNT composites, only low concentrations of MWCNTs can be used to avoid conductivity and premature failure of the composites. Among several methods that were reported to prevent undesired electrical conductivity in the elastomers, most of the works were focused on keeping the filler content below their percolation threshold in order to achieve non-conducting composites. That was the encouragement behind performing the final work in this project which focused on preparing PDMS composites with MWCNT content above the percolation threshold without exhibiting percolative behaviour.

1.7 Outline of the thesis

From the motivation of the study presented in the previous section several steps into the realization of the project objectives were taken which include,

- formation of IPNs based on two different poly(propylene glycols) (PPGs) having different molecular weights and end groups and poly(propylene oxide) (PPO) composites containing

treated fumed silica as new elastomeric materials having high relative permittivity, low elastic modulus and low viscous losses.

- preparation and characterization of platinum free UV cured PDMS soft elastomeric networks.
- incorporation of modified MWCNTs in PDMS matrix to increase overall permittivity of the composites containing percolative amount of MWCNTs.

In Chapter 2, an overview of using PPG having no pre-stretch as basis for developing new DEAP actuator material, is given. Development of new IPNs based on two different molecular weights of PPGs having different end groups has been discussed in the chapter. Mechanical characterizations are performed by shear rheology. Thermal characterizations of the IPNs are done by differential scanning calorimetry (DSC) and thermogravimetric analysis (TGA). Dielectric relaxation spectroscopy (DRS) is used to determine relative permittivity and dielectric losses of prepared IPNs.

In Chapter 3 studies on PPO-fumed silica composites as a probable candidate for DEAP actuator are shown. Mechanical, dielectric and actuation studies performed on PPO composites are presented and the results obtained are compared with acrylic VHB4910.

In Chapter 4 precious metal free UV curing method to obtain soft PDMS networks with low viscous losses from commercially available divinyl terminated PDMS is demonstrated. Discussions on sequential network formation approach and kinetics of network formation measured by rheological studies are presented.

In Chapter 5, a new method of MWCNT modification is demonstrated which is then used as fillers for the preparation of UV curable MWCNT filled PDMS composites with enhanced permittivity. In addition to rheological studies, electrical breakdown tests and dielectric spectroscopy, a thorough study on temperature dependence of AC conductivity is also performed for the composites.

Finally, in chapter 6 summary and concluding remarks are given along with future work and outlook of the work presented in this thesis.

Chapter 2

PPG IPNs based on no pre-straining as basis for DEAP actuators

Literature studies revealed that optimization of DEAPs for better actuation performances can be achieved by forming IPNs. As yet, most of the IPNs as DEAP actuators were based on highly pre-strained VHB acrylic elastomers. To overcome the drawbacks of pre-straining as the basis for DEAP actuators, IPNs based on PPGs were proposed.

In this chapter preparation of novel non-acrylic based PPG IPNs are presented followed by discussions on the results obtained from mechanical, dielectric and thermal characterizations of the prepared IPNs. The following chapter is based on the article **"Silicone resembling poly (propylene glycol) interpenetrating networks based on no pre-stretch as basis for electrical actuators"** published in the proceedings of SPIE smart structures and materials + nondestructive evaluation and health monitoring conference, *see* Appendix B1.

2.1 Introduction

An IPN is a network that consists of two or more polymers that are both crosslinked to give interlaced networks. IPNs have different and often superior properties compared to the respective homo networks of polymers, which is due to stabilized bulk and surface morphologies created by the interlaced networks. There are two main ways to prepare IPNs, either through a sequential or a simultaneous approach. In the sequential method, the IPN is formed in two consecutive steps, where initially a homo network of polymer (I) is formed through cross-linking. This network is then swollen with a monomer

(II), cross-linker and an initiator and the IPN is formed through *in-situ* polymerization. The second method consists of forming two independent networks simultaneously. This is either done by cross-linking two sets of prepolymers or through polymerization and cross-linking of two monomers by non-interfering reactions. Figure 2.1 shows these two synthesis routes.

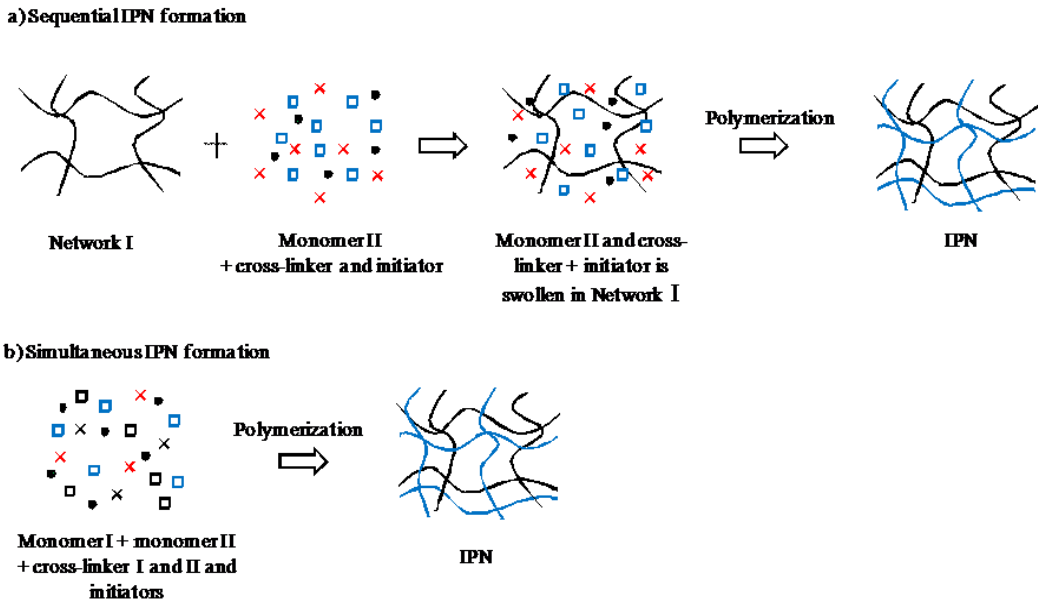

Figure 2.1: IPN synthesis routes: a) Sequential IPN; b) Simultaneous IPN. Monomer I and II could also consist of a prepolymer I and II

Other types of IPNs include: Latex IPN, gradient IPN, thermoplastic IPN and semi-IPN. Latex IPNs are prepared in the form of latexes, typically with a core and shell structure. Gradient IPNs have compositions or cross-linking densities that vary depending on location in the sample. Thermoplastic IPNs are hybrids between IPNs and polymer blends and have physical rather than chemical cross-links and semi-IPNs consist of one or more polymers being cross-linked into networks and one or more polymers being linear or branched[72].

For many years the main focus of IPNs as DEAP actuators was on highly pre-strained acrylic 3M VHB tape due to this materials high electric breakdown field and large strains. The VHB IPNs were created via a sequential approach by treating the pre-strained acrylic VHB film with crosslinkable monomer and initiator and then allowed the monomer and initiator to diffuse into the film. The monomer, upon thermal curing, formed a second polymer network, interlaced with the acrylic network. The formed IPN was allowed to relax to zero stress which made the acrylic network contract and the second network to be compressed. [36,40,41] A schematic representation can be seen in Figure 2.2.

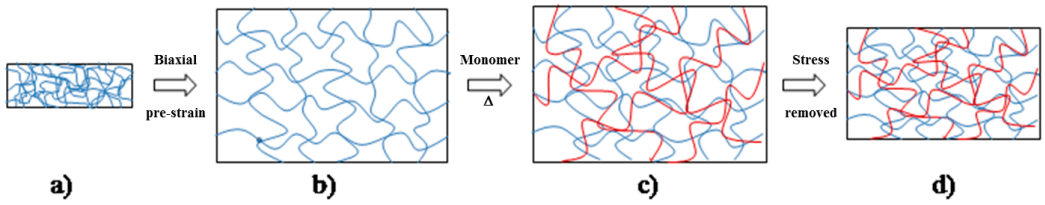

Figure 2.2: Schematic illustration of IPN formation based on 3M VHB tape: a) VHB acrylic tape before pre-strain; b) VHB acrylic tape after biaxial pre-strain; c) cross-linkable monomer is cured and interlaced with the acrylic network forming an IPN; d) stress is removed and the film retains most of the pre-strain

The resultant interpenetrating networks were now in equilibrium with one network highly stressed and the other highly compressed. The formed IPNs were able to withstand strains up to 300% which is comparable to the untreated pre-strained VHB tape[36].

A lot of work had been conducted within the area of VHB acrylic based IPNs with curable multifunctional monomers such as bifunctional 1,6-hexandiol diacrylate (HDDA)[40,42] and trifunctional trimethylolpropane trimethacrylate (TMPTMA) monomers[36,41]. Literature had also been published regarding VHB acrylic elastomers combined with a PDMS. The PDMS chains were swollen with a co-solvent into the acrylic film and subsequently cross-linked. The resultant IPN

material was shown to possess properties between the properties of the homo networks thus eliminating some of the disadvantages that acrylic networks experience[73]. Limited literature has however been published regarding the use of non-acrylic based IPNs as dielectric elastomers; however several articles were published regarding poly(3,4-ethylenedioxythiophene) (PEDOT) which was used in three-component IPNs where PEDOT acted as a electronically conducting polymer embedded in an elastic polymer electrolyte network to form solid polymer electrolytes (SPEs)[74]. Several studies had used poly(ethylene oxide) and poly(butadiene) IPNs as the polymer electrolyte network with the PEDOT conducting polymer. The combination of poly(ethylene oxide) and poly(butadiene) in IPNs was shown to have suitable properties for actuator applications[75–77]. IPNs had also been prepared combining cellulose and chitosan as electroactive paper actuators[78]. These IPNs were synthesised by dissolving cellulose and chitosan in a co-solvent followed by treatment with glutaraldehyde and cross-linking. The resulting films showed good bending displacement but experienced severe degradation at high humidity due to electrode damage. As limited research has been published regarding the use of non-acrylic based IPNs as actuators, there is clearly a need for the development of new materials within this area.

This work focuses on the use of two types of PPGs as IPNs due to the low elastic modulus of this polymer. The difference between the two polymers is the molecular weight and the functional end-groups. The term PPG-OH is used to describe the low molecular weight polymer which contains hydroxyl end-groups and the term PPG-V is used to describe the higher molecular weight polymer which is vinyl terminated.

Combination of PPGs as IPN is envisioned as an alternative to the commonly used PDMS and acrylic elastomers. PDMS as DEAP has been shown to have poor mechanical properties without added

fillers[79]. Acrylic elastomers such as VHB on the other hand have high viscous loss, poor response speed and stringent requirement of pre-strain that limit the use of VHB as DEAPs[43]. The mechanical properties of the PPG based IPN will be greatly improved due to the morphological stability that these interlaced networks experience. By varying the compositions of the two networks it could be possible to achieve tuneable properties and high actuation without pre-straining.

2.2 Experimental

2.2.1 Materials

Hydroxyl terminated poly (propylene glycol) (PPG-OH) of approximate molecular weight 4000 g/mol (Pluriol P 4000) was purchased from BASF, Germany and vinyl terminated poly (propylene glycol) (PPG-V) of molecular weight of 13500 g/mol from Kaneka Corp., Japan. The 3.4-functional crosslinker for PPG-OH DESMODUR N3300 was purchased from Bayer, Germany. All other chemicals were acquired from Sigma-Aldrich.

2.2.2 Methods

Rheological tests were performed in AR2000 stress controlled rheometer at 25°C with parallel plate geometry. Frequency sweep experiments were performed from 10^2 Hz to 10^{-3} Hz with 1mm thick samples at a fixed strain of 1% (the linear viscoelastic region was determined from initial strain sweeps). Glass transition temperature (T_g) of both homo network and IPN was measured by differential scanning calorimetry (DSC) using TA Instruments Q1000 differential scanning calorimeter under nitrogen flow rate of 50 mL/min. Measurements were performed from -85°C to 60°C at a heating rate of 10°C/min. Thermal degradation behaviour was studied by thermogravimetric analysis (TGA). The apparatus used was TA instrument's Q500 TGA analyser from room temperature to 600°C at a heating

rate of 20°C/min in air flow rate of 90 mL/min. Dielectric Relaxation Spectroscopy (DRS) was performed on a Novocontrol Alpha-A high performance frequency analyser from 1Hz to 10^6Hz.

2.2.2.1 Preparation of PPG-V homo network

Pentaerythritol tetrakis (3-mercaptopropionate) (tetra functional crosslinker, 488.66 g/mol, 0.24 g, 0.49 mmol) and 2, 2-dimethyl-2-phenylacetophenone (DMPA) (photo initiator, 256.3 g/mol, 0.13 g, 0.50 mmol) were dissolved in minimum volume of toluene. PPG-V (10 g, 13500 g/mol, 0.74 mmol) was added to the toluene solution and the solution was mixed in a SpeedMixer™ at 2000 rpm for 3 minutes. The mixture was poured into an 8 cm × 10 cm steel mould placed over a glass plate lined with Parafilm® M. This setup was kept in a well-ventilated place for 30 minutes and subsequently transferred to the UV chamber (λ= 365nm) and irradiated for 45 minutes.

2.2.2.2 Preparation of PPG-OH homo network

The PPG-OH homo networks were prepared at room temperature by mixing DESMODUR N3300 (3.4 functional crosslinker, 656.2 g/mol, 1.21 g, 1.84 mmol), dibutyltin dilaurate (catalyst, 631.56 g/mol, 0.016 g, 0.026 mmol) with PPG-OH (10 g, 4000 g/mol, 2.5 mmol) and the mixture was poured into the mould and left for 24 hours at ambient temperature.

2.2.2.3 Preparation of IPNs

IPNs of PPG-V and PPG-OH were prepared by mixing all of the above mentioned components together and keeping the stoichiometric imbalance fixed for both PPG-V and PPG-OH. The mixture was poured into the mould and placed in the UV chamber for 45 minutes and then stored at ambient temperature for 24 hours to ensure complete curing.

2.3 Results and Discussion

2.3.1 Sample preparation and characterization

The generation of IPNs were carried out by a simultaneous approach using two non-interfering chemical reactions (orthogonal reactions). PPG-OH was cross-linked using an isocyanate type cross-linker via a tin-catalyzed reaction and PPG-V was cross-linked with the use of pentaerythritol tetrakis(3-mercaptopropionate), a tetra-functional thiol. Thiol-ene reactions are a type of "click" reactions that are characterised by being mild, having high yields and being orthogonal with other common organic synthesis reactions[46] which makes this type of reaction ideal for simultaneous IPN formation. In this approach the thiol-ene "click" reaction was used as a cross-linking reaction in a new type of system with the PPG-V polymer. The reaction was carried out by free radical addition which is promoted by UV light[47]. As the PPG-OH tin-catalysed cross-linking reaction is facilitated by heat the two cross-linking reactions will be non-interfering, forming two independent networks. A schematic representation of the IPN formation can be seen in Figure 2.3.

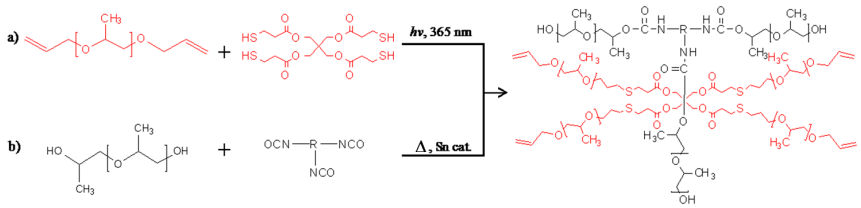

Figure 2.3: Schematic illustration of IPN formation based on PPG-V and PPG-OH: a) PPG-V is cross-linked via a tetra-functional thiol cross-linker using thiol-ene "click" chemistry and UV light; b) PPG-OH is cross-linked with heat, a tin catalyst and an isocyanate crosslinker with an average functionality of 3.4.

PPG-V and PPG-OH homo networks and IPNs consisting of both PPG-V and PPG-OH with varying weight ratios were prepared with this fixed '*r*', which is defined as [80],

$r = [\text{thiol}]/[\text{vinyl/ hydroxyl}] = f[crosslinker]/2[PPG-V / PPG-OH]$, where f is the average functionality of the crosslinker used and [crosslinker] and [PPG-V/PPG-OH] are the molar concentrations of the crosslinker and PPG, respectively. The compositions are listed in Table 2.1.

Table 2.1: Composition of homo and interpenetrating networks

Sample name	PPG-V(wt%)	PPG-OH(wt%)
PPG-V	100	-
I-95/5	95	5
I-90/10	90	10
I-85/15	85	15
I-80/20	80	20
I-75/25	75	25
I-70/30	70	30
PPG-OH	-	100

In order to obtain mechanically strongest crosslinked network rheological tests were performed on the PPG IPNs and '*r*' was determined to be 1.35 for the PPG-V and 1.25 for the PPG-OH systems corresponding to highest *G′*. Any further small increase in the '*r*' resulted in a decrease in *G′* which was consistent with the results obtained by Larsen *et al*.[80] in a vinyl terminated PDMS network.

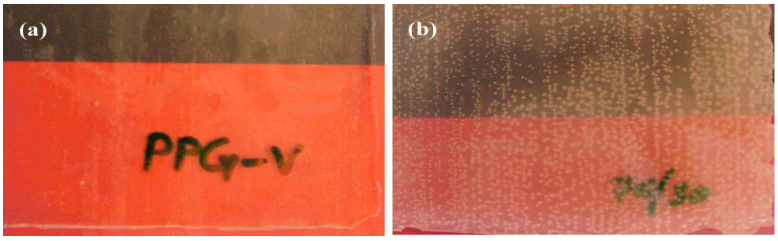

Figure 2.4: Digital images of a part of 8 cm × 10 cm prepared networks (a) PPG-V (b) I-70/30

Samples I-70/30 (Figure 2.4(b)) and I-75/25 had numerous bubbles inside and as this bubble formation was repeatable, they were rejected from further testing.

2.3.2 Rheological measurement

The linear viscoelastic (LVE) properties of the PPG networks were measured to obtain the elastic modulus (*G* or Young's modulus *Y=3G*) and to investigate the mechanical performances of the PPG homo networks and IPNs. Figure 2.5 shows the LVE diagrams for the prepared networks.

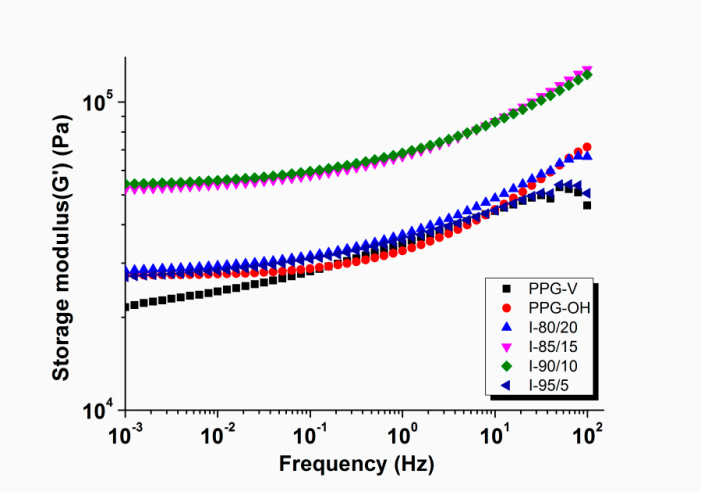

Figure 2.5: Storage modulus versus frequency for homo networks and IPNs at 25°C

As can be seen from Figure 2.5 the two components in the IPN system are fairly similar in their rheological properties. However, in the IPN materials the combination results in a system with improved storage moduli.

Table 2.2 the storage moduli as well as Tan delta values (see Figure 2.6) at low frequencies (10^{-3}Hz) are extracted for comparison.

Table 2.2: LVE data for homo networks and IPNs

Sample name	Storage modulus (kPa) at 10^{-3} Hz	Tan delta at 10^{-3} Hz
PPG-V	22	0.05
I-95/5	27	0.03
I-90/10	54	0.02
I-85/15	52	0.02
I-80/20	28	0.02
PPG-OH	27	0.02

As evident from Table 2.2 the storage moduli (G') at the plateau terminal region (10^{-3} Hz) is approximately 22 and 27 kPa, respectively, for PPG-V and PPG-OH homo networks which is very low compared to commercially available PDMS elastomers as well as non-filled silicone elastomers[80]. Reported G' for Elastosil RT 625 is 77 kPa[79] in very thin films. In IPN compositions I-85/15 and I-90/10 the shear storage modulus increases abruptly indicating additional chain restriction imposed by the PPG-OH networks. The shorter chains in PPG-OH results in higher crosslink density and behave as hard phase acting as anchor points hindering chain movements. No such increase in modulus is observed at the two extremes of the IPN compositions.

The Tan delta plots (Figure 2.6) and the values reported in Table 2.2 can also give some insight into the molecular motion and damping behaviour of the elastomer networks.

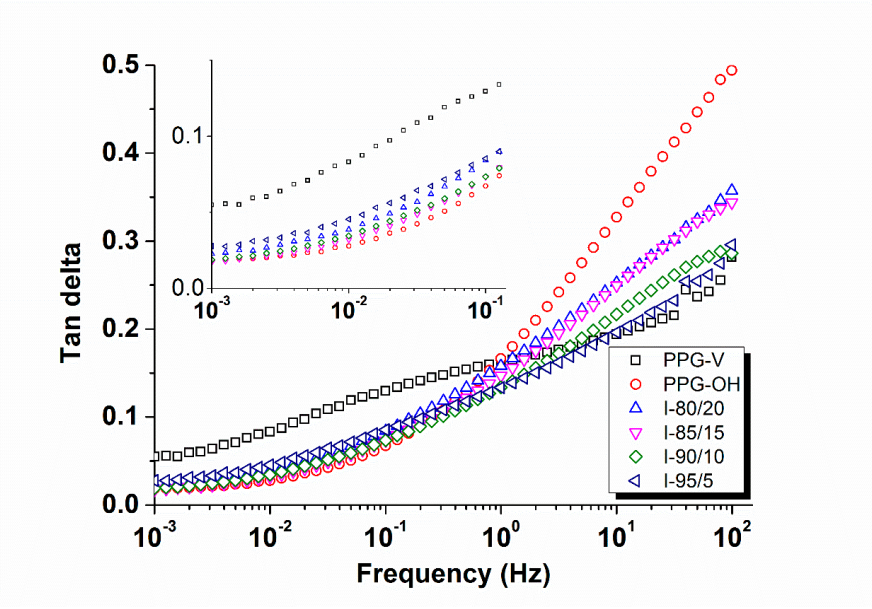

Figure 2.6: Tan delta as a function of frequency for homo networks and IPNs at 25°C. The inset shows the tan delta curves of homo networks and IPNs at the terminal region

The frequency dependency of Tan delta at the terminal frequency region is not significant for homo network and IPNs which is typical of crosslinked elastomers. Moreover the dissipative nature of the homo and interpenetrating networks is evident from the increasing trend in the Tan delta curves at frequencies above 1Hz. A close inspection of the curves at the terminal region reveals that I-85/15 and I-90/10 have very low Tan delta similar to PPG-OH, indicating low loss while PPG-V remains well above any of the IPNs and PPG-OH.

2.3.3 Differential scanning calorimetry

The glass transition temperature of the homo networks and IPNs was studied by DSC and reported in Table 2.3.

Table 2.3: DSC results of homo networks and IPNs

Sample name	Tg(°C)
PPG-V	-64.0
I-95/5	-64.0
I-90/10	-65.1
I-85/15	-64.6
I-80/20	-64.8
PPG-OH	-64.9

Few polymers are completely miscible, which often results in gelation and phase separation during IPN formation. Both phenomena influence the stability of the IPN produced. If gelation occurs first then the phase domains remain small in contrast to when phase separation occurs before gelation where domains are larger [72]. Since the backbone structures of both polymers are identical in this study, phase separation is expected to be limited. Both networks are formed simultaneously, which ensures good mixing until the gelation point of one of the networks. This is evident from the T_g values, which are comparative for both the homo networks and the IPNs.

2.3.4 Thermogravimetric analysis

Thermal degradation of IPNs can be best understood when compared to the thermal behaviour of the homo networks as shown in Figure 2.7 where the Thermo Gravimetric Analysis (TGA) of homo networks and IPNs are compared.

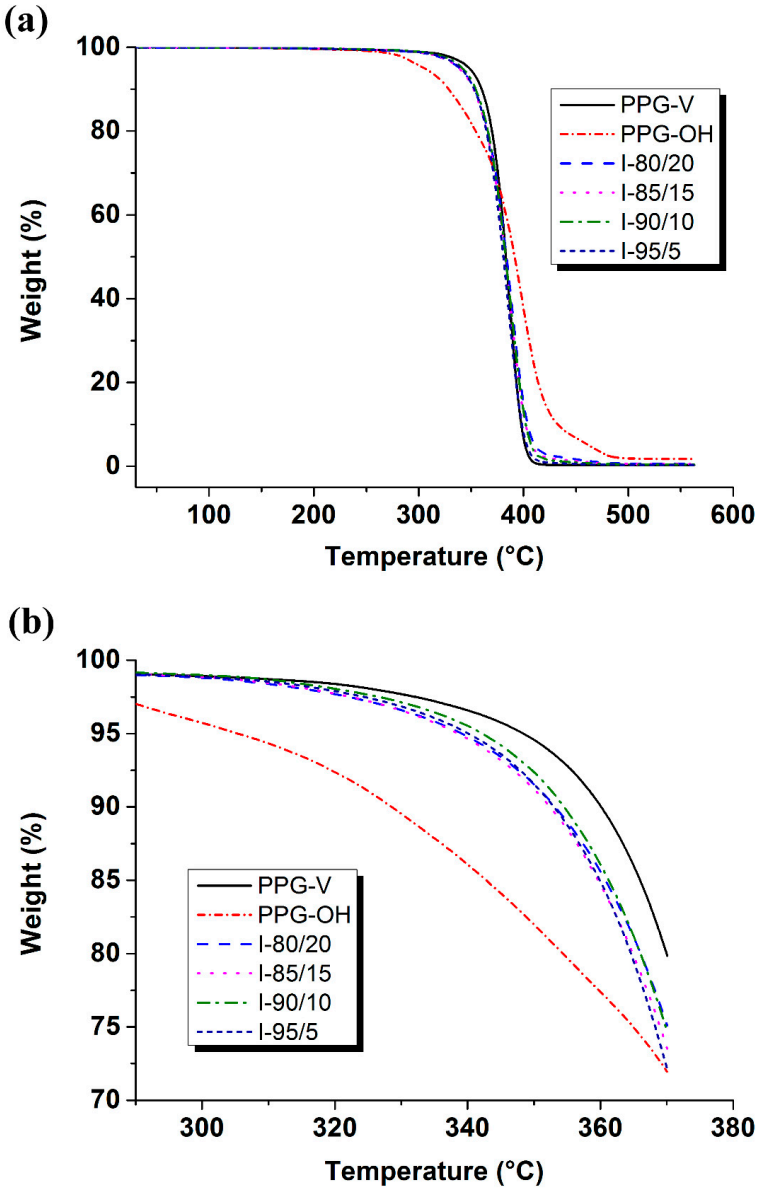

Figure 2.7: (a) TGA of homo networks and IPNs (b) magnified view of T_5

As seen from Figure 2.7, both the homo network and IPNs show single step degradation process corresponding to complete decomposition of polymer backbone. Different temperatures attributed to various levels of thermal stability of a polymer can be identified from the TGA curve, namely T_5, T_{50}, and T_{95}, defined as the temperature where 5, 50 and 95% mass loss of the polymer occurs. In this case there is an improvement in the onset of degradation, which is illustrated from Figure 2.7 (b).

The T_5 values of homo networks and IPNs are extracted from Figure 2.7 (b) and listed in Table 2.4 for easy comparison.

Table 2.4: T_5 temperature for homo networks and IPNs

Sample name	T_5(°C)
PPG-V	344
I-95/5	340
I-90/10	342
I-85/15	339
I-80/20	339
PPG-OH	306

The T_5 degradation temperatures from Table 2.4 clearly show only a minor reduction in thermal stability of the IPN than PPG-V homo network, as the PPO-OH content is increased. This corroborates the DSC results indicating a completely miscible polymer system with a homogeneous distribution of the two components in the IPN.

2.3.5 Dielectric spectroscopy

For applications of DEAP materials relative permittivity and the dielectric losses are important design parameters and all the materials were investigated by dielectric relaxation spectroscopy (DRS) as shown in Figure 2.8.

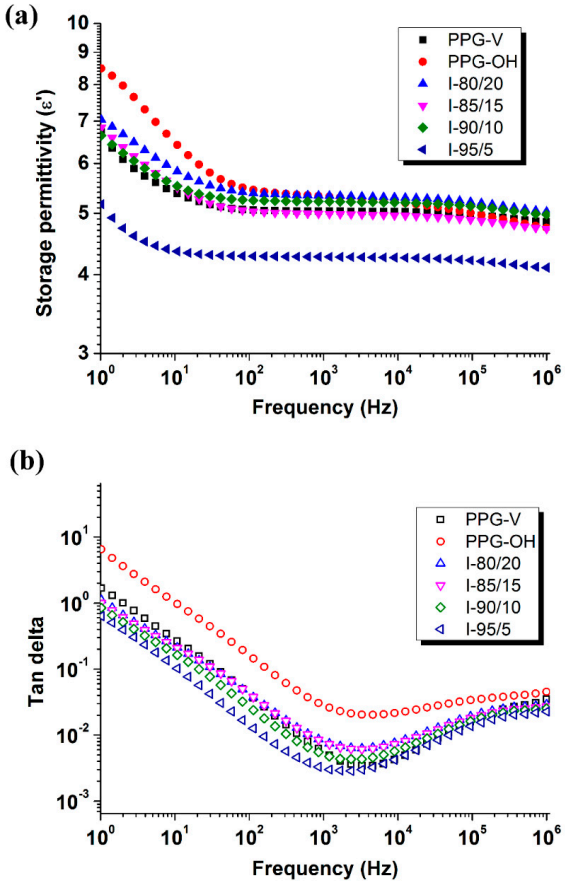

Figure 2.8: (a) Storage permittivity and (b) Tan delta vs. frequency for homo networks and IPNs obtained from DRS.

From Figure 2.8(a) it is apparent that the system is homogeneous resulting in no dielectric transitions from interfacial polarizations in the IPNs. In the medium to high frequency range (10^2-10^6Hz) where the dielectric property depends on the bulk polarization process[81], the ε' for the homo and interpenetrating networks are almost constant. The relative permittivity for homo networks and IPNs,

except for I-95/5, is calculated to be 5.0-5.2 at 10^4 Hz, which is about 67% higher than pure or fumed silica reinforced PDMS[79].

All compositions have same trend in dielectric loss behaviour as seen from Figure 2.8(b). The Tan delta of PPG-V networks and IPNs start from 1 at 1Hz and gradually decrease as the frequency is increased with the minimum in Tan delta at ~10^3Hz. PPG-OH although follows the same trend as the rest, shows a much Tan delta in the entire frequency range, which is a result of higher losses.

For evaluation of the proposed PPG material for DEAP applications some of the essential properties of PPG-V homo networks are compared to a commercial PDMS (Elastosil RT625) in Table 2.5.

Table 2.5: Comparison of different properties of Elastosil RT625 and PPG-V

Property	**Elastosil RT625**	**PPG-V**
Permittivity (ε')	3.0	5.0
Dielectric breakdown strength(DBS) (V/μm)[79]	60	60[a]
Young's modulus (Y) (kPa)[79]	227	66
Figure of merit ($F_{om} = \frac{\varepsilon'(\mathrm{DBS})^2}{Y}$) [18]	48	273

[a]Breakdown strength of fumed silica filled PPG-V system.

It is clear from Table 2.5 that the PPG material has superior properties in some of the critical design parameters which are required for an efficient DEAP material. The PPG has a substantially improved permittivity as well as a low Young's modulus, which both look very promising for the further investigations of PPG based systems.

2.4 Conclusion

Interpenetrating polymer networks (IPNs) are promising materials as applicable to DEAP actuators. The main focus of IPNs as DEAP actuators have previously been based on pre-strained acrylic 3M VHB tape due to the large achievable strain of this material. Therefore, to eliminate the requirements of pre-straining of VHB acrylics, this work was focused on developing new type of non-acrylic based PPG IPNs as DEAPs. The initial results showed that the IPNs exhibited low elastic modulus, low tendency towards viscous losses and good thermal stability. In addition to this, the one pot procedure for the preparation of the IPNs resulted in a homogenous distribution of the two networks illustrated by several different techniques. The DRS investigations revealed a high dielectric permittivity (ε' = 5.0) of the IPNs in the medium to high frequency range. The PPG IPNs showed clear improvements over the VHB acrylics, however it was judged that the curing process for obtaining the IPNs was not industrially suitable due to long time requirements therefore, it was decided to conduct further studies on vinyl terminated PPG homo networks as DEAPs.

Chapter 3

Reinforced PPO as soft and extensible DEAP

As shown in chapter 2, vinyl terminated PPG (hereafter mentioned as PPO) homo networks and PPG IPNs are promising DEAPs having excellent relative permittivity, low viscous and dielectric losses. Nevertheless, PPO homo networks possessed poor mechanical stabilities which posed as a limitation when handling thin films. It was expected that this issue could be resolved by incorporating reinforcing filler into PPO homo networks.

The following chapter highlights on preparations and characterizations of treated fumed silica reinforced PPO composites. Mechanical, dielectric and actuation studies are performed and the results are directly compared to widely used VHB acrylic elastomers. This chapter is based on the article **"Reinforced poly(propylene oxide): A very soft and extensible dielectric electroactive polymer"** published in Smart Materials and Structures, *see* Appendix B2

3.1 Introduction

In this study PPO and its composites have been investigated as a new DEAP material and the results are compared against commercially available acrylic (VHB4910). The aim is to develop a new DEAP material with enhanced electromechanical response, compared to VHB. In addition, a thorough electrical breakdown measurement of this system could also be done in future in order to investigate the effect of filler addition on electrical breakdown strength, as it is known that such particulate filled system could suffer from low breakdown strength. Jensen *et al.*[82,83] investigated the networks from PPO as materials for very soft skin adhesives. They applied silicone hydride functional crosslinkers to crosslink the end-linked vinyl functional PPO, which was found to be inefficient. In the presented work, a novel, fast and efficient UV photo-crosslinking is employed to crosslink PPO

and its composites with treated fumed silica. Mechanical, dielectric, rheological and electromechanical characterizations are performed on both this new material and its composites in order to evaluate the potential of PPO as a new DEAP.

3.2 Experimental

3.2.1. Materials

Vinyl terminated PPO of approximate molecular weight 16500 g/mol (Kaneka Silyl ACS 003) was obtained from Kaneka Corp., Japan. 2,4,6-trimethylbenzoylphenylphosphinic acid ethyl ester (Lucirin TPO-L) was purchased from BASF, Germany. VHB 4910 was obtained as 1 mm and 0.5 mm thick films with polyethylene backing material from 3M. The filler used for the elastomeric composites was hexamethyldisilazane (HMDS) treated fumed silica AEROSIL® R812, from Evonik Industries. The reported Brunauer, Emmett and Teller (BET) surface area of AEROSIL® R812 was 260±30 m^2/g. All the other chemicals used in this work were purchased from Sigma-Aldrich.

3.2.2. Methods

Rheological tests were performed in a stress controlled rheometer (AR2000) from TA Instruments, with 25 mm parallel plate geometry. Measurements conditions were set to controlled strain mode at 1% strain, which was ensured to be within the linear viscoelastic region as determined from initial strain sweeps. Frequency sweep experiments were performed from 10^2 Hz to 10^{-3} Hz at 25°C. Broadband dielectric spectroscopy was carried out on disc-shaped samples of both the pure matrix and the composites (diameter of 25 mm and thickness 1 mm) at 25°C in the frequency range 20 Hz to 2 MHz by means of an ARES G2 rheometer equipped with DETA accessory including an inductance (L)-capacitance (C)-resistance (R) (LCR) meter (Agilent E4980A). Actuation behavior of the PPO films, shaped in rectangular material strips of dimension 20 × 25 mm^2 and thickness varying between 80-226 μm, was studied after they were provided with opposed compliant electrodes by

smearing a carbon based conductive grease (Nyogel 755G, Tecnolube Seal, USA) on both their major surfaces. For each sample a vertical prestrain of 100% and a dc high voltage with stepwise increment of 250V were applied across the elastomer by means of power supply (HV-DC 205A-30P, Bertan, USA). At each voltage level isotonic transverse strains were measured by a displacement transducer and waited until a constant deformation was obtained. One sample for each composition was measured. A two-column ultimate testing machine (5500R, Instron, UK) was used to perform uniaxial elongation tests for PPO and the composites at a constant deformation rate of 25 mm/min with a 10 N load cell. Molecular weights and polydispersity index (PDI) were estimated by size exclusion chromatography (SEC) using Viscotek GPCmax VE-2001. The machine was equipped with Viscotek TriSEC Model 302 triple detector array (refractive index detector, viscometer detector, and laser light scattering detector with the light wavelength of 670 nm, and measuring angles of 90° and 7°) and a Knauer K-2501 UV detector using two PLgel mixed-D columns from Polymer Laboratories (PL). The samples were run in tetrahydrofuran (THF) at 30°C (1 mL/min). Molecular weights were calculated using polystyrene (PS) standards from PL. Nuclear Magnetic Resonance (NMR) spectroscopy was performed on a 300 MHz Cryomagnet from Spectrospin & Bruker, in $CDCl_3$ at room temperature. Fourier Transform Infrared Spectroscopy (ATR-FTIR) was performed on a Nicolet iS50 from Thermo Fischer Scientific with a universal Attenuated Total Reflection sampling accessory on a diamond crystal.

3.2.2.1 Standard procedure for preparation of PPO networks

Pentaerythritol tetrakis (3-mercaptopropionate) (tetra functional crosslinker, 488.66 g/mol, 0.24 g, 0.49 mmol) and 2,4,6-trimethylbenzoylphenylphosphinic acid ethyl ester (Lucirin TPO-L) (photo initiator, 316.33 g/mol, 0.19 g, 0.60 mmol) were added to α,ω-divinyl PPO (10 g, 16500 g/mol, 0.60 mmol) and mixed in a SpeedMixer™ (DAC 150 FVZ, Hauschild Co., Germany) at 3500 rpm for 5 minutes. The mixture was poured into an 8 cm × 10 cm steel mould placed over a glass plate

lined with Parafilm® M. This setup was kept in a well-ventilated place for 45-60 minutes and subsequently transferred to the UV chamber (λ=365 nm, 4.5 mW/cm^2) and irradiated for 45 minutes in ambient atmosphere.

3.2.2.2 Standard procedure for filled PPO systems.

The system was prepared as above for pure PPO networks. The filler was added with 40-60 wt% toluene directly into the PPO-crosslinker mixture prior to speed mixing, otherwise, the procedure was unchanged. The resulting films were studied by scanning electron microscopy (SEM) to ensure proper mixing of the fillers into the elastomer.

3.3 Results and discussions

3.3.1. Sample preparation and characterization

In this study a novel network material for DEAP applications based on PPO was prepared. The network was prepared through a highly efficient crosslinking of a commercially available α,ω-divinyl PPO with pentaerythritol tetrakis(3-mercaptopropionate), a tetra-functional thiol. Thiol-ene reactions are a type of "click" reactions that are characterised by being highly efficient and easy to perform in bulk processes[46,47]. The reaction is tolerant to a large number of functional groups and can be initiated through both thermal and photochemical initiators, as shown in Scheme 3.1 for the photochemical initiator (Lucirin) applied here.

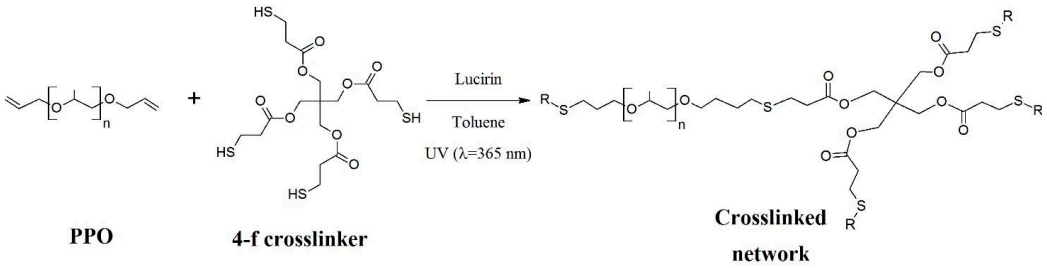

Scheme 3.1:Photoinitiated crosslinking of α,ω–divinyl PPO by thiol-ene chemistry, where R signifies the network.

The thiol-ene crosslinking reaction shown in Scheme 3.1 relies on a high degree of end-group functionality in order to be efficient and produce a crosslinked network with a minimum of dangling chains. The presence of the end groups on the commercial α,ω-divinyl PPO base material has been confirmed by ^{1}H-NMR spectroscopy, where the presence of the vinyl end group was confirmed with a characteristic set of doublets at 5.2 ppm and a multiplet at 5.9 ppm. The presence of the vinyl end-groups were also confirmed by FT-IR, where the double bond stretching was found at ~ 1600 cm^{-1}.

The crosslinked PPO networks were prepared with a controlled stoichiometric imbalance [84], which is defined as $r = [\text{thiol}]/[\text{vinyl}] = f[\text{crosslinker}]/2[\text{PPO}]$ where f is the average functionality of the crosslinker used and [crosslinker] and [PPO] are the molar concentrations of the crosslinker and PPO, respectively.

In order to obtain the mechanically strongest network, rheological tests were performed on pure PPO networks by monitoring the storage modulus (G') in the linear viscoelastic region for different crosslinker compositions. The storage moduli at 10^{-3} Hz are summarized in Table 3.1.

Table 3.1 : Storage modulus (G') of networks at different crosslinker contents at 10^{-3}Hz [a)]

Stoichiometric imbalance (*r*)	0.8	1.0	1.2	1.32	1.65	1.85
***G′* (kPa)**	0.49	0.30	0.43	25.2	34.7	27.9

[a)] The complete data series have been included in Appendix A1.

From Table 3.1, it can be seen that the mechanically strongest network was obtained at approximately r = 1.65 corresponding to highest G' among other pure PPO networks and this stoichiometric imbalance was thereafter kept constant throughout the study for the pure PPO network and PPO composites.

Pure PPO network was prepared as shown in Scheme 3.1. Particle composites were prepared as for the pure PPO network, with addition of the different amounts of filler before mixing and UV crosslinking. In the compositions, the non-rubber ingredients (such as fillers in this case) are expressed by parts per hundred rubber (phr). In this convention, the filler amount is taken as the ratio against 100 parts (by weight) of rubber. In a typical composition, PPO_10 indicates 10 phr (1 g) treated fumed silica was mixed with 10 g pure PPO.

3.3.2. Rheological measurement

Mechanical tests were performed on pure and composite PPO networks in order to measure linear viscoelastic (LVE) properties. Figure 3.1(a) shows the storage modulus (G') and Figure 3.1(b) shows loss tangent (Tan delta) of the materials. Tan delta is also known as the damping of the material. It is obvious that, with respect to the viscous loss in the investigated frequency regime, all PPO networks are superior to VHB (see insert in Figure 3.1(b) for comparison).

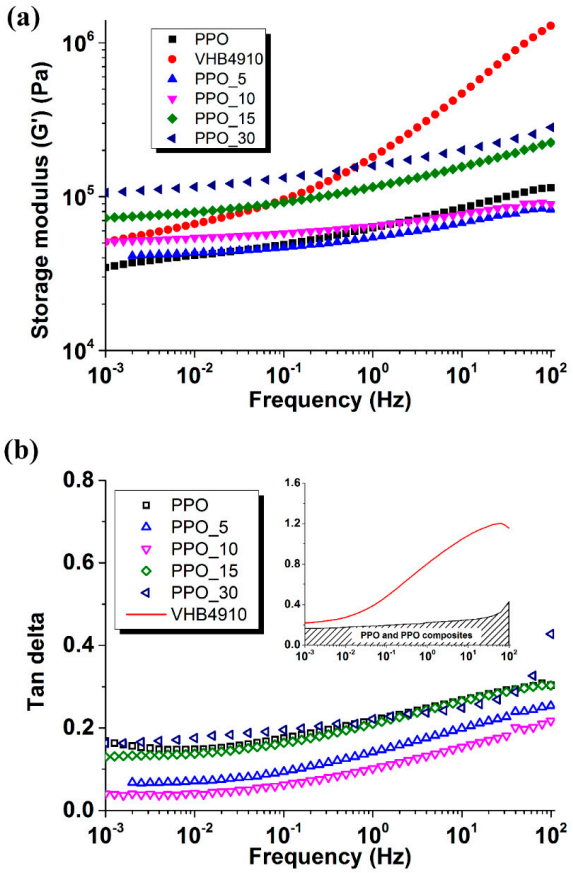

Figure 3.1: (a) Storage modulus and (b) Tan delta versus frequency for pure PPO and filled PPO networks at 25°C. Inset shows the difference in Tan delta between the PPO formulations (shaded region) and VHB

From Figure 3.1(a) it can be seen that the G' at the plateau (terminal) region (10^{-3}Hz) is approximately 35 kPa for pure PPO which is very low compared to VHB as well as for non-filled silicone elastomers[84]. On addition of treated fumed silica into the soft PPO network, the storage modulus (G') at low frequencies gradually increases from 35 kPa to 106 kPa due to the hindrance in chain movement imposed by the filler.

The Tan delta plots (Figure 3.1(b)) also give some insight into the damping behaviour of the polymers. At 5 phr treated fumed silica loading, the viscous loss of pure PPO network is reduced significantly in the entire frequency range, and it continues to decrease as the filler content is raised up to 10 phr. However, upon addition of 15 and 30 phr treated fumed silica the composites show increased Tan delta, indicating prominent damping behavior of the composites and hence a possible destruction of the network properties[84]. Moreover, at low frequencies the samples containing treated fumed silica exhibit an almost stable Tan delta, as is typical for a loaded crosslinked rubber in which chain movements are further restricted due to the presence of filler particles. Compared to PPO, VHB remains a material with a significant loss, a higher Tan delta and showing a much more dispersive behavior than PPO and any of the composites (Figure 3.1b).

3.3.3. Dielectric spectroscopy

One interesting aspect of this study is to measure the effect of incorporating treated fumed silica as a reinforcing agent on dielectric permittivity of PPO. Figure 3.2(a) and Figure 3.2(b) show dielectric spectra for PPO and its composites.

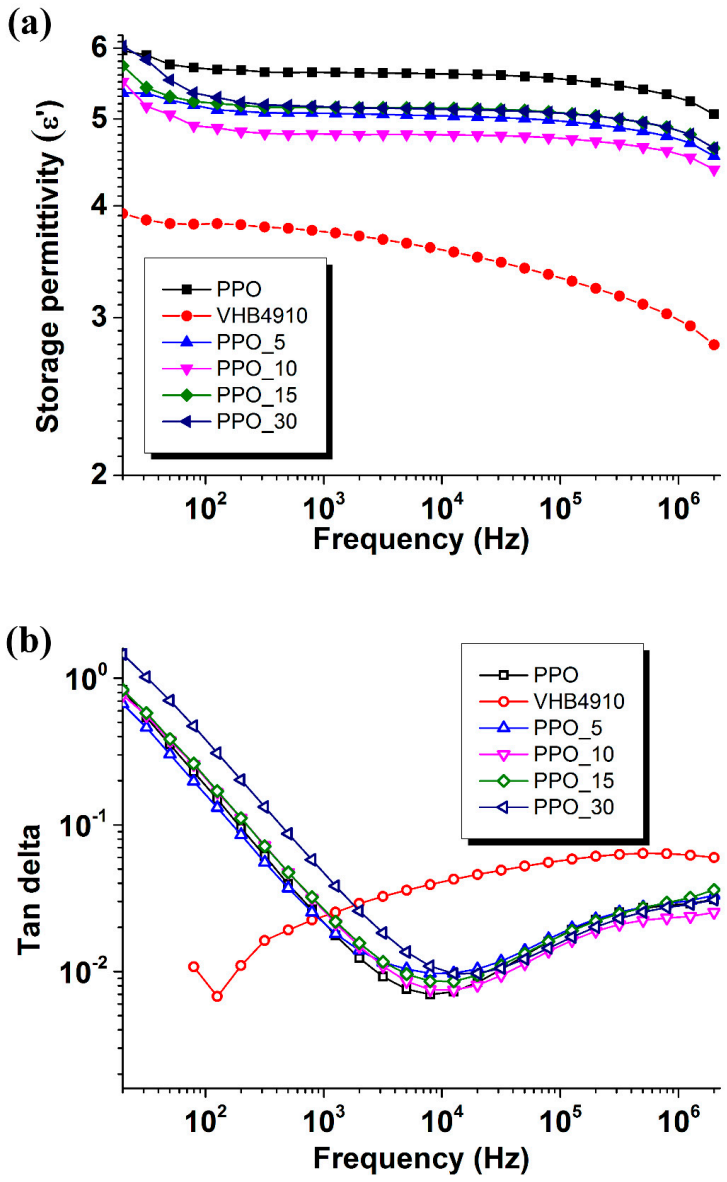

Figure 3.2: Dielectric spectroscopy plot (a) Storage permittivity versus frequency and (b) Tan delta versus frequency for PPO and the composites.

At low frequencies, an increase in the dielectric constant of both PPO and its composites is observed as frequency is progressively lowered from about 10^2 Hz down to 20 Hz (Figure 3.2(a)), which is accompanied by a parallel increase of the Tan delta (Figure 3.2(b)). Such an increase, which shows up as a low frequency dispersion in all the dielectric spectra, can be ascribed to a Maxwell-Wagner polarization, which is caused by a limited displacement of charges induced by the electric field in correspondence of interfaces between different phases. While in the case of pure PPO network such dispersion could arise only from a polarization contribution at the level of the sample/electrode interface and in the composites it could be indicative of the presence of further interfaces. Indeed, the fact that in the composites such polarization effects are more significant than in pure PPO network is likely due to the presence of interfaces between the PPO matrix and the filler. Coherently, it is also found that as the filler amount is increased the interface polarization effect increases. In the region of the medium-high frequencies (10^2 – 10^6 Hz), where the dielectric response mainly depends on the bulk polarization processes[81], there are no significant changes in the ε' (Figure 3.2(a)) for all the materials. However, the dielectric constant varies with the composites compared to that of the pure matrix. From Figure 3.2a the relative dielectric constant for pure PPO network at 1 kHz can be determined to be 5.6, which is higher than the value reported for VHB4910 (3.21 at 1 kHz)[85,86]. Treated fumed silica was used as a filler for reinforcing purposes, and since it is a low dielectric constant filler (ε_r = 3.9) it gives a minor decrease in the dielectric permittivity, as predicted by common mixing rules[50]. Although, at higher treated fumed silica contents the bulk permittivity of PPO_15 and PPO_30 becomes higher than PPO_5 and PPO_10, it remains lower than the pure matrix. This change in the behavior of the dielectric properties at higher filler loading factors could be the result of a larger contribution from interfaces at filler/matrix boundaries as the filler volume fraction is increased. Some studies have already revealed that the presence of such boundary layers inside a material increases the dielectric permittivity. For instance, at the interface between matrix and filler

in a particulate composite or between two immiscible phases in a polymer blend, intermediate interaction regions can provide additional polarization properties, which can play a major role in determining the final permittivity of such material[87–90].

3.3.4. Mechanical analysis

The mechanical properties of the PPO and the reinforced composites were investigated by tensile testing as shown in Figure 3.3.

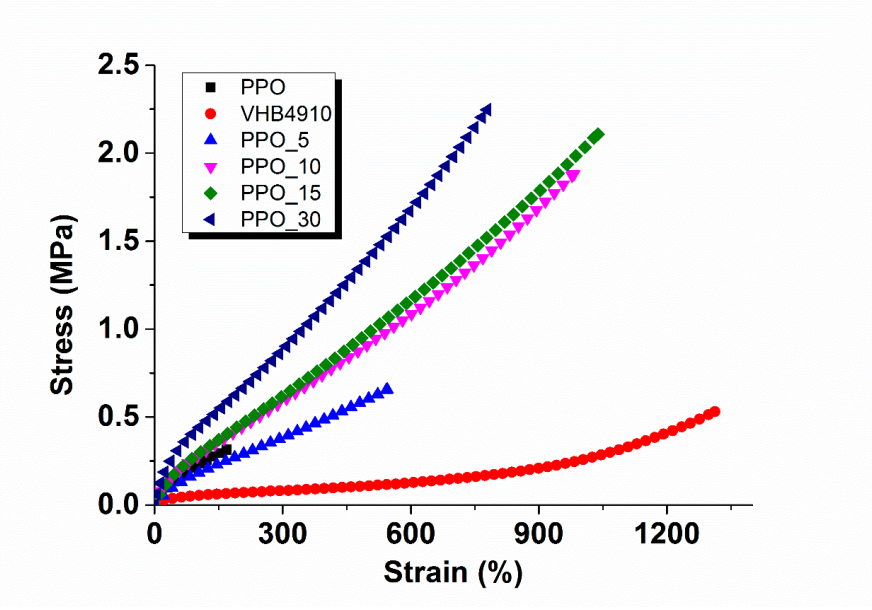

Figure 3.3: Tensile testing of PPO and the reinforced composites

Each test was stopped either at sample break, which occurred for all samples except PPO_30, or when the load cell reached maximum limit (10 N). Observed elongation at break of pure PPO network is 170% while all the composites show maximum elongation exceeding 500%. Thus, filler incorporation in PPO network increases the extensibility of the networks, clearly showing the desired improvement in mechanical stability of the prepared composites.

Table 3.2 summarizes the local elastic moduli (tangent slope) at different strains of PPO and the composites.

Table 3.2: Local elastic moduli of PPO and its composites at different strain.

Sample	Modulus at 25% strain (kPa)	Modulus at 50% strain (kPa)	Modulus at 100% strain (kPa)
PPO	264	205	143
VHB4910	78	31	19
PPO_5	200	160	119
PPO_10	327	241	176
PPO_15	338	240	178
PPO_30	474	344	239

From the table, it is clear that for PPO composites the local elastic moduli steadily decrease as the strain is increased up to about 100%, which is a common feature of the elastomeric behavior. At higher elongations the situation changes and a steeper monotonic increase in the stress curves is observed (except for pure PPO network as the sample failed at about 170% strain), recognizable as an up-swing after a flex point above 100% strain, which is due to the preferred orientation of the polymer chains in the direction of extension. When the filler amount is increased, the respective curves shift to higher stresses at corresponding strains (Figure 3.3) with the exception of PPO_5, for which the response remains below that of the pure matrix. One plausible reason might be that in case of PPO_5 the reduction of crosslink density is dominating over induced mechanical improvement due to filler addition thereby making the sample softer than PPO. A markedly different stress-strain behavior is observed for VHB, where a very low modulus at strains below 600% is observed, which is advantageous to electromechanical actuation, followed by a moderate increase at strains beyond 900%.

3.3.5. Actuation study

Electromechanical actuation tests were performed on 100% pre-strained samples of both PPO and its composites, and the results are presented in Figure 3.4. The electromechanical response of pre-strained VHB4910 is included in Figure 3.4 for easy comparison. Due to the detection of a partial electrical conduction at fields over 20 V/μm in samples containing treated fumed silica, the effective electric field acting on these samples was not considered reliable beyond this threshold value. Therefore, data have been reported only for reliable values below 20 V/μm (with the exception of PPO_30, which showed reliable actuation at electric field as high as 27 V/μm). For pure PPO network the sample failed at fields around 17 V/μm, while VHB4910 did not show any such failure.

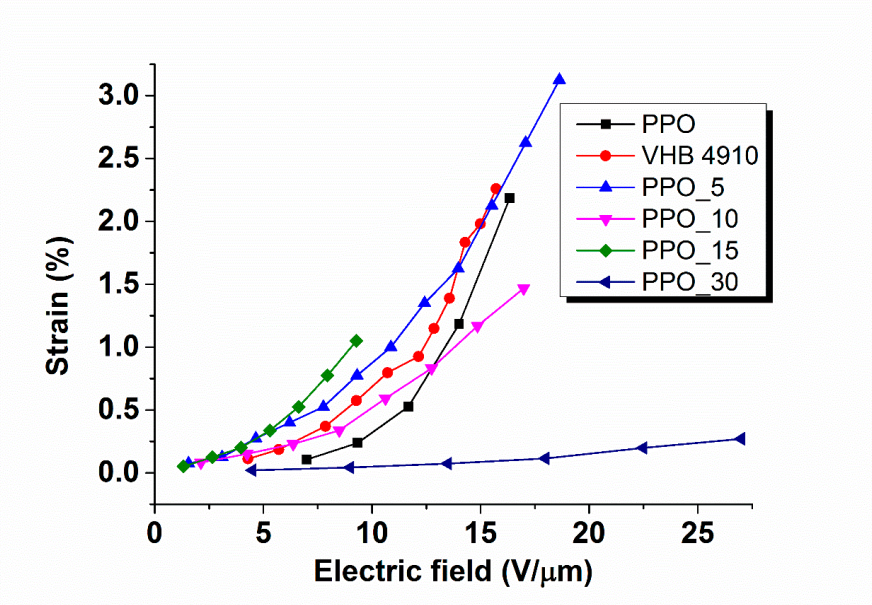

Figure 3.4: Electromechanical response of PPO and the composites.

As seen in Figure 3.4, the actuation response of pure PPO network is very close to that of VHB4910. Addition of filler significantly reduces the stickiness of PPO and improves its mechanical performance manifold (Figure 3.1 and Figure 3.3). The decrease in Young's modulus at low filler

loading followed by an increase as filler amount is increased, directly reflects on the electromechanical response of PPO composites. From Figure 3.4, it can be seen that PPO_5 shows the maximum actuation strain among the studied PPO composites, followed by PPO_10 and PPO_15. The relatively low actuation strain of PPO_10 and PPO_15 is due to the higher modulus and lower dielectric permittivity compared to pure PPO network and PPO_5. At higher content of treated fumed silica the strain induced by the Maxwell stress becomes very small as can be seen for PPO_30. These observations are in good agreement with equation(1.2) and all measurements agree well at low voltages whereas the different losses start to play an important role at higher voltages for all types of materials investigated here. Considering the results obtained from actuation studies, PPO filled with small amounts of filler has very good actuation behavior and good mechanical properties. Higher filler content gave better mechanical property, but severely hindered the actuation performances of the material. Therefore a convenient tradeoff between the required mechanical reinforcement of PPO composites and the electromechanical response opens a pathway into the development of stacked actuators[9,10]. The PPO samples possess natural adhesiveness, which would be beneficial for sandwiching several actuators on top of each other. Future development of this material would be to strike a balance between improving mechanical properties and electromechanical response by either employing chemical modification of the base polymer or using novel filler materials. However, the filler selection is limited to fillers with little UV absorption.

Table 3.3 summarizes and compares all the material data for PPO, PPO_5 and VHB4910 obtained in this study.

Table 3.3: Material data comparison between PPO, PPO_5 and VHB4910

Sample	Shear modulus (kPa) at 10^{-3} Hz	Tan delta from rheology at 10^{-3} Hz	Storage permittivity at 1kHz	Tensile modulus (kPa) at 100 % strain	Electrically induced strain (%) at ~ 14 V/μm
PPO	34.7	0.16	5.6	143	1.2
PPO_5	41.2	0.07	5.1	119	1.6
VHB4910	50.7	0.2	3.7	19	1.8

From Table 3.3 it is seen that pure PPO network is relatively soft material however, it shows high viscous loss owing to high Tan delta. When treated fumed silica is added the shear modulus increases indicating reinforcement effect of PPO matrix with a parallel decrease in viscous loss. The storage permittivity of pure PPO network is about 1.5 times higher than VHB4910 although a slight decrease in permittivity can be seen in case of PPO_5 as predicted by mixing rule mentioned earlier. PPO_5 and VHB4910 shows similar electromechanical behaviour, which is an improvement over pure PPO network.

3.4 Conclusion

This study reveals the potential of PPO reinforced with treated fumed silica filler as a new DEAP material. A novel PPO elastomer and its composites were developed by a simple and easily manageable processing scheme. Shear rheology showed enhancement in the mechanical stability of PPO composites over the mechanically weak pure PPO network, and additionally both PPO and its composites showed significantly less viscous loss as compared to the widely used VHB acrylic elastomer. The reinforcement effect was also reflected in the mechanical tests, where the composites showed elongations of more than 500% compared to the 150% for the pure network. The relative permittivity of pure PPO network at 10^3 Hz was found to be 5.6, and all the PPO composites showed permittivities above 4.8, which is significantly higher than VHB4910. The electromechanical

actuation test showed that PPO composites with small amounts of filler (5-10 phr) have the best electromechanical behavior. Stickiness of PPO composites was identified as the drawback while handling thin films. Although increasing the filler concentration solved the issue to some extent, but at the cost of marked reduction in actuation strain due to stiffening of the films. No further tests were carried out to optimize the stickiness of PPO composites and the focus was shifted from PPO to a well known DEAP material, PDMS.

Chapter 4

Platinum free UV cured soft PDMS networks

Findings in literature showed that platinum catalyzed addition reactions are the most common method for curing vinyl terminated PDMS. It was envisioned that the drawbacks of using platinum could be corrected by using an alternative approach of UV induced thiol-ene reactions for the preparation of PDMS networks. Furthermore, advanced sequential (stepwise) curing emerged as a promising approach towards achieving PDMS elastomers with reduced elastic modulus without increase in viscous losses. This chapter focuses on using UV curing method for the preparation of PDMS networks by employing two types of crosslinking procedures involving a one step and a two step processes, respectively.

In this chapter the preparation procedures for obtaining PDMS networks from commercially available divinyl terminated PDMS by both one step and two step processes are demonstrated. Mechanical characterizations and curing kinetics of the prepared networks are investigated by shear rheology and the results are presented. This chapter is based on the article **"UV-Cured, Platinum-Free, Soft Poly(dimethylsiloxane) Networks"** published in Chemistry: A European Journal, *see* Appendix B3.

4.1 Introduction

Depending on the types of photo initiators used, UV curing follows either free radical or cationic mechanisms. In the free radical mechanism, the photo initiator absorbs UV light and generates free radicals, which react with unsaturated bonds and initiate the crosslinking process. However when cationic photo initiator is used, the photo initiator absorbs UV light and forms cationic species which then react with the reactive groups (e.g. epoxy) present on the polymer and initiates the crosslinking process. Free radical initiated reactions are very fast and thus, most of the available UV curable

systems are based on free radical mechanism as for example acrylates or urethane acrylates[91,92]. Curing of acrylates and urethane acrylate systems by free radical mechanisms are generally fast but they show serious drawbacks such as inhibition by atmospheric oxygen which can be restricted by carrying out the crosslinking reactions in an inert atmosphere [93] or by using thiol-ene reactions. Although thiol-ene reactions generally follow free radical mechanisms atmospheric oxygen does not show any negative effect on the curing process [94].

In silicone industries, the majority of vinyl terminated silicones that are cured at low temperatures use platinum catalyzed addition reactions. Only a few of silicone formulations use UV curing method solely, while most of the UV curable silicones still use platinum for additional addition crosslinking reactions. Some of the major drawbacks of platinum catalyzed crosslinking of silicones include highly priced catalyst requirement in the crosslinking reaction and poisoning of catalyst by compounds containing nitrogen, sulfur, phosphorus and tin[44]. Studies have also been done extensively on UV curable silicone copolymers [95–97] but very few examples on UV curable silicone homopolymers are available in literature [98,99]. Previously prepared UV curable PDMS systems rely on significant lower molecular weight PDMS than the PDMS used in this study. Consequently, the previously prepared networks are harder than the networks prepared in this study[99]. To overcome the drawbacks exhibited by platinum catalyzed curing of silicones and to prepare soft PDMS networks, UV chemistry can be used in combination with thiol-ene reactions to crosslink vinyl containing silicones provided the crosslinking reaction can proceed with large conversion.

The first objective of the present study is to develop a platinum free UV curable system to prepare PDMS networks. For this, UV photo crosslinking is employed to crosslink a α,ω- vinyl terminated PDMS by a six functional thiol crosslinker in a single step at ambient atmosphere via a free radical pathway. Though the above reaction produces soft crosslinked PDMS network, it is slow and

inefficient. Therefore, the second objective is to develop a platinum free thiol-ene based UV photo crosslinking system to produce soft PDMS networks in a fast and efficient way. This approach involves crosslinking a commercially available vinyl PDMS in a stepwise manner that will ensure fast and efficient crosslinking of PDMS. The prepared two step networks are also termed as heterogeneous bimodal networks [69,100]. In the stepwise mixing procedure, the short-chain and long chain polymers are separately reacted with crosslinker below their gelation threshold to produce pre-reacted mixtures. These pre-reacted mixtures are subsequently mixed and crosslinked with additional crosslinker where short chain domains are created within the long chain network and gives better control over network formation. Rheological studies are performed for mechanical characterizations and to study curing kinetics after UV exposure on both the prepared one and two step PDMS networks.

4.2 Experimental

4.2.1 Materials

α,ω-vinyl terminated PDMS (DMS-V35 and DMS-V05) with $\bar{M}_n$ = 49500 g/mol and 800 g/mol respectively, were purchased from Gelest Inc., USA. DMS-V35 and DMS-V05 are hereinafter mentioned as long chain and short chain, respectively. A (Mercaptopropyl) methylsiloxane-dimethylsiloxane copolymer (GP 367) used as a six functional crosslinker was obtained from Genesee Polymers Corp., USA. All other chemicals used in this study were purchased from Sigma-Aldrich and used as received.

4.2.2 Methods

Mixing of the components required for the network formation was done in a SpeedMixer™ (DAC 150 FVZ, Hauschild Co., Germany) at 3500 rpm for 2 minutes in case of one step networks and 1minute for two stage networks. Rheological tests were performed in a strain controlled rheometer

(ARES G2) from TA Instruments, USA with 25 mm parallel plate geometry. Measurement condition was set to controlled strain mode at 2% strain, which was ensured to be within the linear viscoelastic region as determined from initial strain sweeps. Frequency sweep experiments were performed from 10^2 Hz to 10^{-3} Hz at 23°C. Characterizations of the pre-reacted structures were carried out by size exclusion chromatography (SEC) using Viscotek GPCmax VE-2001. The machine was equipped with Viscotek TriSEC Model 302 triple detector array (refractive index detector, viscometer detector, and laser light scattering detector with the light wavelength of 670 nm, and measuring angles of 90° and 7°) and a Knauer K-2501 UV detector using two PLgel mixed-D columns from Polymer Laboratories (PL), USA. The samples were run in tetrahydrofuran (THF) at 30°C (1 mL/min). Molecular weights were calculated using polystyrene (PS) standards from PL. Nuclear magnetic resonance (NMR) spectroscopy was performed on a 300 MHz cryomagnet from Spectrospin and Bruker, in $CDCl_3$ at room temperature. Fourier transform infrared spectroscopy (ATR-FTIR) was performed on a Nicolet iS50 from Thermo Fischer Scientific with a universal attenuated total reflection sampling accessory on a diamond crystal.

4.2.2.1 Standard procedure for preparation of PDMS one-step networks

(Mercaptopropyl)methylsiloxane-dimethylsiloxane copolymer (hexa functional crosslinker, 3600 g/mol, 0.15 g, 0.039 mmol, 0.24 mmol of thiol group) and 2, 2-dimethyl-2- phenylacetophenone (DMPA) (photo initiator, 256.3 g/mol, 1-2 mL, 0.017 g/mL, 0.066 mmol) were added to α,ω-vinyl PDMS (3 g, 49500 g/mol, 0.061 mmol, 0.13 mmol of vinyl groups) to prepare the one step networks. The mixture was then mixed in the SpeedMixer™. After the mixing step, the mixture was poured into a 4 cm × 3 cm steel mold placed over a glass plate lined with Parafilm® M. This setup was kept in a well-ventilated place for 10-15 minutes and subsequently transferred to the UV chamber (λ=365 nm, 4.5 mW/cm^2) and irradiated for 20 minutes in ambient atmosphere. One step network based on

short PDMS chains (800 g/mol) with overall stoichiometric imbalance of 2 was brittle and further mechanical characterizations were not performed on the sample.

4.2.2.2 Standard procedure for preparation of PDMS Two step networks:

In the first step, the six functional crosslinker (3600 g/mol, 0.045 g, 0.012 mmol, 0.073 mmol of thiol group) was mixed with DMPA (photo initiator, 256.3 g/mol, 0.05-0.06 mL, 0.017 g/mL, 0.004 mmol). Thereafter short chain PDMS (800 g/mol, 0.3 g, 0.38 mmol, 0.88 mmol of vinyl group) was added to give a stroichiometry of $r \sim 0.10$. The whole mixture was mixed in the SpeedMixer™ for a minute and subsequently transferred to the UV chamber (λ=365 nm, 4.5 mW/cm^2) and irradiated for 20 minutes in ambient atmosphere. Next, long chain PDMS (49500 g/mol, 2.7 g, 0.054 mmol, 0.11 mmol of vinyl group) was mixed with the same hexa functional crosslinker (3600 g/mol, 0.0069g, 0.0019 mmol, 0.011 mmol of thiol group) and DMPA (photo initiator, 256.3 g/mol, 0.05-0.06 mL, 0.0173 g/mL, 0.004 mmol) to give stoichiometric imbalance $r \sim 0.10$. The mixture was then mixed in the SpeedMixer™ for a minute and subsequently transferred to the UV chamber (λ=365 nm, 4.5 mW/cm^2) and irradiated for 20 minutes in ambient atmosphere. In the second step, the reacted short chain and long chain PDMS was combined together and mixed with additional six functional crosslinker (3600 g/mol, 0.72 g, 0.20 mmol, 1.2 mmol of thiol group) and DMPA (photo initiator, 256.3 g/mol, 0.5-0.6 mL, 0.0173 g/mL, 0.04 mmol) to give an overall stoichiometric imbalance of $r = 1.5$. It was observed in our system that if stoichiometric imbalance was used above 0.14 then gels were formed after mixing the two pre-reacted mixtures together in the second step even before the UV irradiation. The reason of gel formation is probably due to very fast reactions between the pre-reacted mixtures. Therefore, to ensure that no such gels were formed before UV irradiation, the stoichiometric imbalance was kept low in cases of both short and long chains. The mixture was then mixed in the SpeedMixer™ and after mixing the mixture was poured into a 4 cm × 3 cm steel mold placed over a glass plate lined with Parafilm® M. This setup was kept in a well-ventilated place for

10-15 minutes and subsequently transferred to the UV chamber (λ=365 nm, 4.5 mW/cm^2) and irradiated for 20 minutes in ambient atmosphere. Long and short chain contents were varied to create two step networks with weight ratios of long chain: short chain= 90:10, 85:15, 80:20, 75:25 and 70:30.

4.3 Results and Discussions

4.3.1 Sample preparation and characterization

A commercially available PDMS was crosslinked by using UV exposure in presence of a photoinitiator without the use of platinum catalyst. The network was prepared through crosslinking between α,ω- vinyl terminated PDMS with a commercially available six functional (Mercaptopropyl)methylsiloxane-dimethylsiloxane copolymer as a crosslinker. The reaction in Scheme 4.1 shows crosslinking of a vinyl terminated PDMS by (mercaptopropyl) methylsiloxane-dimethylsiloxane copolymer in presence of UV light for the photochemical initiator (DMPA) applied here.

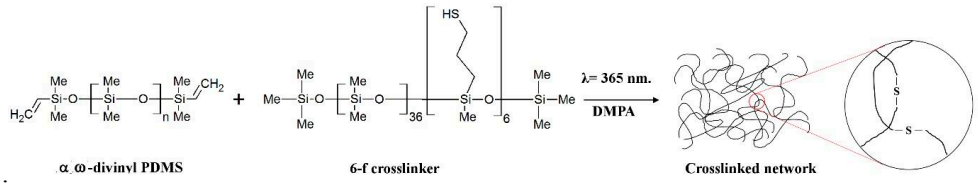

Scheme 4.1: Photoinitiated crosslinking of α,ω- vinyl terminated PDMS by thiol-ene chemistry

The photoinitiated crosslinking shown in Scheme 4.1 is a type of thiol-ene reactions where double bonds (-enes) present on the polymer chains are allowed to react with thiol (-SH) on the crosslinker under UV light and in presence of a photoinitiator to form a crosslinked network.

The fraction of unreacted polymer chains in the pre-reacted mixtures is calculated as $(1-r)^2$=0.81, since an unreacted polymer chain requires that both chain ends are unreacted, i.e. with a probability of $(1-r)^2$ [84]. Similarly, fraction of polymer chains reacted with the crosslinker at both ends

(probability of r^2) and dangling polymer chains (probability of $2r\times[1-r]$) present in the pre-reacted mixtures are found to be 0.01 and 0.18, respectively. The pre-reacted short and long chain structures are investigated by ^{1}H NMR, FTIR and SEC. (Appendix A2-A5). Compositions are summarized in Table 4.1

Table 4.1: Compositions of the two step networks

Sample ID	Bi90-10	Bi85-15	Bi80-20	Bi75-25	Bi70-30
Ratio of long and short chains (wt./ wt.)	90:10	85:15	80:20	75:25	70:30

The crosslinked one and two step PDMS networks were prepared with a controlled *r*. In order to obtain mechanically strongest network rheological tests were performed on both one and two step PDMS networks by monitoring the storage modulus (G') in the linear viscoelastic region. Four samples of Bi90-10 with varying stoichiometric imbalance (r = 1.25, 1.5, 1.75, 2.0) was used to prepare four different samples and G' of those samples were measured in order to obtain the optimum stoichiometry. The obtained optimum stoichiometry for Bi90-10 was then taken as the reference for all other two step networks prepared in this study. The one step network was prepared with $r = 2$. The storage moduli of one step and Bi90-10 network at 10^{-3} Hz are summarized in Table 4.2.

Table 4.2: Storage moduli (G') at 10^{-3} Hz of Bi90-10 prepared with different stoichiometric imbalance. G' of the one step network has been included as a comparison between the storage moduli of one and two step networks (The complete data series has been included in Appendix A6)

	Two step network (Bi90-10)				**One step network**
Stoichiometric imbalance (*r*)	1.25	1.5	1.75	2.0	2.0
***G′* (kPa) at 10^{-3} Hz**	11	26	25	20	20

From Table 4.2 the stoichiometric imbalance corresponding to highest *G′* was chosen as 1.5 and the stoichiometric imbalance was thereafter kept constant throughout the study for all two step network compositions shown in Table 4.1.

4.3.2 Rheological measurement

The prepared one and two step networks were tested mechanically in order to measure the linear viscoelastic (LVE) properties of the material. Figure 4.1(a) shows the storage modulus (*G′*) and Figure 4.1(b) shows loss tangent (Tan delta) of the materials as a function of applied frequency. Tan delta is also known as the damping of the material.

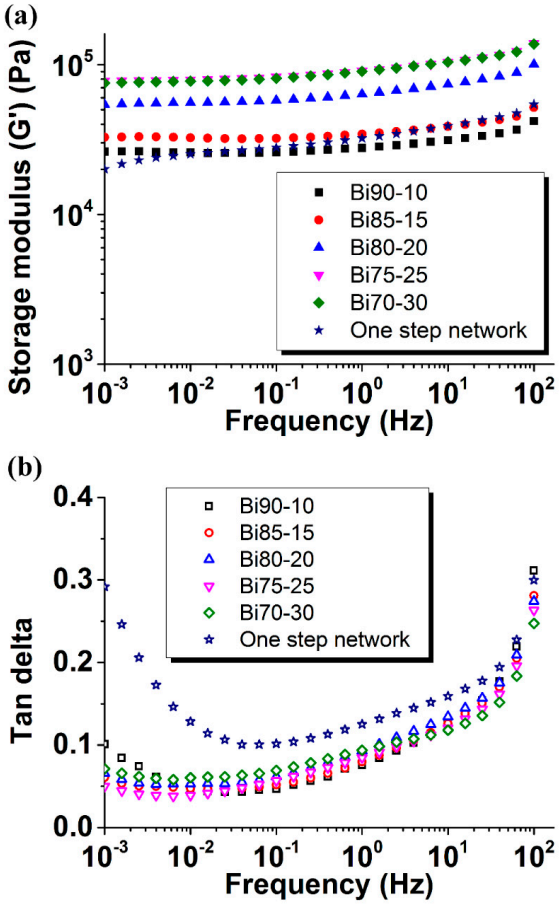

Figure 4.1: (a) Storage modulus (G') and (b) Tan delta as function of frequencies for one and two step networks at 23°C

It can be seen from Figure 4.1(a) that the two step networks show a gradual increase in G' in the studied frequency range as the amount of short chain is increased. Moreover the prepared one step network shows G' of 20 kPa at 10^{-3} Hz. This can be compared to 135 kPa for a similar molecular weight PDMS obtained from conventional platinum catalyzed addition cured PDMS [69]. In the two step networks short chain clusters act as apparent crosslinkers of the long chain and the network remains soft until the point where the stress becomes sufficiently large to initiate deformations of the

short chain clusters which can be seen from the low G' at 10^{-3} Hz exhibited by Bi90-10 and Bi85-15 with low short chain content [69,100]. Since the molecular weight of the short chain PDMS (800 g/mol) used within this study is significantly lower than the entanglement molecular weight (M_e) of PDMS (~12000 g/mol) [101], the elastic modulus of the short chain cluster within the two step networks will be dominated by crosslinks rather than entanglements. Therefore, at higher loadings of short chain PDMS (more than 15%) the short chain clusters act as reinforcing domains and restrict chain movements significantly thereby increasing the modulus of Bi80-20, Bi75-25 and Bi70-30, respectively.

The Tan delta plots (Figure 4.1(b)) also give some insight into the molecular motion and damping behaviour of the polymers. From the figure, it is seen that the one step network shows higher Tan delta than the two step networks at all frequencies. The sharp increase in Tan delta of the one step network at frequencies less than 10^{-1} Hz is due to long relaxations exhibited by the long dangling chains. However, in the two step networks no such relaxations were present at these frequencies. Moreover the low Tan delta shown by the two step networks at frequencies less than 10^{-1} Hz indicates that the prepared two step networks have significantly less dangling chains and lower viscous losses than the one step network.

Figure 4.2 shows evolution of normalized storage moduli ($G^{\#}_{0,Dayi} = G'_{0,Dayi} / G'_{0,Day0}$) at 10^{-3} Hz of both one and two step network with time after UV exposure. The complete set of data on the time dependent mechanical properties has been included in the Appendix (A7 and A8). Storage moduli of one and two step networks were measured for several days after UV exposure until the difference between two successive G' at 10^{-3} Hz at two successive days became 10% or less. The obtained storage moduli of one and two step networks at 10^{-3} Hz were then normalized by the storage modulus obtained at day 0 at the same frequency to illustrate the differences in curing kinetics of both the

networks after the UV exposure. Since development of storage modulus throughout the curing is related to kinetics of network formation, it is reasonable to take $G^{\#}_{0,Dayi}$ as a measure of curing kinetics in this study.

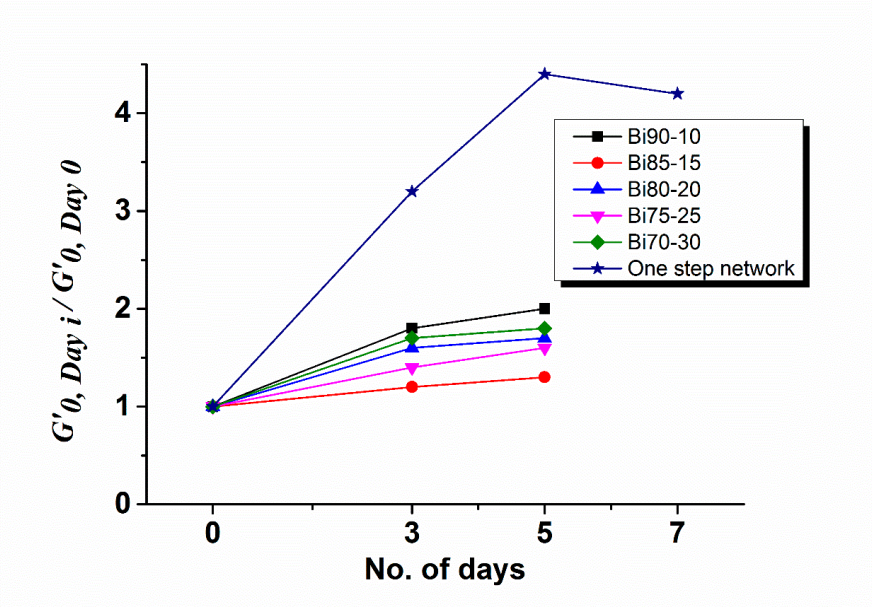

Figure 4.2: Investigation of curing kinetics after UV exposure of one and two step PDMS networks

As seen from the figure (Figure 4.2) the one step network takes longer time to reach stable $G^{\#}_{0,Dayi}$, indicating slow and inefficient curing than the two step networks. Such slow curing kinetics is due to slow diffusion of crosslinker molecule, which in turn slows down the crosslinking reaction. Silicones having vinyl groups as the reactive sites are either crosslinked at low temperatures by addition reactions, or at elevated temperatures by peroxides. Study shows [102] that silicones crosslinked by peroxide are more prone to slow curing kinetics due to the formation of volatiles during the crosslinking reaction than the addition cured silicones. Although addition curing of silicones are generally fast, some studies show that it can also suffer from slow curing kinetics similar to peroxide crosslinked silicones due to the presence of excess hydride crosslinkers in the system [103–105].

Shama *et al.* showed that in UV curable urethane acrylate and vinyl ether urethane systems slow curing kinetics similar to that of the silicones can be observed [106]. However, studies on development of mechanical properties throughout the curing process of UV initiated free radical curing of silicones are not well documented in literature. Therefore, development of storage modulus over time during curing of UV initiated free radical curing of silicone has been studied here extensively. From Figure 4.2 all compositions of the two step networks show a less pronounced $G^{\#}_{0,Dayi}$ with time due to step wise mixing procedure used in the two step networks which makes curing faster and gives control over network formation. In the two step networks the crosslinking reaction procedure first allows for the short and long chains to react separately with the crosslinker and form pre-reacted structures. After mixing the short and long chain pre-reacted structures together in the second step, the rest of the crosslinker is added in order to fully crosslink the system. By using step wise mixing procedure for creating two step networks, the crosslinker molecule is allowed to interact easily with the crosslinking sites on the polymer thereby speeding up the crosslinking reaction to a large extent. Due to fast reactions, $G^{\#}_{0,Dayi}$ shows less time dependency than the network prepared in a single step. The crosslinking reactions used in this study involve formation of free radicals. However, not all of the generated free radicals are consumed in the crosslinking and some of the radicals can be trapped inside the reaction media even after the UV source has been switched off. These trapped free radicals are responsible for the slow curing kinetics exhibited by the one step network but the large increase in $G^{\#}_{0,Dayi}$ from day 0 to day 3 in the one step network cannot be explained solely based on the trapped free radical species in the network structure. Nevertheless, it is possible that the effect is a combination of trapped living free radical and relieved built-in stresses that was frozen in the network during crosslinking. On the other hand, two step networks prepared by a controlled reaction procedure have limited tendency of trapped free radical species due to faster reactions than the one

step network. Because of fast and efficient reactions, two step networks show less time dependent mechanical behavior than the one step network depicted in Figure 4.2.

4.4 Conclusion

This study shows that PDMS one step networks can be prepared by using UV initiated thiol-ene chemistry as the crosslinking method. Moreover, the applied curing method does not require the use of platinum catalyst, which is otherwise an essential component in the addition crosslinking of vinyl terminated PDMS. Rheological studies revealed that the prepared UV cured PDMS network was softer than the corresponding platinum catalyzed addition cured network. However, the one step network showed slow curing kinetics manifested in the increase in G' several days after the UV exposure. It was also shown in the study that it is possible to synthesize UV curable PDMS networks in an efficient way by using a controlled two step reaction procedure where the network is allowed to form stepwise. In the two step process, first, pre-reacted structures of the two polymers with widely separated molecular weight is formed by reacting with deficient amount of crosslinker to avoid gelation. Then these two pre-reacted clusters are connected via covalent bond by the use of additional crosslinker. In this way domains of short chain clusters and long chain clusters are formed within the network. Thus, in the two step networks the short chain clusters act as reinforcing domains of the long chains and the networks showed significantly low viscous losses with softness comparable to the one step network. Due to the formation of pre-reacted structures before the final crosslinking, two step networks showed stable mechanical properties than the one step network even several days after the UV exposure due to a faster curing kinetics.

Chapter 5

Multiwalled carbon nanotube/poly(dimethyl siloxane) (MWCNT/PDMS) composites

In chapter 4, PDMS networks prepared by a two step process showed stable mechanical properties and low viscous losses due to controlled distributions of short chain clusters acting as reinforcing domains within the long chain networks. On the other hand, incorporation of conductive fillers below the percolation threshold is a common approach for increasing the otherwise low relative permittivity of PDMS elastomers. It was envisioned that the control of network heterogeneity as demonstrated in chapter 4 could be utilized for incorporation of conductive fillers in higher concentrations than usual without making the composites conductive.

In this chapter procedure for incorporating MWCNT in PDMS matrix and subsequent crosslinking by UV for the preparation of MWCNT-PDMS composites are presented. Furthermore, the results obtained on mechanical, dielectric and AC conductivity studies on the prepared PDMS composites are discussed. A publication is planned based on the work presented in this chapter.

5.1 Introduction

Several methods to prevent formation of conductive paths inside the elastomers containing conductive or semi-conductive fillers have already been reported [65]. However, most of the works were focused on keeping the filler contents below their percolation threshold in order to achieve non-conductive composites. The objective of the present study is to prepare PDMS composites containing loadings of MWCNT above the percolation threshold without exhibiting percolative behaviour. Modified MWCNT filled PDMS networks are prepared by using UV chemistry in a controlled two-step process. At first, pre-reacted mixtures of short chain PDMS with MWCNTs and long chain

PDMS with treated fumed silica are formed separately by reacting with deficient amount of crosslinker to avoid gelation. In the second step, these two pre-reacted clusters are covalently connected by using additional crosslinker.

5.2 Experimental

5.2.1 Materials

α,ω-vinyl terminated PDMS (DMS-V35 and DMS-V05) with $\bar{M}_n$ = 49500 g/mol and 800 g/mol, respectively, were purchased from Gelest Inc., USA. DMS-V35 and DMS-V05 are hereinafter mentioned as long chain and short chain PDMS, respectively. A (mercaptopropyl) methylsiloxane-dimethylsiloxane copolymer (GP 367) used as a six functional crosslinker was obtained from Genesee Polymers Corp., USA. Hexamethyldisilazane (HMDS) treated fumed silica (SIS6962) was purchased from Fluorochem, UK. Thin multiwalled carbon nanotubes (MWCNTs) (NANOCYL^{TM} NC7000) having average diameter of 9.5 nm and average length of 1.5 microns were obtained from Nanocyl s.a., Belgium. All other chemicals used in this study were purchased from Sigma-Aldrich and used as received.

5.2.2 Methods

Dispersion of MWCNTs was achieved by sonication using a sonication probe (UP200S, Hielscher – Ultrasound Technology, Germany, 200 W, 24 kHz) for 10 minutes. Mixing of the components required for the network formation was done in a SpeedMixer™ (DAC 150 FVZ, Hauschild Co., Germany) at 3500 rpm. Rheological tests were performed in a strain controlled rheometer (ARES G2) from TA Instruments, USA, with 25 mm parallel plate geometry. Measurement conditions were set to controlled strain mode at 2% strain, which was ensured to be within the linear viscoelastic region as determined from initial strain sweeps. Frequency sweep experiments were performed from

10^2 Hz to 10^{-3} Hz at 23°C. Dielectric relaxation spectroscopy (DRS) was performed on a Novocontrol Broadband Dielectric Spectrometer BDS-40 (Novocontrol Technologies GmbH & Co. KG, Germany) fitted with a Novocontrol Quattro Cryosystem temperature controller at 23°, 50°, 75°, 100°, 125° and 150°C operating in the frequency range 10^{-1}-10^6 Hz . Electrical break down tests were performed on an in-house built device based on international standards (IEC 60243-1 (1998) and IEC 60243-2 (2001)). The thicknesses of films (105-150 μm) were measured by optical microscopy of cross-sectional cuts. The film was placed in between the two spherical electrodes of radius 20 mm and the breakdown was measured at the point of contact with a stepwise increasing voltage (50-100 V/step) at a rate of 0.5-1 steps/s. Each sample was subjected to eight breakdown measurements and an average of these values was indicated as the breakdown strength of the sample.

5.2.2.1 Standard procedure for preparation of modified MWCNTs

Pristine MWCNTs (0.12 g) were dispersed in N-methyl pyrrolidone (NMP) (30 mL) by sonication for 15 minutes. (Mercaptopropyl)methylsiloxane-dimethylsiloxane copolymer (hexa functional crosslinker, 3600 g/mol, 0.15 g, 0.042 mmol, 0.24 mmol of thiol group) and 2,2-dimethyl-2-phenylacetophenone (DMPA) (photo initiator, 256.3 g/mol, 0.0029 g, 0.012 mmol) were added to the dispersed MWCNTs. Thereafter, short chain PDMS (0.86 g, 800 g/mol, 1.1 mmol, 2.6 mmol of vinyl groups) was added to give a stoichiometric imbalance of r ~ 0.1 and mixed in the SpeedMixer™ for 1 minute. The whole mixture was then added drop wise to methanol (about 500 mL) under stirring. Next, the methanol mixture was irradiated by ultraviolet (UV) light (λ=365 nm, 2 mW/cm^2) for 30 minutes under stirring to form pre-reacted short chain PDMS in presence of MWCNTs. The methanol mixture was then vacuum filtered using a 0.45 μm. poly (tetrafluoro ethylene) (PTFE) filter. The obtained modified MWCNTs were washed with ~100 mL methanol to remove any excess NMP. Washed modified MWCNTs were then left to dry at room temperature for three days.

Thermogravimetric analysis (TGA) was performed on the modified MWCNTs to determine the ratio of pre-reacted short chain and MWCNTs.

5.2.2.2 Standard procedure for preparation of silica filled PDMS reference material

(Mercaptopropyl)methylsiloxane-dimethylsiloxane copolymer (hexa functional crosslinker, 3600 g/mol, 0.15 g, 0.042 mmol, 0.24 mmol of thiol group) was mixed with DMPA in heptane (photo initiator, 0.5-0.6 mL, 0.036 mmol). Thereafter, 1 g treated fumed silica and α,ω-vinyl PDMS (3 g, 49500 g/mol, 0.061 mmol, 0.12 mmol of vinyl groups) was added to give an overall $r = 2$ where r is defined as $r = [\text{thiol}]/[\text{vinyl}] = f[\text{crosslinker}]/2[\text{PDMS}]$. The mixture was then mixed in the SpeedMixer™ for 2 minutes. The mixture was poured into a 4 cm × 3 cm × 1 cm steel mold placed over a glass plate lined with Parafilm® M. This setup was kept in a well-ventilated place for 30 minutes and subsequently transferred to the UV chamber (λ=365 nm, 4.5 mW/cm^2) and irradiated for 20 minutes in ambient atmosphere.

5.2.2.3 Standard procedure for preparation of PDMS composites containing 0.33 wt% modified MWCNTs

Six functional crosslinker (3600 g/mol, 0.0069 g, 0.0019 mmol, 0.011 mmol of thiol group) was mixed with DMPA in heptane (photo initiator, 0.5-0.6 mL, 0.036 mmol). Thereafter long chain PDMS (49500 g/mol, 3 g, 0.061 mmol, 0.12 mmol of vinyl group) and 1 g treated fumed silica (25 wt% relative to long chain) was added to give a stoichiometric imbalance of $r \sim 0.10$. The whole mixture was mixed in the SpeedMixer™ for 2 minutes and subsequently transferred to the UV chamber (λ=365 nm, 4.5 mW/cm^2) and irradiated for 20 minutes in ambient atmosphere. In the second step, treated fumed silica filled pre-reacted long chain PDMS was mixed with 0.024 g modified MWCNT containing 0.013 g MWCNT and 0.011 g pre-reacted short chain PDMS and 1-1.5 mL heptane. Next, additional six functional crosslinker (3600 g/mol, 0.13 g, 0.036 mmol, 0.21 mmol of

thiol group) and DMPA in heptane (photo initiator, 0.5-0.6 mL, 0.036 mmol) was added to give an overall stoichiometric imbalance $r = 1.5$. The mixture was then mixed in SpeedMixer™ for 2 minutes and then poured into a 4 cm × 3 cm × 1 cm steel mold placed over a glass plate lined with Parafilm® M. This setup was kept in a well-ventilated place for 30 minutes and subsequently transferred to the UV chamber (λ=365 nm, 4.5 mW/cm^2) and irradiated for 60 minutes (30 minutes from each side) in ambient atmosphere. Modified MWCNT contents were varied to create PDMS networks with different weight ratios of modified MWCNTs= 0.33%, 0.66% and 1%.

Addition of unmodified MWCNT in α,ω-vinyl terminated PDMS and subsequent curing by photochemical crosslinking of PDMS resulted in a partially crosslinked sample due to UV absorption capabilities of unmodified MWCNTs. Therefore, a commercially available platinum catalyzed two part addition curing PDMS (Elastosil RT625, Wacker Chemie AG, Germany) was used as a reference material containing 1wt % unmodified MWCNTs. Unmodified MWCNTs were at first dispersed in heptane prior to addition into the commercially available platinum catalyzed PDMS and the whole mixture was crosslinked subsequently to obtain MWCNT-PDMS reference sample.

5.3 Results and Discussion

5.3.1 Sample preparation and characterization

The aim of this work was to prepare sub percolative PDMS composites containing percolative amount of modified MWCNTs as DEAPs. For this, the first step involved modification of MWCNTs following the pathway as shown in Scheme 5.1.

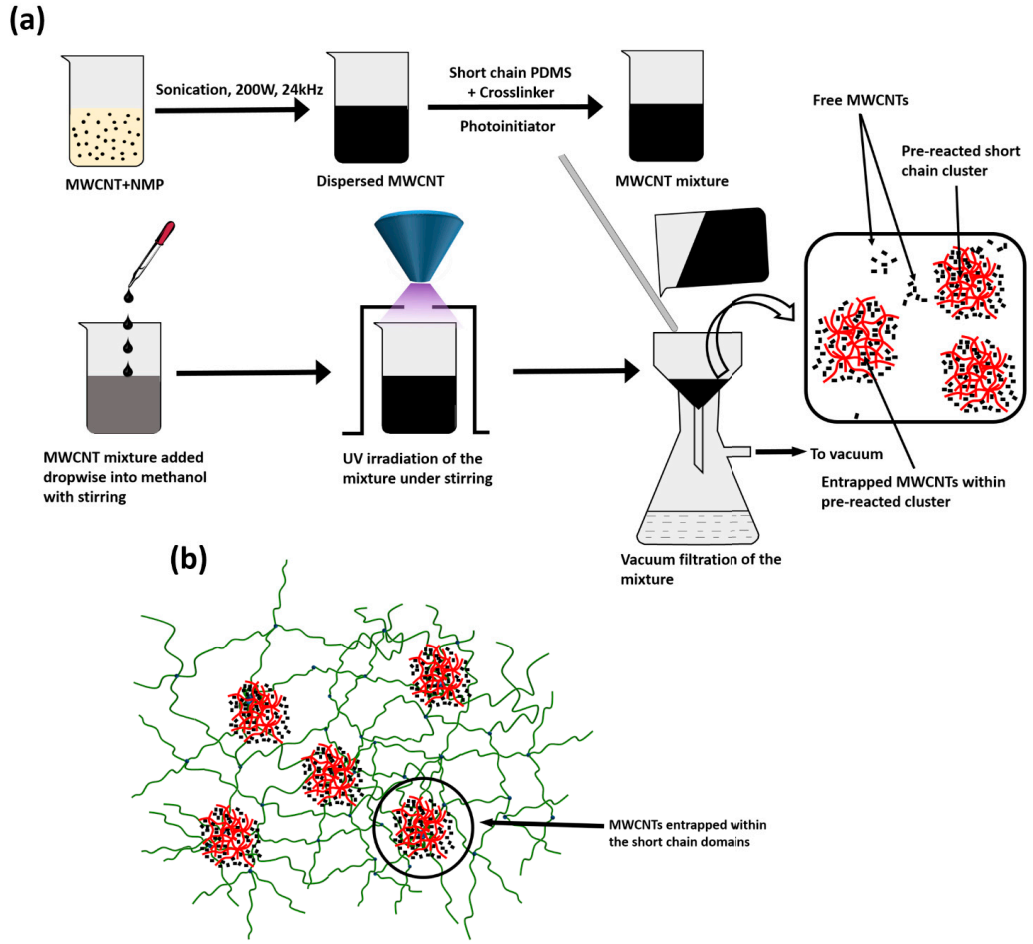

Scheme 5.1: (a) Schematic representation of the formation of modified MWCNTs (b) localized distribution of modified MWCNTs in the UV curable PDMS network

The first step of modification of MWCNTs involved precipitation of MWCNTs in methanol in presence of short chain PDMS, which were reacted with deficient amount of crosslinker below their gelation threshold to form pre-reacted mixtures. The critical stoichiometric ratio (r_c) at the gel point was calculated from the Flory-Stockmayer equation: $r_c = 1/(f-1)$, where f is the functionality of the crosslinker used. For the PDMS-crosslinker system used in this study, r_c was determined to be 0.2. To prevent premature gelation of the PDMS pre-reacted mixtures, r was kept at 0.1 which was found

from our previous study[107]. The modified MWCNTs were thereafter used as fillers for the long chain PDMS, which was crosslinked by the reaction scheme described in section 4.2.2.2 of chapter 4. The two step process of incorporating modified MWCNTs in the PDMS matrix is similar to the heterogeneous bimodal networks where the short chain domains were created within the long chain networks that gave controlled network structure [69,100].

Modified MWCNT content was determined from the total weight of the mixture containing polymer, modified MWCNT and treated fumed silica. Similarly in the treated fumed silica filled PDMS reference composite, silica content was calculated based on total weight of polymer and treated fumed silica. The compositions of modified MWCNT filled composites are summarized in Table 5.1.

Table 5.1: Compositions of PDMS networks filled with modified MWCNTs

Sample name	Modified MWCNT (wt%)	Treated fumed silica (wt%)
HPD_0	0	25
HPD_0.33	0.33	25
HPD_0.66	0.66	25
HPD_1	1	25

In a typical composition, HPD_X refers to 25 wt% treated fumed silica filled PDMS network with X wt% of modified MWCNTs. To study the effects of MWCNT modification on the dielectric nature of the prepared composites, a reference PDMS composite, PD_1, containing 1 wt% unmodified MWCNTs was studied along with the others.

5.3.2 Rheological measurement

Mechanical tests were performed on the prepared PDMS networks with and without modified MWCNTs in order to measure the linear viscoelastic (LVE) properties. Figure 5.1(a) shows the

storage modulus (G') and Figure 5.1(b) shows loss tangent (Tan delta) of the materials as a function of applied frequency.

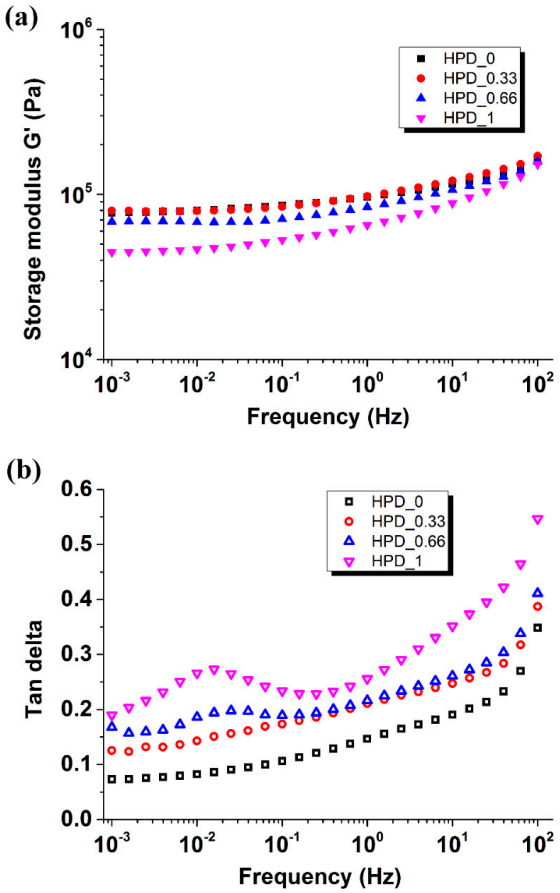

Figure 5.1: (a) Storage modulus (G') and (b) Tan delta as function of frequency for the prepared PDMS networks at 23°C

It is observed from Figure 5.1(a) that all the composites containing modified MWCNT exhibit a reduction in G' compared to the non-filled network HPD_0 in the studied frequency range. The decrease in G' is explained by a reduction in crosslink density imposed by the presence of large aspect ratio MWCNT fillers. A recent study on PDMS networks in presence of MWCNTs performed by

Li *et al.* [108] also showed a similar reduction in crosslink density of the composites due to destruction of network structures imposed by the long aspect ratio MWCNTs.

Damping behaviour of the composites can be seen in the Tan delta plots (Figure 5.1(b)). It is seen from Figure 5.1(b) that HPD_0.33, HPD_0.66 and HPD_1 show an increase in Tan delta in the investigated frequency range as the modified MWCNT content increases. At a frequency of ~ 10^{-2}Hz, an increase in Tan delta is observed for the modified MWCNT filled PDMS composites due to long relaxations exhibited by the long dangling chains. The dangling chains are formed by the destruction of network structure around the MWCNTs as seen by an increase in Tan delta with an increase in modified MWCNT content in Figure 5.1(a). The observed reduction in crosslink density increases with the increase in the amount of modified MWCNTs in the composites whereas no such effect is observed for HPD_0 due to the absence of the modified MWCNTs.

5.3.3 Dielectric spectroscopy

The dielectric properties of the composites were also investigated. Figure 5.2 shows storage permittivity (ε') and loss permittivity (ε'') of treated fumed silica filled PDMS networks with and without modified MWCNTs as a function of frequency at 23 °C.

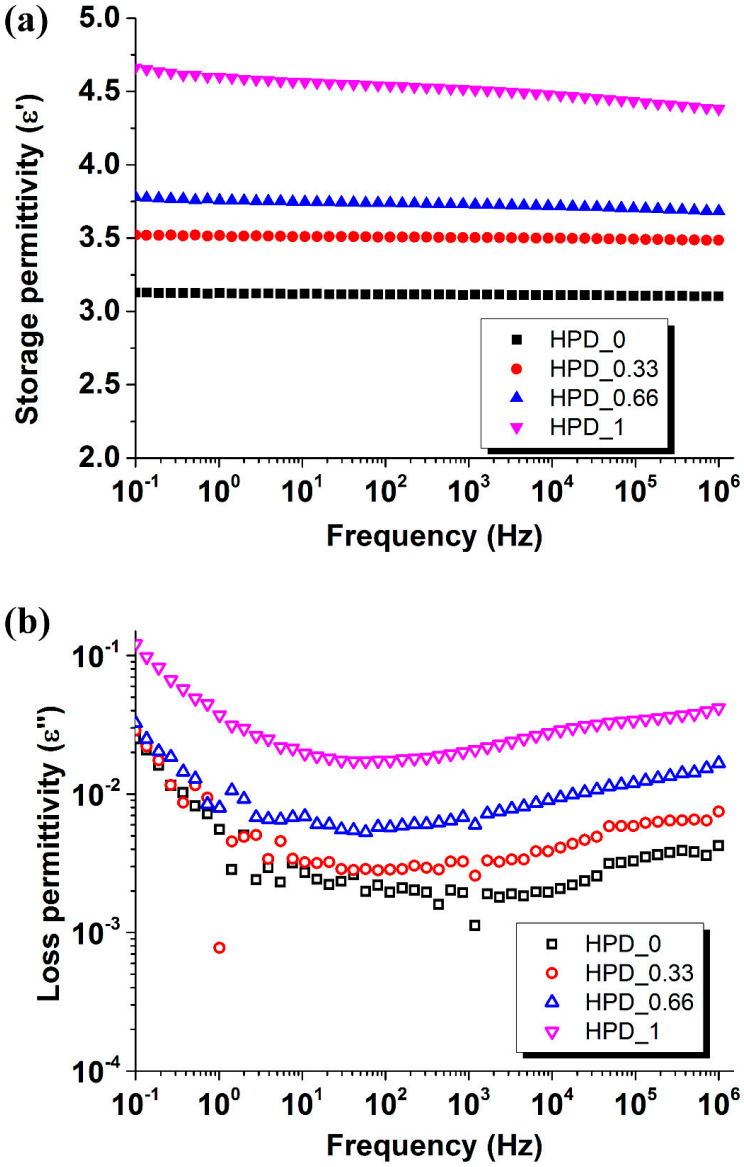

Figure 5.2: Dielectric relaxation spectroscopy data (a) storage permittivity and (b) loss permittivity as a function of frequency for PDMS composites at 23 °C.

It is seen from Figure 5.2(a) that the storage permittivity of the composites increases gradually with increasing modified MWCNT content and the highest storage permittivity is obtained for HPD_1 ($\varepsilon' = 4.7$ at 1 kHz) which is about 50% higher than HPD_0 ($\varepsilon' = 3.1$) at 1 kHz. The trend of increasing storage permittivity with the increase in modified MWCNT content in this study can be explained by the boundary capacitor model [109,110]. The MWCNTs can be considered as micro-capacitors, where the MWCNTs are separated by insulating PDMS. As the modified MWCNT content in the prepared composites increases, more micro-capacitors are formed leading to a higher permittivity of the composites as observed in Figure 5.2(a).

As seen in Figure 5.2(b), increasing the modified MWCNT content increases dielectric loss of all the composites in the low frequency range of 10^{-1}-10 Hz due to dipole relaxations [111] and Maxwell-Wagner polarizations[112]. In the medium frequency range, ($10^2 – 10^6$ Hz) HPD_0.33 and HPD_0.66 exhibit higher losses than HPD_0 due to the motion of highly mobile conducting electrons generated from the modified MWCNTs[113,114]. With the increase in modified MWCNT content, more closely spaced micro capacitors are formed which favors electron flow by means of tunneling effect and thus show higher losses in HPD_1[115].

5.3.4 Room temperature AC conductivity studies

The most vital requirement of DEAP transducers is the non-conductivity of the elastomers. Therefore, it is necessary to measure the effect of incorporating modified MWCNTs on the AC conductivities of the PDMS composites. Figure 5.3 shows frequency dependent real part of AC conductivities (σ') of the PDMS composites measured at 23°C as a function of modified MWCNT content.

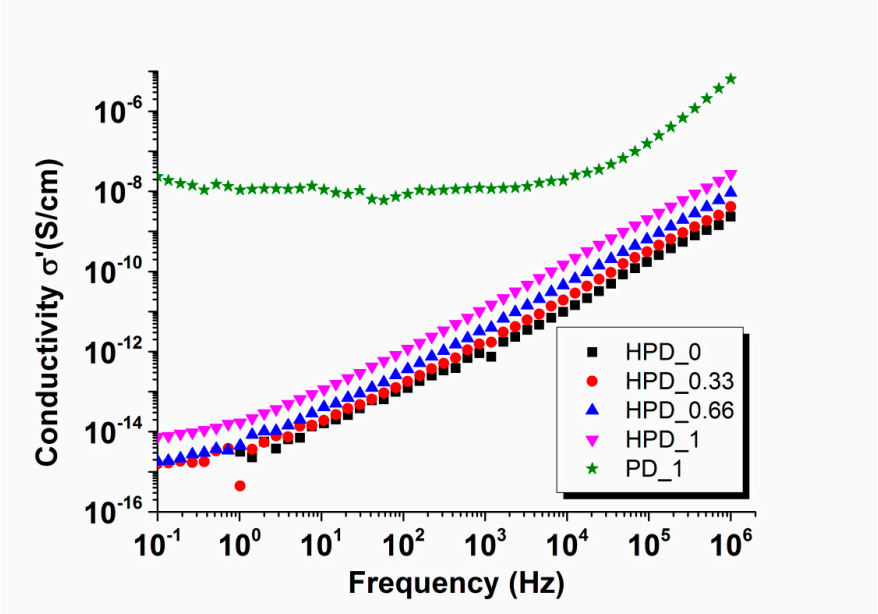

Figure 5.3: Variation of AC conductivities as a function of frequency for PDMS composites at 23°C.

From Figure 5.3 it is seen that the AC conductivity of HPD_0 increases with increasing frequency as is expected for an insulator material with a value of about 10^{-15} S/cm at 10^{-1} Hz. In the low frequency region (10^{-1}-1 Hz), HPD_0.33 and HPD_0.66 show non-conductive behaviour evident from frequency dependent σ' whereas HPD_1 exhibits signs of frequency independent σ' indicating conductive behaviour of the composite. Non-conductivities shown by HPD_0.33 and HPD_0.66 are due to localized distribution of the MWCNTs in the composites, that does not allow formation of any conductive paths across the sample volume. Whereas, PD_1 shows AC conductivities several decades higher than HPD_1 due to formation of conductive paths across the sample volume.

5.3.5 Dielectric breakdown study

Figure 5.4 shows dielectric breakdown strength and leakage current flowing through the sample as a function of modified MWCNT content in the PDMS composites.

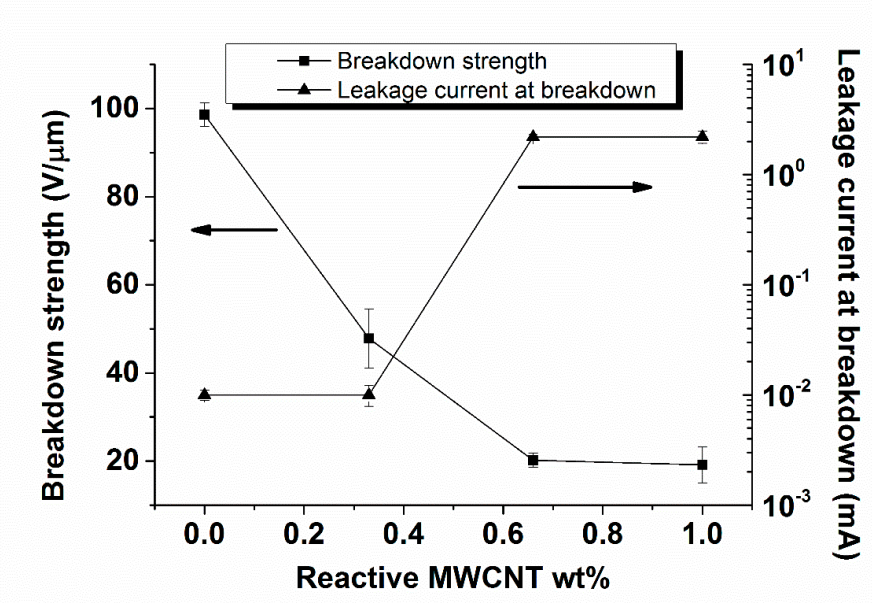

Figure 5.4: Variation of breakdown strength and leakage current of the PDMS composites as a function of modified MWCNT content. The reference sample PD_1 breaks down immediately due to the conductive nature.

From Figure 5.4 it is seen that there is a gradual reduction in breakdown strength from 100 V/μm in HPD_0 to 20 V/μm in HPD_1 and an increase in leakage current at breakdown in the composites as the modified MWCNT content is increased. The reduction in breakdown strength can be explained by easy flow of charges through the samples when modified MWCNTs in the composites is increased. In HPD_0 charges cannot flow due to absence of modified MWCNTs, hence a higher electric field is needed to induce electron avalanches[116], and thus the film possess high breakdown strength among the other PDMS composites examined in this study. Generation of heat during breakdown tests can lead to increased conductivities of polymer composites containing conductive or semi-conductive fillers [117]. This increase in conductivity leads to further increase in sample temperature due to Joule heating, which is proportional to electrical conductivity [118] until a point is reached where the

composites fail catastrophically due to electro thermal breakdown [119]. This strong influence of temperature and electric field dependency of electrical conductivity on electro thermal breakdown in PDMS films was also reported by Zakaria *et al.*[117].

5.3.6 Temperature dependent AC conductivity studies

To investigate more on premature breakdown of modified MWCNT filled PDMS composites, AC conductivities were measured at different temperatures as a function of applied frequency and the results obtained are presented in Figure 5.5.

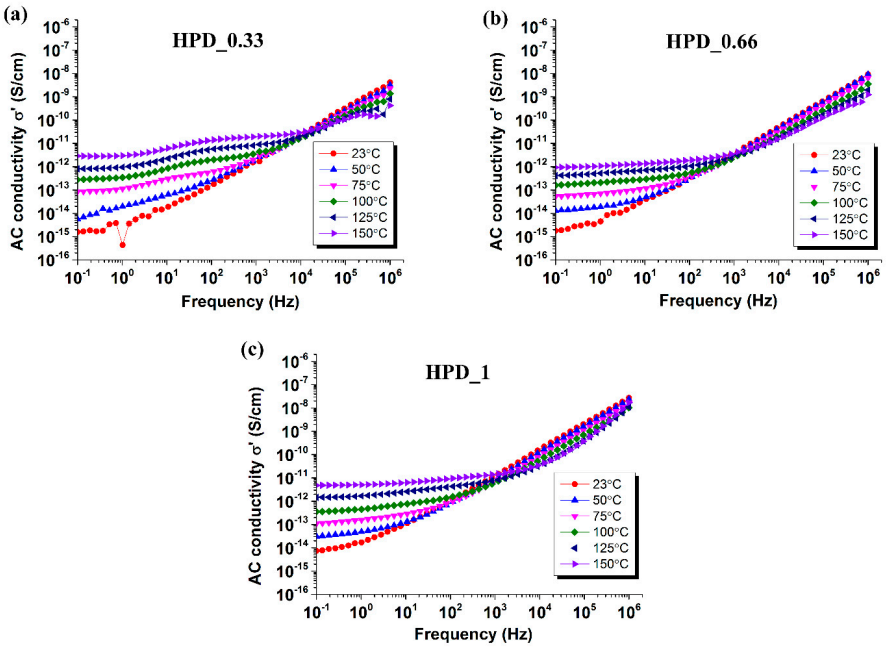

Figure 5.5:Temperature dependency of AC conductivities of (a) HPD_0.33 (b) HPD_0.66 (c) HPD_1 as a function of frequency.

From Figure 5.5, it is seen that the AC conductivities of all composites containing modified MWCNTs increase as the temperature is increased from 50 °C to 150 °C. HPD_0.33 (Figure 5.5(a))

shows non-conductive behaviour at 50 °C, evident from the frequency dependent AC conductivity in the entire frequency range. However, when temperature is increased to 75 °C, a frequency independent behaviour is observed at frequencies <1Hz, indicating a transition from a non-conductive to a conductive composite. Whereas, at 50 °C both HPD_0.66 and HPD_1 (Figure 5.5(b) and Figure 5.5(c), respectively) exhibit current conduction through the material that can also be seen in Figure 5.4 where leakage current flows through the material during breakdown test indicating non-dielectric nature of the composites. Further upon step-wise increase in temperature from 75 °C to 150 °C all composites (HPD_0.33, HPD_0.66 and HPD_1) show increased conductivities indicated by an upward shift of the AC conductivities at frequencies <1 Hz which indicates strong influence of temperature on AC conductivities of the composites. The increase in AC conductivities is due to increased thermal emission of electrons between two separated MWCNTs when temperature is increased [120]. Strong influence of temperature on AC conductivities of the composites is shown in Figure 5.5. During electrical breakdown tests heat generated within the film cannot be dissipated sufficiently and thereby leads to an increase in film temperature, which leads to electro thermal breakdown of the PDMS composites due to increased conductivity of the films. Therefore, it is clear that the results obtained in electrical breakdown tests are influenced by increased temperature of the sample that leads to increase in conductivity and decreased breakdown strength with increasing modified MWCNT content[117].

5.4 Conclusion

The study shows a novel method of modifying MWCNTs, which is used to prepare PDMS composites exhibiting sub percolative behaviour at room temperature with percolative content of MWCNTs. Modified MWCNT filled PDMS networks are obtained by using UV chemistry in a controlled two-step process. Shear rheology showed a gradual reduction in G' and an increase in Tan delta as the modified MWCNT content was increased in the composites due to destruction of network structure

around the MWCNTs. Storage permittivity of the composites increased from 3.1 to 4.7 at 1 kHz as the modified MWCNT content was increased from 0 to 1 wt%. AC conductivity studies at 23°C revealed that HPD_0.33 and HPD_0.66 exhibited non-conductive behaviour whereas HPD_1 showed signs of conductive behaviour of the composite. Modified MWCNT-PDMS composites showed decrease in dielectric breakdown strength from 100 V/μm to 20 V/μm as the modified MWCNT content was increased from 0 to 1wt%. Temperature dependent AC conductivity studies revealed that increase in conductivities of the composites with temperature lead to premature electro thermal breakdown when the modified MWCNT loading was above 0.66 wt%. Therefore it has been demonstrated that AC conductivities of elastomers filled with semi conductive fillers possess strong dependence on temperature. When these composites are used in high voltage operations such as DEAP transducers, an accelerating effect is observed where an increase in sample temperature causes an increase in conductivity and vice versa that leads to premature breakdown of the film. Therefore, in order to characterize such composites as probable candidates for DEAP transducers, it is desirable to obtain a thorough knowledge by studying conductivities of the composites at several different temperatures.

Chapter 6

Conclusion

6.1 Summary and concluding remarks

The goal of this Ph.D. project has been preparation and characterizations of high permittivity UV cured soft elastomeric networks and composites applicable as DEAP actuators.

Simultaneous IPNs were prepared using two non-interfering chemical reactions for crosslinking PPGs of two different molecular weights having vinyl (PPG-V) and hydroxyl (PPG-OH) end groups. PPG-OH was cross-linked using an isocyanate type cross-linker via a tin-catalyzed reaction while PPG-V was cross-linked by UV induced thiol-ene reactions in presence of a tetra-functional thiol crosslinker and a photo initiator. Mechanical characterizations of PPG IPNs revealed enhancement of elastic modulus and tendency towards lower viscous losses compared to the pure networks as a result of the stabilized morphology of the interconnected networks. Thus the improved mechanical properties exhibited by this new non-acrylic based PPG IPNs could be used to overcome the mandatory requirement of pre-straining which is a limitation of VHB acrylics used as DEAPs. Moreover, the relative permitivitties in medium to high frequency range for both the PPG homo networks and the prepared IPNs, were found to be about 67% higher than the widely used pure or fumed silica reinforced PDMS elastomers as applied to DEAP actuators[79]. However, due to the requirement of long curing time it was judged that it would be difficult to prepare the IPNs by suitable industrial processes and therefore the IPNs were not further investigated. The study also revealed that the pure vinyl terminated PPG (hereafter mentioned as PPO) networks exhibited excellent relative permittivity, reduced viscous and dielectric losses but possessed poor mechanical stabilities.

Treated fumed silica was incorporated into the otherwise weak pure PPO networks to improve its mechanical properties. The positive effects of silica reinforcement were clearly visible both by shear rheology and by uniaxial stress-strain measurements in terms of increased elastic modulus and maximum elongation, respectively. When compared to commonly used acrylic VHB elastomers, the new PPO composites showed a marked improvement in terms of significantly low viscous losses, higher relative permittivity and comparable actuation behaviour at low filler loadings. However, PPO elastomeric composites showed significant stickiness which posed as challenge when handling thin films. No further attempts were made for reducing the stickiness of PPO networks by increasing filler concentrations since highly loaded PPO networks showed reduced actuation strains and it was decided to focus on PDMS instead.

UV induced thiol-ene "click" chemistry was successfully established to crosslink vinyl terminated PDMS. The fast and efficient UV curing method eliminated the use of platinum catalyst, which otherwise plays vital role in addition curing of vinyl terminated PDMS. Two different types of network structures were prepared, either by employing a single step (one step network) or an advanced sequential mixing (two step network). Extensive rheological studies conducted on both the networks showed that the prepared networks possessed lower elastic modulus when compared to the literature reported platinum catalyzed addition cured PDMS networks. Additionally the two step networks possessed lower viscous losses than the one step network. This was attributed to the presence of short chain PDMS domains acting as reinforcements within the long chain networks. Curing kinetics study was carried out to determine the development of the mechanical properties of both the networks after UV exposure. There again, the more controlled two steps network showed faster curing than the one step network.

In order to improve relative permittivity of PDMS a unique method of MWCNT incorporation was successfully demonstrated. Pre-reacted short chain PDMS layers were formed on MWCNTs when the mixture containing dispersed MWCNTs and short chain PDMS were exposed to UV radiation in presence of deficient amount of hexa functional thiol PDMS crosslinker and a photoinitiator. These pre-reacted short chain PDMS encapsulated MWCNTs (modified MWCNTs) were then used as fillers in the long chain PDMS and crosslinked subsequently via UV induced thiol-ene reactions. The composites were designed to contain loadings of MWCNT above the percolation threshold without becoming conductive which was confirmed by room temperature AC conductivity studies and attributed to a localized distribution of MWCNTs. The composites showed a decrease in elastic modulus, increase in relative permittivities and a decrease in breakdown strength with increasing content of modified MWCNTs. Temperature dependent AC conductivity studies revealed that due to an accelerating effect, an increase in the sample temperature led to an increase in sample conductivities and vice versa which caused premature breakdown of the composites.

Considering all the steps taken into the realization of the project objectives for developing elastomeric materials having high relative permittivity, low elastic modulus along with low viscous and dielectric losses applicable as DEAP actuators, this thesis showed that

- a novel non-acrylic PPG/PPO elastomer was identified and developed with properties specific for application as DEAP actuators. Both PPG IPNs and filled PPO networks showed improved elastic modulus, high relative permittivities, low viscous and dielectric losses thus overcoming some of the drawbacks of commercially available DEAP actuator materials namely VHB acrylics and silicone elastomers.
- Platinum free UV cured PDMS soft elastomeric networks were successfully prepared. Two step networks formed by advanced mixing sequence showed better control over network

formation which was reflected in a lower elastic modulus and lower viscous losses than the one step network and other platinum cured PDMS networks.

- Overall increase in relative permittivity of PDMS networks were obtained by preparing modified MWCNTs-PDMS composites. Unique modification method allowed incorporation of percolative content of MWCNTs without making the composites conductive due to localized distribution of MWCNTs. The composites also showed low elastic modulus and low viscous and dielectric losses.

The properties of the elastomeric materials developed throughout this project comply well with the overall objectives and thus can be considered as potential DEAPs.

6.2 Future work and outlook

In this section, future possibilities and recommendations derived from the work conducted in the thesis are outlined.

Stickiness of PPO networks posed a challenge while handling thin films. Increasing filler concentration in PPO networks substantially reduced the stickiness although at the cost of poor actuation strain due to stiffening of the films. At this point an alternative approach of reducing stickiness of PPO networks could be done by forming bimodal networks composed of short and long chains of PPO where the networks are expected to show reduced viscous losses due to lower tendency towards formation of network irregularities. On the other hand stickiness could be used as a positive quality of PPO networks in the field of multilayered stacked actuator configuration. VHB acrylics are most commonly used in stacked actuator configurations due to the stickiness of the films which is a prime requirement for maintaining structural integrity of the actuator devices. Since VHB exhibits

high viscous losses and requires pre-strain for better actuation performances, PPO networks could be used as an alternative to VHB in the field of stacked actuators.

While preparing MWCNT filled UV curable PDMS composites, it was observed that at high MWCNT loadings, crosslinking was difficult to achieve as MWCNTs block UV radiation. An alternative approach could be to use thermal curing, initiated by microwave to prepare MWCNT filled PDMS composites where an electromagnetic field is applied to the material which results in rapid and uniform heating throughout the sample[121–123]. AC conductivity studies performed on the modified MWCNT filled UV curable PDMS composites revealed a strong relationship between conductivity and sample temperature. Therefore thermal effects on conductivities of the composites containing conductive or semi conductive fillers as potential DEAPs should be thoroughly investigated, since increase in sample temperature during high voltage operations can lead to premature breakdown of composites due to increased conductivity of elastomers.

Bibliography

[1] Pelrine, R., Kornbluh, R., and Kofod, G., "High-Strain Actuator Materials Based on Dielectric Elastomers," Advanced Materials 12(16), 1223–1225 (2000).

[2] Madden, J.D.W., [Dielectric elastomers as high-performance electroactive polymers] , in Dielectr. elastomers as electromechanical transducers, F. Carpi, D. De Rossi, R. Kornbluh, R. Pelrine, and P. Sommer-Larsen, Eds., Elsevier, Amsterdam, 13–21 (2008).

[3] Kofod, G., "Dielectric elastomer actuators," in Tech. Univ. Denmark, Ph. D. thesis(September), Technical University of Denmark, Denmark, pp. 1–132 (2001).

[4] Chiba, S., Waki, M., Kornbluh, R., and Pelrine, R., "Innovative power generators for energy harvesting using electroactive polymer artificial muscles," in Proc. SPIE 6927, Y. Bar-Cohen, Ed., 692715–1–9 (2008).

[5] Chiba, S., Waki, M., Wada, T., Hirakawa, Y., Masuda, K., and Ikoma, T., "Consistent ocean wave energy harvesting using electroactive polymer (dielectric elastomer) artificial muscle generators," Applied Energy 104, 497–502 (2013).

[6] Rosenthal, M., Bonwit, N., Duncheon, C., and Heim, J., "Applications of dielectric elastomer EPAM sensors," in Proc. SPIE 6524, Y. Bar-Cohen, Ed., 65241F–1–7 (2007).

[7] Akbari, S., Rosset, S., and Shea, H.R., "More than 10-fold increase in the actuation strain of silicone dielectric elastomer actuators by applying prestrain," in Proc. SPIE 8687, Y. Bar-Cohen, Ed., 86871P–1–13 (2013).

[8] Schlaak, H.F., Jungmann, M., Matysek, M., and Lotz, P., "Novel multilayer electrostatic solid state actuators with elastic dielectric," in Proc. SPIE, Y. Bar-Cohen, Ed., 121–133 (2005).

[9] Kovacs, G., Düring, L., Michel, S., and Terrasi, G., "Stacked dielectric elastomer actuator for tensile force transmission," Sensors and Actuators A: Physical 155(2), 299–307 (2009).

[10] Bar-Cohen, Y., "Electroactive polymer (EAP) actuators for future humanlike robots," in Proc. SPIE 7287, Y. Bar-Cohen and T. Wallmersperger, Eds., 728703–1–6 (2009).

[11] Matysek, M., Lotz, P., Winterstein, T., and Schlaak, H.F., "Dielectric elastomer actuators for tactile displays," in World Haptics 2009 - Third Jt. EuroHaptics Conf. Symp. Haptic Interfaces Virtual Environ. Teleoperator Syst., 290–295 (2009).

[12] Jungmann, M., and Schlaak, H.F., "Miniaturised electrostatic tactile display with high structural compliance," in Proc. Conf. Eurohaptics, 12–17 (2002).

[13] Webpage, “Bayer Material Science,” http://www.vivitouch.com, 2011.

[14] Yu, L., Gonzalez, L.B., Hvilsted, S., and Skov, A.L., “Soft silicone based interpenetrating networks as materials for actuators,” in Proc. SPIE 9056, Y. Bar-Cohen, Ed., 90560C–1–9 (2014).

[15] Pelrine, R., and Kornbluh, R., [Electromechanical transduction effects in dielectric elastomers: actuation, sensing, stiffness modulation and electric energy generation] , in Dielectr. elastomers as electromechanical transducers, F. Carpi, D. De Rossi, R. Kornbluh, R. Pelrine, and P. Sommer-Larsen, Eds., Elsevier, Amsterdam, 1–12 (2008).

[16] De Tommasi, D., Puglisi, G., and Saccomandi, G., “A micromechanics-based model for the Mullins effect,” Journal of Rheology 50(4), 495–512 (2006).

[17] Cantournet, S., Desmorat, R., and Besson, J., “Mullins effect and cyclic stress softening of filled elastomers by internal sliding and friction thermodynamics model,” International Journal of Solids and Structures 46(11-12), 2255–2264 (2009).

[18] Sommer-Larsen, P., and Larsen, A.L., “Materials for dielectric elastomer actuators,” in Proc. SPIE 5385, Y. Bar-Cohen, Ed., 68–77 (2004).

[19] Vudayagiri, S., Junker, M.D., and Skov, A.L., “Factors affecting the surface and release properties of thin polydimethylsiloxane films,” Polymer Journal 45(8), 871–878 (2013).

[20] Pelrine, R., Kornbluh, R., Pei, Q., and Joseph, J., “High-speed electrically actuated elastomers with strain greater than 100%,” Science 287(5454), 836–839 (2000).

[21] Sheng, J., Chen, H., Li, B., and Chang, L., “Temperature dependence of the dielectric constant of acrylic dielectric elastomer,” Applied Physics A511–515 (2012).

[22] Jean-Mistral, C., Sylvestre, A., Basrour, S., and Chaillout, J.-J., “Dielectric properties of polyacrylate thick films used in sensors and actuators,” Smart Materials and Structures 19(7), 075019–1–9 (2010).

[23] Kofod, G., Sommer-Larsen, P., Kornbluh, R., and Pelrine, R., “Actuation Response of Polyacrylate Dielectric Elastomers,” Journal of Intelligent Materials Systems and Structures 14(12), 787–793 (2003).

[24] Wissler, M., and Mazza, E., “Mechanical behavior of an acrylic elastomer used in dielectric elastomer actuators,” Sensors and Actuators A: Physical 134(2), 494–504 (2007).

[25] Skov, A.L., Vudayagiri, S., and Benslimane, M., “Novel silicone elastomer formulations for DEAPs,” in Proc. SPIE 8687, Y. Bar-Cohen, Ed., 86871I–1–8 (2013).

[26] Galantini, F., Carpi, F., and Gallone, G., “Effects of plasticization of a soft silicone for dielectric elastomer actuation,” Smart Materials and Structures 22(10), 104020–1–7 (2013).

[27] Benslimane, M.Y., Kiil, H.-E., and Tryson, M.J., "Dielectric electro-active polymer push actuators: performance and challenges," Polymer International 59(3), 415–421 (2010).

[28] Kussmaul, B., Risse, S., Kofod, G., Waché, R., Wegener, M., McCarthy, D.N., Krüger, H., and Gerhard, R., "Enhancement of dielectric permittivity and electromechanical response in silicone elastomers: Molecular grafting of organic dipoles to the macromolecular network," Advanced Functional Materials 21(23), 4589–4594 (2011).

[29] Carpi, F., Gallone, G., Galantini, F., and De Rossi, D., "Silicone–Poly(hexylthiophene) Blends as Elastomers with Enhanced Electromechanical Transduction Properties," Advanced Functional Materials 18(2), 235–241 (2008).

[30] Ueda, T., Kasazaki, T., Kunitake, N., Hirai, T., Kyokane, J., and Yoshino, K., "Polyurethane elastomer actuator," Synthetic Metals 85(1-3), 1415–1416 (1997).

[31] Jo, N.-J., Lim, D.-H., Bark, G.-M., Chun, H.-H., Lee, I.-W., and Park, H., "Polyurethane-based actuators with various polyols," Journal of Materials Science & Technology 26(8), 763–768 (2010).

[32] Jung, K., Lee, J., Cho, M., Koo, J.C., Nam, J., Lee, Y., and Choi, H.R., "Development of enhanced synthetic elastomer for energy-efficient polymer actuators," Smart Materials and Structures 16(2), S288–S294 (2007).

[33] Cheng, Z.-Y., Bharti, V., Xu, T.-B., Xu, H., Mai, T., and Zhang, Q.M., "Electrostrictive poly(vinylidene fluoride-trifluoroethylene) copolymers," Sensors and Actuators A: Physical 90(1-2), 138–147 (2001).

[34] Pei, Q., Pelrine, R.E., and Kornbluh, R.D., "Electroactive polymers," U.S. Patent No. 09/619,847, Google Patents, US (2004).

[35] Kofod, G., Stoyanov, H., Kollosche, M., Risse, S., Ragusch, H., McCarthy, D.N., Waché, R., Rychkov, D., and Dansachmüller, M., "Molecular level materials design for improvements of actuation properties of dielectric elastomer actuators," in Proc. SPIE 7976, Y. Bar-Cohen and F. Carpi, Eds., 79760J–1–12 (2011).

[36] Ha, S.M., Yuan, W., Pei, Q., Pelrine, R., and Stanford, S., "Interpenetrating networks of elastomers exhibiting 300% electrically-induced area strain," Smart Materials and Structures 16(2), S280–S287 (2007).

[37] Pei, Q., Pelrine, R., Rosenthal, M.A., Stanford, S., Prahlad, H., and Kornbluh, R.D., "Recent progress on electroelastomer artificial muscles and their application for biomimetic robots," in Proc. SPIE 5385, Y. Bar-Cohen, Ed., 41–50 (2004).

[38] Palakodeti, R., and Kessler, M.R., "Influence of frequency and prestrain on the mechanical efficiency of dielectric electroactive polymer actuators," Materials Letters 60(29-30), 3437–3440 (2006).

[39] Brochu, P., and Pei, Q., “Advances in dielectric elastomers for actuators and artificial muscles,” Macromolecular Rapid Communications 31(1), 10–36 (2010).

[40] Ha, S.M., Yuan, W., Pei, Q., Pelrine, R., and Stanford, S., “Interpenetrating Polymer Networks for High-Performance Electroelastomer Artificial Muscles,” Advanced Materials 18(7), 887–891 (2006).

[41] Ha, S.M., Park, I.S., Wissler, M., Pelrine, R., Stanford, S., Kim, K.J., Kovacs, G., and Pei, Q., “High Electromechanical Performance of Electroelastomers Based on Interpenetrating Polymer Networks,” in Proc. SPIE 6927, Y. Bar-Cohen, Ed., 69272C–1–9 (2008).

[42] Ha, S.M., Yuan, W., Pei, Q., Pelrine, R., and Stanford, S., “New high-performance electroelastomer based on interpenetrating polymer networks,” in Proc. SPIE 6168, Y. Bar-Cohen, Ed., 616808–1–12 (2006).

[43] Biggs, J., Danielmeier, K., Hitzbleck, J., Krause, J., Kridl, T., Nowak, S., Orselli, E., Quan, X., Schapeler, D., et al., “Electroactive polymers: developments of and perspectives for dielectric elastomers.,” Angewandte Chemie (International ed. in English) 52(36), 9409–9421 (2013).

[44] Fawcett, A.S., Grande, J.B., and Brook, M. a., “Rapid, metal-free room temperature vulcanization produces silicone elastomers,” Journal of Polymer Science Part A: Polymer Chemistry 51(3), 644–652 (2013).

[45] Decker, C., “Kinetic Study and New Applications of UV Radiation Curing,” Macromolecular Rapid Communications 23(18), 1067–1093 (2002).

[46] Hoyle, C.E., and Bowman, C.N., “Thiol-ene click chemistry.,” Angewandte Chemie (International ed. in English) 49(9), 1540–73 (2010).

[47] Lowe, A.B., “Thiol-ene ‘click’ reactions and recent applications in polymer and materials synthesis,” Polymer Chemistry 1(1), 17–36 (2010).

[48] Wu, Y., Zhao, X., Li, F., and Fan, Z., “Evaluation of Mixing Rules for Dielectric Constants of Composite Dielectrics by MC-FEM Calculation on 3D Cubic Lattice,” Journal of Electroceramics 11(3), 227–239 (2003).

[49] Wakino, K., “A new proposal on mixing rule of the dielectric constant of mixture,” in Proc. 1994 IEEE Int. Symp. Appl. Ferroelectr., 33–38 (1847).

[50] Gallone, G., Carpi, F., De Rossi, D., Levita, G., and Marchetti, A., “Dielectric constant enhancement in a silicone elastomer filled with lead magnesium niobate–lead titanate,” Materials Science and Engineering: C 27(1), 110–116 (2007).

[51] Carpi, F., and De Rossi, D., “Improvement of electromechanical actuating performances of a silicone dielectric elastomer by dispersion of titanium dioxide powder,” IEEE Transactions on Dielectrics and Electrical Insulation 12(4), 835–843 (2005).

[52] Szabo, J.P., Hiltz, J.A., Cameron, C.G., Underhill, R.S., Massey, J., White, B., and Leidner, J., "Elastomeric composites with high dielectric constant for use in Maxwell stress actuators," in Proc. SPIE 5051, Y. Bar-Cohen, Ed., 180–190 (2003).

[53] Yu, L., Vudayagiri, S., Zakaria, S., Benslimane, M.Y., and Skov, A.L., "Filled liquid silicone rubbers: possibilities and challenges," in Proc. SPIE 9056, Y. Bar-Cohen, Ed., 90560S–1–9 (2014).

[54] Liu, B., and Shaw, M.T., "Electrorheology of filled silicone elastomers," Journal of Rheology 45(3), 641–657 (2001).

[55] Khastgir, D., and Adachi, K., "Piezoelectric and dielectric properties of siloxane elastomers filled with bariumtitanate," Journal of Polymer Science Part B: Polymer Physics 37(21), 3065–3070 (1999).

[56] Kofod, G., McCarthy, D.N., Stoyanov, H., Kollosche, M., Risse, S., Ragusch, H., Rychkov, D., Dansachmüller, M., and Waché, R., "Materials science on the nano-scale for improvements in actuation properties of dielectric elastomer actuators," in Proc. SPIE 7642(2), Y. Bar-Cohen, Ed., 76420J–1–12 (2010).

[57] Stoyanov, H., Kollosche, M., McCarthy, D., Becker, A., Risse, S., and Kofod, G., "Sub-percolative composites for dielectric elastomer actuators," in Proc. SPIE 7493, J. Leng, A. K. Asundi, and W. Ecke, Eds., 74930Q–1–8 (2009).

[58] Matsumoto, M., and Miyata, Y., "Complex permittivity based on equivalent circuit model for polymer/metal composite. Frequency dependence of permittivity as function of concentration," IEEE Transactions on Dielectrics and Electrical Insulation 6(1), 27–34 (1999).

[59] Iijima, S., "Helical microtubules of graphitic carbon," Nature 354(6348), 56–58 (1991).

[60] Baughman, R.H., Zakhidov, A.A., and de Heer, W.A., "Carbon nanotubes--the route toward applications.," Science (New York, N.Y.) 297(5582), 787–92 (2002).

[61] Galantini, F., Bianchi, S., Castelvetro, V., and Gallone, G., "Functionalized carbon nanotubes as a filler for dielectric elastomer composites with improved actuation performance," Smart Materials and Structures 22(5), 055025–1–10 (2013).

[62] Cameron, C.G., Underhill, R.S., Rawji, M., and Szabo, J.P., "Conductive filler: elastomer composites for Maxwell stress actuator applications," in Proc. SPIE 5385, Y. Bar-Cohen, Ed., 51–59 (2004).

[63] Zhang, X., Wissler, M., Jaehne, B., Breonnimann, R., and Kovacs, G., "Effects of crosslinking, prestrain and dielectric filler on the electromechanical response of a new silicone and comparison with acrylic elastomer," Proceedings of SPIE 5385(0), 78–86 (2004).

[64] Chwang, C.-P., Liu, C.-D., Huang, S.-W., Chao, D.-Y., and Lee, S.-N., "Synthesis and characterization of high dielectric constant polyaniline/polyurethane blends," Synthetic Metals 142(1-3), 275–281 (2004).

[65] Molberg, M., Crespy, D., Rupper, P., Nüesch, F., Månson, J.-A.E., Löwe, C., and Opris, D.M., "High Breakdown Field Dielectric Elastomer Actuators Using Encapsulated Polyaniline as High Dielectric Constant Filler," Advanced Functional Materials 20(19), 3280–3291 (2010).

[66] Butkewitsch, S., and Scheinbeim, J., "Dielectric properties of a hydrated sulfonated poly(styrene–ethylene/butylenes–styrene) triblock copolymer," Applied Surface Science 252(23), 8277–8286 (2006).

[67] Lehmann, W., Skupin, H., Tolksdorf, C., Gebhard, E., Zentel, R., Krüger, P., Lösche, M., and Kremer, F., "Giant lateral electrostriction in ferroelectric liquid-crystalline elastomers.," Nature 410(6827), 447–450 (2001).

[68] Madsen, F.B., Daugaard, A.E., Hvilsted, S., Benslimane, M.Y., and Skov, A.L., "Dipolar cross-linkers for PDMS networks with enhanced dielectric permittivity and low dielectric loss," Smart Materials and Structures 22(10), 104002–1–11 (2013).

[69] Bejenariu, A.G., Yu, L., and Skov, A.L., "Low moduli elastomers with low viscous dissipation," Soft Matter 8(14), 3917–3923 (2012).

[70] Mark, J.E., "Molecular aspects of rubberlike elasticity," Accounts of Chemical Research 18(7), 202–206 (1985).

[71] Wang, S., and Mark, J.E., "Unimodal and bimodal networks of poly(dimethyl-siloxane) in pure shear," Journal of Polymer Science Part B: Polymer Physics 30(8), 801–807 (1992).

[72] Sperling, L.H., [Interpenetrating Polymer Networks: An Overview] , in Interpenetr. Polym. Networks, D. Klempner, L. H. Sperling, and L. A. Utracki, Eds., American Chemical Society, Washington, DC, 3–38 (1994).

[73] Mathew, G., Rhee, J., Nah, C., and Leo, D., "Effects of silicone rubber on properties of dielectric acrylate elastomer actuator," Polymer Engineering & Science 46(10), 1455–1460 (2006).

[74] Plesse, C., Khaldi, A., Wang, Q., Cattan, E., Teyssié, D., Chevrot, C., and Vidal, F., "Polyethylene oxide–polytetrahydrofurane–PEDOT conducting interpenetrating polymer networks for high speed actuators," Smart Materials and Structures 20(12), 124002–1–8 (2011).

[75] Brandell, D., Kasemägi, H., and Aabloo, A., "Poly(ethylene oxide)–poly(butadiene) interpenetrated networks as electroactive polymers for actuators: A molecular dynamics study," Electrochimica Acta 55(4), 1333–1337 (2010).

[76] Plesse, C., Vidal, F., Randriamahazaka, H., Teyssié, D., and Chevrot, C., "Synthesis and characterization of conducting interpenetrating polymer networks for new actuators," Polymer 46(18), 7771–7778 (2005).

[77] Plesse, C., Vidal, F., Gauthier, C., Pelletier, J.-M., Chevrot, C., and Teyssié, D., "Poly(ethylene oxide)/polybutadiene based IPNs synthesis and characterization," Polymer 48(3), 696–703 (2007).

[78] Cai, Z., and Kim, J., "Cellulose-chitosan interpenetrating polymer network for electro-active paper actuator," Journal of Applied Polymer Science 114(1), 288–297 (2009).

[79] Skov, A.L., Bejenariu, A., Bøgelund, J., Benslimane, M., and Daugaard, A.E., "Influence of micro- and nanofillers on electro-mechanical performance of silicone EAPs," in Proc. SPIE 8340, Y. Bar-Cohen, Ed., 83400M–1–10 (2012).

[80] Larsen, A.L., Hansen, K., Sommer-Larsen, P., Hassager, O., Bach, A., Ndoni, S., and Jørgensen, M., "Elastic properties of nonstoichiometric reacted PDMS networks," Macromolecules 36(26), 10063–10070 (2003).

[81] Carpi, F., Gallone, G., Galantini, F., and De Rossi, D., [Enhancing the dielectric permittivity of elastomers] , in Dielectr. elastomers as electromechanical transducers, F. Carpi, D. De Rossi, R. Kornbluh, R. Pelrine, and P. Sommer-Larsen, Eds., Elsevier, Amsterdam, 51–68 (2008).

[82] Jensen, M.K., Bach, A., Hassager, O., and Skov, A.L., "Linear rheology of cross-linked polypropylene oxide as a pressure sensitive adhesive," International Journal of Adhesion and Adhesives 29(7), 687–693 (2009).

[83] Jensen, M.K., Hassager, O., Rasmussen, H.K., Skov, A.L., Bach, A., and Koldbech, H., "Planar elongation of soft polymeric networks," Rheologica Acta 49(1), 1–13 (2009).

[84] Frankær, S.M.G., Jensen, M.K., Bejenariu, A.G., and Skov, A.L., "Investigation of the properties of fully reacted unstoichiometric polydimethylsiloxane networks and their extracted network fractions," Rheologica Acta 51(6), 559–567 (2012).

[85] Website, "www.3M.com."

[86] Molberg, M., Leterrier, Y., Plummer, C.J.G., Walder, C., Löwe, C., Opris, D.M., Nüesch, F.A., Bauer, S., and Månson, J.-A.E., "Frequency dependent dielectric and mechanical behavior of elastomers for actuator applications," Journal of Applied Physics 106(5), 054112–1–7 (2009).

[87] Gallone, G., Galantini, F., and Carpi, F., "Perspectives for new dielectric elastomers with improved electromechanical actuation performance: composites versus blends," Polymer International 59(3), 400–406 (2010).

[88] Ozmusul, M.S., and Picu, R.C., "Elastic moduli of particulate composites with graded filler-matrix interfaces," Polymer Composites 23(1), 110–119 (2002).

[89] Todd, M.G., and Shi, F.G., "Characterizing the interphase dielectric constant of polymer composite materials: Effect of chemical coupling agents," Journal of Applied Physics 94(7), 4551–4557 (2003).

[90] Todd, M.G., and Shi, F.G., "Complex permittivity of composite systems: a comprehensive interphase approach," IEEE Transactions on Dielectrics and Electrical Insulation 12(3), 601–611 (2005).

[91] Yang, Z., Wicks, D.A., Yuan, J., Pu, H., and Liu, Y., "Newly UV-curable polyurethane coatings prepared by multifunctional thiol- and ene-terminated polyurethane aqueous dispersions: Photopolymerization properties," Polymer 51(7), 1572–1577 (2010).

[92] Studer, K., Decker, C., Beck, E., and Schwalm, R., "Overcoming oxygen inhibition in UV-curing of acrylate coatings by carbon dioxide inerting, Part I," Progress in Organic Coatings 48(1), 92–100 (2003).

[93] Studer, K., Decker, C., Beck, E., and Schwalm, R., "Overcoming oxygen inhibition in UV-curing of acrylate coatings by carbon dioxide inerting: Part II," Progress in Organic Coatings 48(1), 101–111 (2003).

[94] Kade, M.J., Burke, D.J., and Hawker, C.J., "The power of thiol-ene chemistry," Journal of Polymer Science Part A: Polymer Chemistry 48(4), 743–750 (2010).

[95] Masson, F., Decker, C., Andre, S., and Andrieu, X., "UV-curable formulations for UV-transparent optical fiber coatings," Progress in Organic Coatings 49(1), 1–12 (2004).

[96] Kim, H.K., Ju, H.T., and Hong, J.W., "Characterization of UV-cured polyester acrylate films containing acrylate functional polydimethylsiloxane," European Polymer Journal 39(11), 2235–2241 (2003).

[97] Müller, U., Timpe, H.-J., and Neuenfeld, J., "Photocrosslinking of silicones—5. Photo-induced polymerization of silicone with pendant acrylate groups in the presence of oxygen," European Polymer Journal 27(7), 621–625 (1991).

[98] Zhang, G.-B., Fan, X.-D., Kong, J., and Liu, Y.-Y., "Kinetic Study on UV-curing of Hyperbranched Polysiloxane," Polymer Bulletin 60(6), 863–874 (2008).

[99] Müller, U., Kunze, A., Herzig, C., and Weis, J., "Photocrosslinking of Silicones. Part 13. Photoinduced Thiol-Ene Crosslinking of Modified Silicones," Journal of Macromolecular Science, Part A 33(4), 439–457 (1996).

[100] Madsen, F.B., Daugaard, A., Fleury, C., Hvilsted, S., and Skov, A.L., "Visualisation and Characterisation of Heterogeneous Bimodal PDMS Networks," RSC Advances 4(14), 6939–6945 (2014).

[101] Fetters, L., Lohse, D., and Richter, D., "Connection between polymer molecular weight, density, chain dimensions, and melt viscoelastic properties," Macromolecules 27(17), 4639–4647 (1994).

[102] Braley, S., "The Chemistry and Properties of the Medical-Grade Silicones," Journal of Macromolecular Science: Part A - Chemistry 4(3), 529–544 (1970).

[103] Quan, X., "Properties of post-cured siloxane networks," Polymer Engineering and Science 29(20), 1419–1425 (1989).

[104] Karlsson, A., Singh, S.K., and Albertsson, A.-C., "Controlled destruction of residual crosslinker in a silicone elastomer for drug delivery," Journal of Applied Polymer Science 84(12), 2254–2264 (2002).

[105] Karlsson, A., "New Analytical Methods For Silicone Elastomers Used in Drug Delivery Systems," in Dep. Polym. Technol. R. Inst., Royal Institute of Technology, Stockholm, pp. 1–107 (2003).

[106] Shama, S.A., "Postcure behavior of UV curable materials: A comparison of urethane acrylates with vinyl ether end-capped urethanes.," Journal of Photopolymer Science and Technology 4(1), 9–22 (1991).

[107] Goswami, K., Skov, A.L., and Daugaard, A.E., "UV-Cured, Platinum-Free, Soft Poly(dimethylsiloxane) Networks," Chemistry - A European Journal 20(30), 9230–9233 (2014).

[108] Li, Z., Moon, K., Lin, Z., Yao, Y., Wilkins, S., and Wong, C.P., "Carbon nanotubes inhibit the free-radical cross-linking of siloxane polymers," Journal of Applied Polymer Science 131(12), 40355–1–6 (2014).

[109] Zhang, J., Mine, M., Zhu, D., and Matsuo, M., "Electrical and dielectric behaviors and their origins in the three-dimensional polyvinyl alcohol/MWCNT composites with low percolation threshold," Carbon 47(5), 1311–1320 (2009).

[110] Dang, Z., Yao, S., Yuan, J., and Bai, J., "Tailored Dielectric Properties based on Microstructure Change in BaTiO 3 -Carbon Nanotube/Polyvinylidene Fluoride Three-Phase Nanocomposites," The Journal of Physical Chemistry C 114(31), 13204–13209 (2010).

[111] Shrivastava, N.K., Kar, P., Maiti, S., and Khatua, B.B., "A facile route to develop electrical conductivity with minimum possible multi-wall carbon nanotube (MWCNT) loading in poly(methyl methacrylate)/MWCNT nanocomposites," Polymer International 61(11), 1683–1692 (2012).

[112] Nalwa, H.S., [Ferroelectric Polymers: Chemistry: Physics, and Applications] , H. S. Nalwa, Ed., Marcel Dekker Inc, New York, 1–912 (1995).

[113] Xiang, C., Pan, Y., Liu, X., Sun, X., Shi, X., and Guo, J., "Microwave attenuation of multiwalled carbon nanotube-fused silica composites," Applied Physics Letters 87(12), 123103–1–3 (2005).

[114] Al-Saleh, M.H., Jawad, S. a., and El Ghanem, H.M., "Electrical and dielectric behaviors of dry-mixed CNT/UHMWPE nanocomposites," High Performance Polymers 26(2), 205–211 (2013).

[115] Nanni, F., and Valentini, M., [Polymer–Carbon Nanotube Composites] , in Polym. Nanotub. Compos., T. McNally and P. Pötschke, Eds., Woodhead Publishing Limited, Cambridge, United Kingdom, 329–346 (2011).

[116] Kim, H.K., and Shi, F.G., "Thickness dependent dielectric strength of a low-permittivity dielectric film," IEEE Transactions on Dielectrics and Electrical Insulation 8(2), 248–252 (2001).

[117] Zakaria, S., Morshuis, P.H.F., Benslimane, M.Y., Gernaey, K. V, and Skov, A.L., "The electrical breakdown of thin dielectric elastomers: thermal effects," in Proc. SPIE 9056, Y. Bar-Cohen, Ed., 90562V–1–11 (2014).

[118] Dissado, L.A., and Fothergill, J.C., [Electrical Degradation and Breakdown in Polymers] , illustrate, G. C. Stevens, Ed., P. Peregrinus, London, United Kingdom, 1–620 (1992).

[119] Whitehead, S., [Dielectric breakdown of solids] , The Clarendon Press, Oxford, United Kingdom, 1–271 (1951).

[120] Mohiuddin, M., and Hoa, S.V., "Temperature dependent electrical conductivity of CNT–PEEK composites," Composites Science and Technology 72(1), 21–27 (2011).

[121] Thostenson, E.T., and Chou, T.-W., "Microwave processing: fundamentals and applications," Composites Part A: Applied Science and Manufacturing 30(9), 1055–1071 (1999).

[122] Mijović, J., and Wijaya, J., "Review of cure of polymers and composites by microwave energy," Polymer Composites 11(3), 184–191 (1990).

[123] Yusoff, R., and Aroua, M., "Curing of polymeric composites using microwave resin transfer moulding (RTM)," Journal of Engineering Science and Technology 2(2), 151–163 (2007).

Appendix A

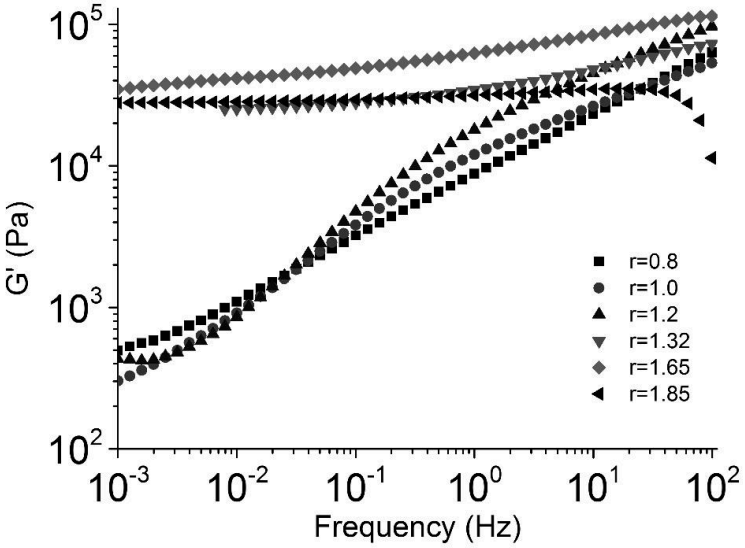

A1: Investigations of storage moduli (G') of PPO pure networks with varying stoichiometric imbalance ratio

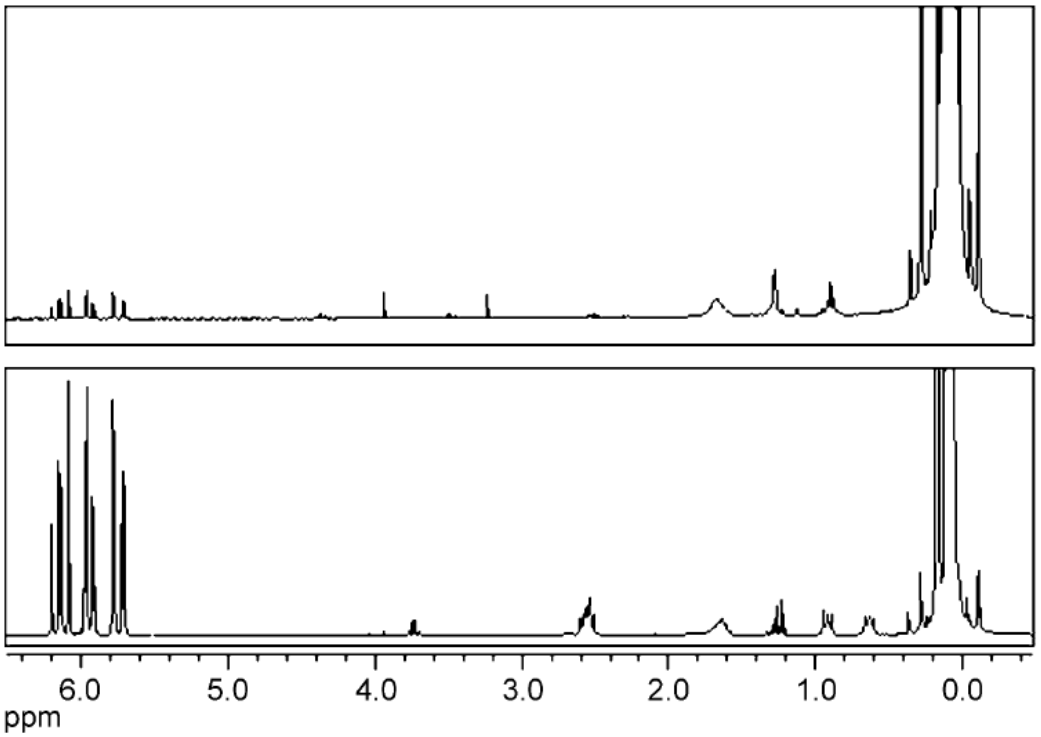

A2:[1]H NMR spectra of the two hyperbranched structures (top: hyperbranched high-molecular-weight PDMS; bottom: hyperbranched low-molecular- weight PDMS), showing full conversion of the thiol cross-linker as well as the excess vinyl groups from the PDMS

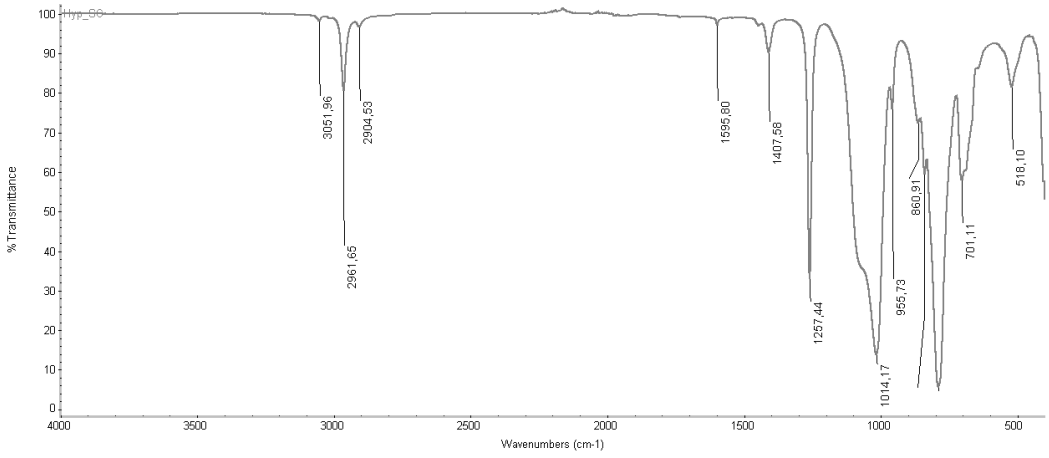

A3: ATR-FTIR spectra of hyperbranched PDMS short chain

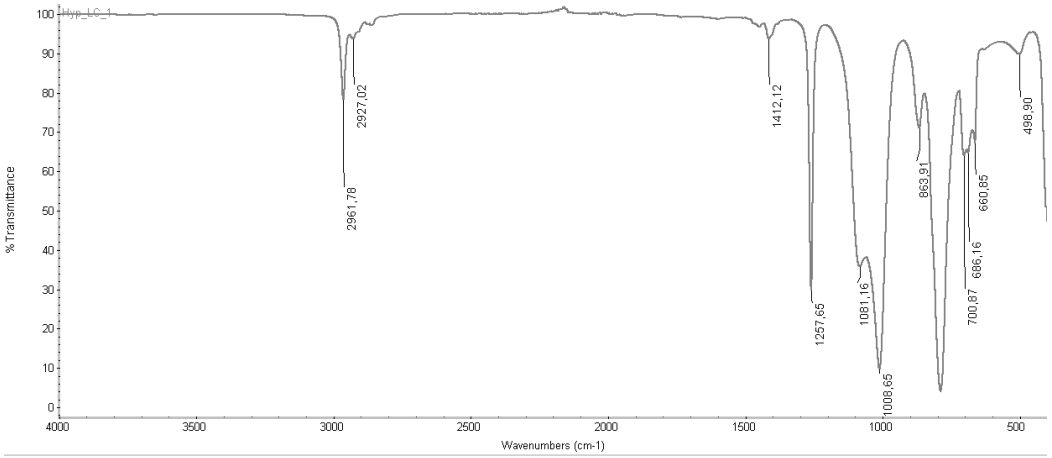

A4: ATR-FTIR spectra of hyperbranched PDMS long chain

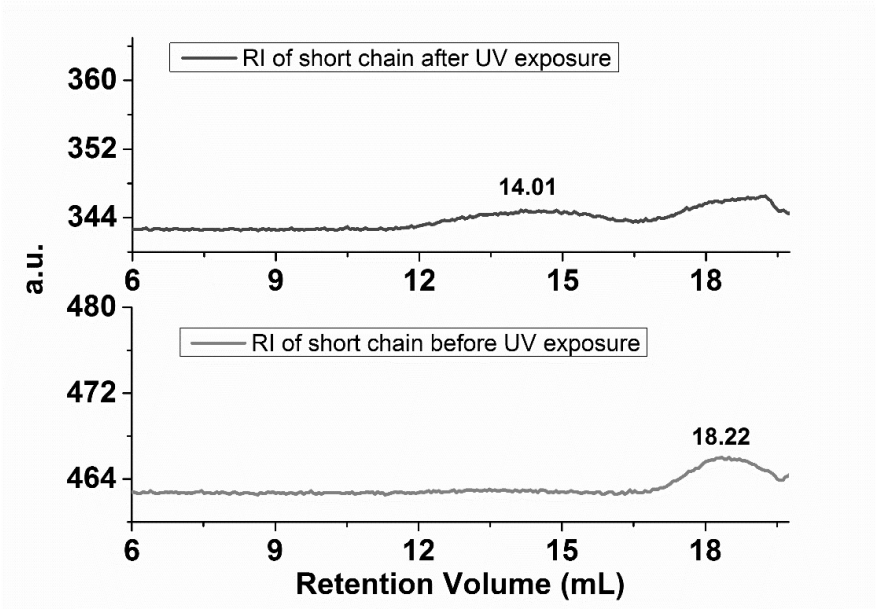

A4: SEC traces of PDMS short chain before and after UV exposure

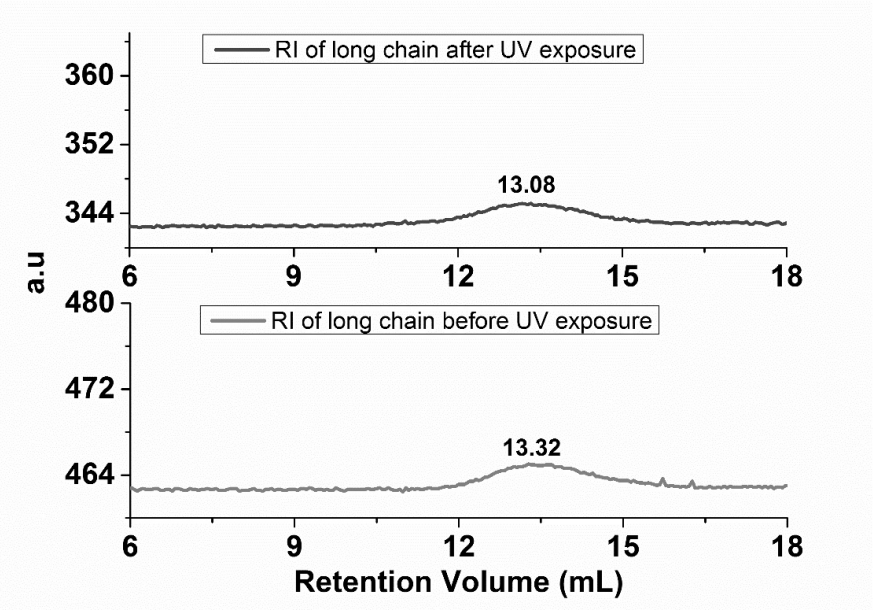

A5: SEC traces of PDMS long chain before and after UV exposure

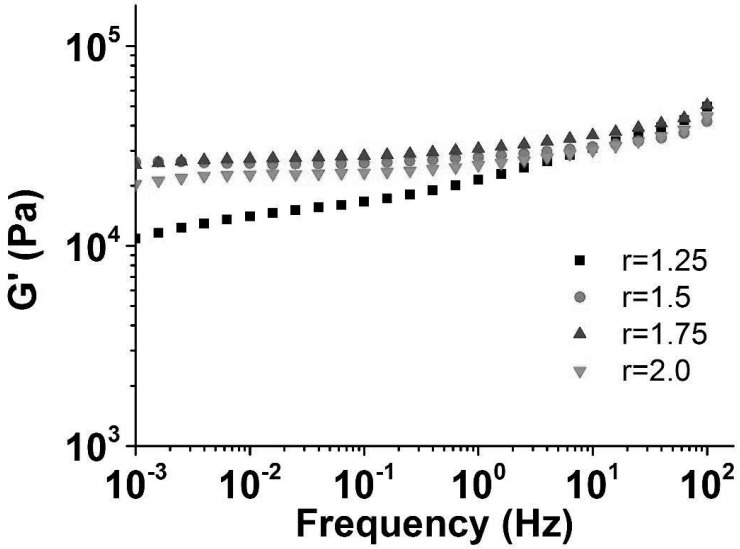

A6: Investigation of storage modulus moduli (G') of the two step networks (Bi90-10) with varying crosslinker amounts

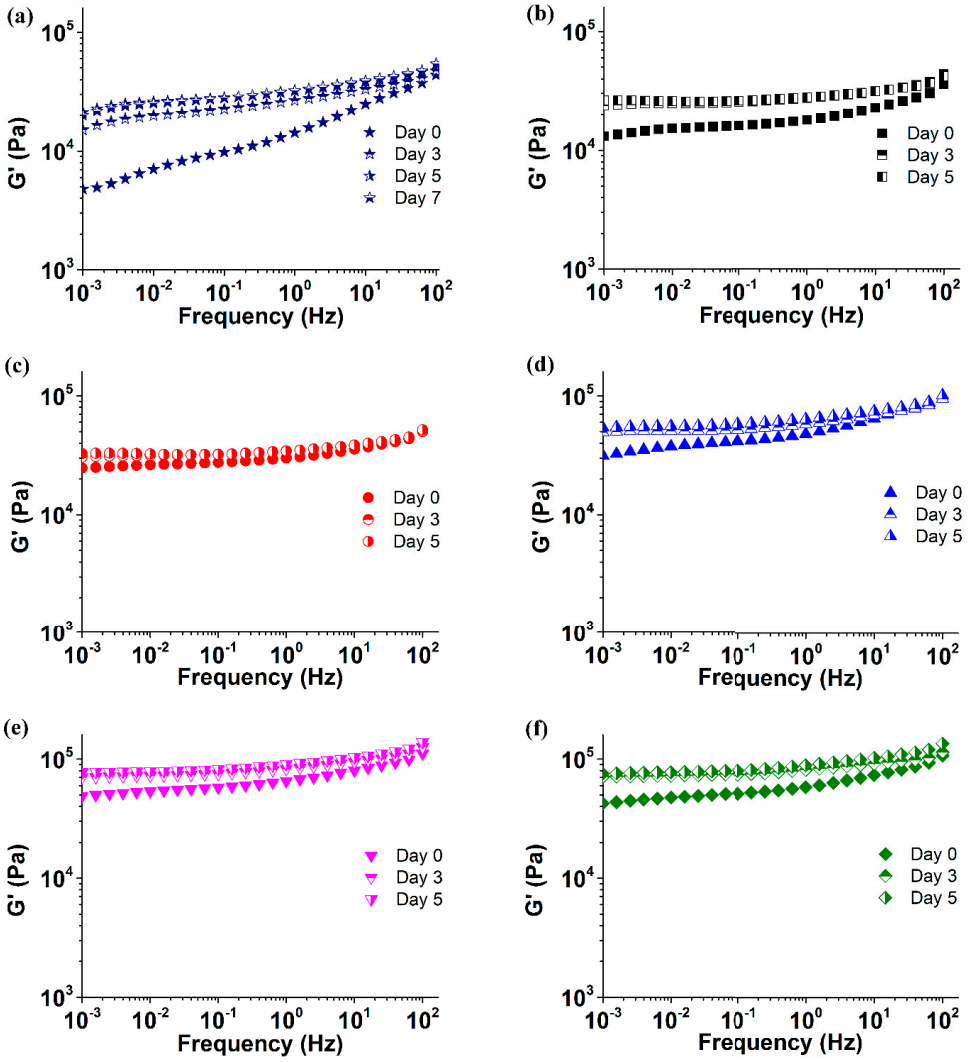

A7: Investigation of storage moduli (G') of (a) one step (b) Bi90-10 (c) Bi85-15 (d) Bi80-20 (e) Bi75-25 (f) Bi70-30 networks after UV exposure at different days

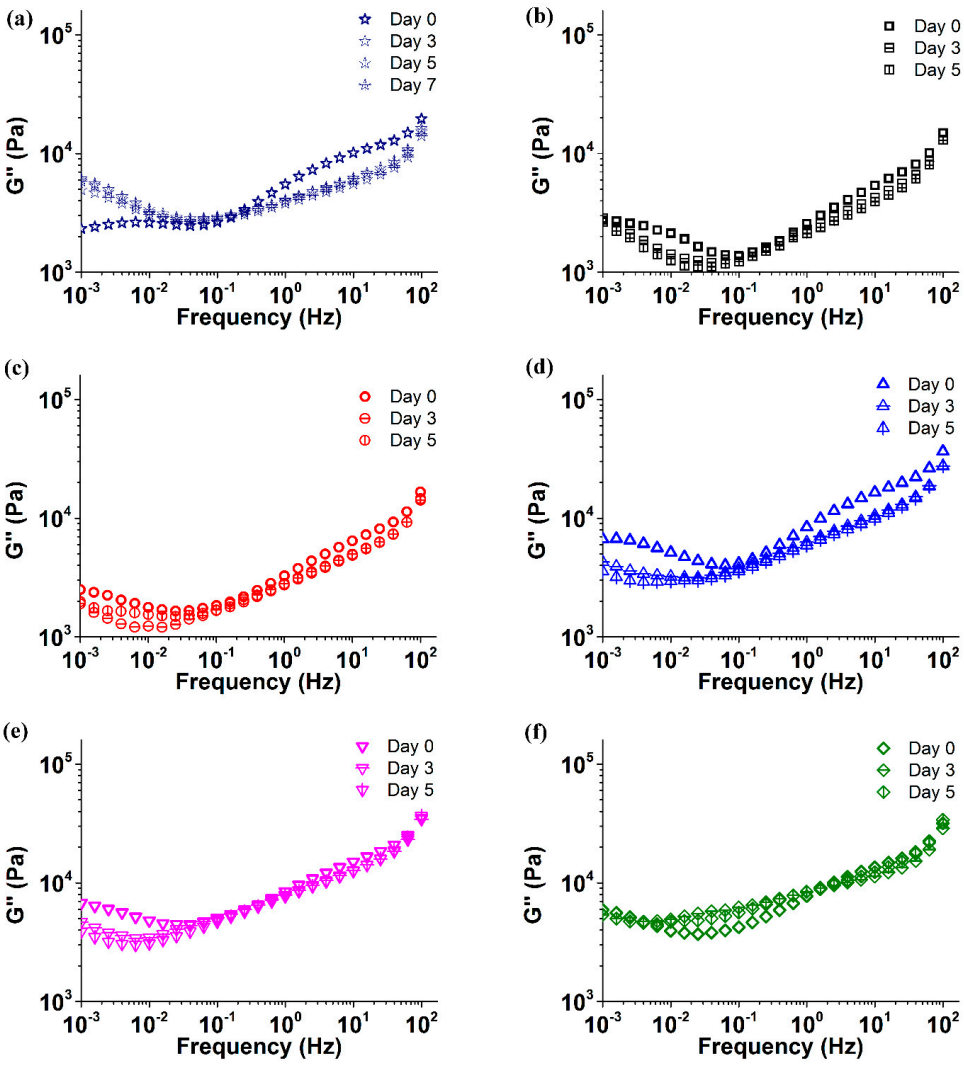

A8:Investigation of loss moduli (G") of (a) one step (b) Bi90-10 (c) Bi85-15 (d) Bi80-20 (e) Bi75-25 (f) Bi70-30 networks after different days of UV exposure

Appendix B

Article B1: *Silicone resembling poly (propylene glycol) interpenetrating networks based on no pre-stretch as basis for electrical actuators*

Goswami, K., Madsen, F.B., Daugaard, A. E. & Skov, A. L. 2013 *Proceedings of SPIE.* Bar-Cohen, Y. (ed.). SPIE - International Society for Optical Engineering, Vol. 8687, 86871Z-1-12

Silicone resembling poly (propylene glycol) interpenetrating networks based on no pre-stretch as basis for electrical actuators

Kaustav Goswami, Frederikke Bahrt Madsen, Anders Egede Daugaard, Anne Ladegaard Skov*.

The Danish Polymer Centre, Department of Chemical and Biochemical Engineering,

Technical University of Denmark, 2800 Kgs. Lyngby, Denmark.

ABSTRACT

Elastomers currently used as transducers have not been designed with this specific application in mind and there is therefore a need for new target engineered materials to bring down driving voltages and increase actuator performance. A proposed method of optimization involves the development of new types of interpenetrating polymer networks (IPNs) to be used as dielectric elastomer (DE) transducers. This work demonstrates the use of polypropylene glycol (PPG) as a novel DE material. The IPNs formed were shown to exhibit excellent thermal stability and mechanical properties including lower tendency for viscous dissipation with higher dielectric permittivity compared to state of the art polydimethylsiloxane (PDMS) materials.

Keywords: Poly (propylene glycol), IPN, actuator, dielectric permittivity

1. INTRODUCTION

The need for new transducer materials is increasing due to the requirements from high-performance applications such as wave energy harvesting[1], valves and flat screen loudspeakers.[2] Although areas such as design and manufacturing of transducers historically have received a lot of attention, less work has been conducted within the area of material optimization. A tendency is, however, that the focus on material optimization has increased during the last few years. Current commercially available elastomers that demonstrate the best actuation characteristics such as silicones and acrylics were not designed to be used as transducers and their performance are consequently not a result of targeted development[3]. Therefore, the design of novel engineered materials with properties targeted towards the use as actuators and generators poses an interesting and imperative task.

The interest in using elastomers for actuators has increased during the last decade due to their large strains, good frequency responses, high work densities and high degree of electromechanical coupling and good overall performance.[4,5] Elastomers are a class of polymer networks that range from soft and gel-like to hard and brittle rubbers. Elastomers are typically formed by cross-linking either by use of a cross-linker or by irradiation, and the resulting material properties depend greatly on the amount of cross-linker or radiation dose used for the network formation.[6] Elastomers with specific properties can be prepared for any application by careful control of reaction parameters and this makes these materials especially well-suited for applications as actuators.

Elastomers for dielectric elastomers (DEs) consist of a thin elastomeric film sandwiched between two compliant electrodes and thereby forming a capacitor. The electrodes can be made from a variety of compliant conductive materials.[5] When an external voltage is applied, the material exhibits a change in size and shape. The capacitor is consequently squeezed together due to the electrostatic forces caused by free charges, which are negative on one electrode and positive on the other. Since the volume is kept constant due to the incompressibility of the elastomer, the elastomer is expanded in the transverse direction of the electric field and the area of the electrodes is consequently increased. The increase in electrode area decreases the charge density, which is energetically favorable. The decrease in charge density is the driving force for the actuation.[7]

* al@kt.dtu.dk; phone +45 45252825

Electroactive Polymer Actuators and Devices (EAPAD) 2013, edited by Yoseph Bar-Cohen,
Proc. of SPIE Vol. 8687, 86871Z · © 2013 SPIE · CCC code: 0277-786X/13/$18 · doi: 10.1117/12.2010494

Since the life time of current DEs are limited to around one million cycles,[4] there is a need for further development in order to meet the demands for high-performance applications. The short life times are often a consequence of pre-straining of the elastomers films. DEs are usually pre-strained as this has been shown to increase the electrical breakdown strength[8-12] and frequency response[3]. Upon pre-stretching, the breakdown strength increases due to realignment of defects, such as voids and particles. However, pre-stretching has the disadvantage of decreasing the overall performance of the actuator because of a large performance gap between the active material and the packaged actuator, lower lifetime due to stress concentration at the film/support structure interface[8,13] and stress relaxation that affects actuation.[14] High loading of fillers are also expected to decrease the life time of the elastomers. Recent research has shown that the dielectric permittivity of silicones can be increased even by very small loadings of fillers[15] but the effect may be limited.

One promising way of optimizing DEs is to create an interpenetrating polymer network (IPN). An IPN is a network that consists of two or more polymers that both are cross-linked to give interlaced networks. The advantage of IPNs is that no pre-stretch is necessary to obtain high actuation.[13] IPNs have different and often superior properties compared to the respective homopolymers, which is due to stabilized bulk and surface morphologies created by the interlaced networks. There are two main ways to prepare IPNs, either through a sequential or a simultaneous approach. In the sequential method, the IPN is formed in two consecutive steps, where initially a homonetwork of polymer (I) is formed through cross-linking. This network is then swollen with a monomer (II), cross-linker and an initiator and the IPN is formed through *in-situ* polymerization. The second method consists of forming two independent networks simultaneously. This is either done by cross-linking two sets of prepolymers or through polymerization and cross-linking of two monomers by non-interfering reactions. Figure 1 shows these two synthesis routes.

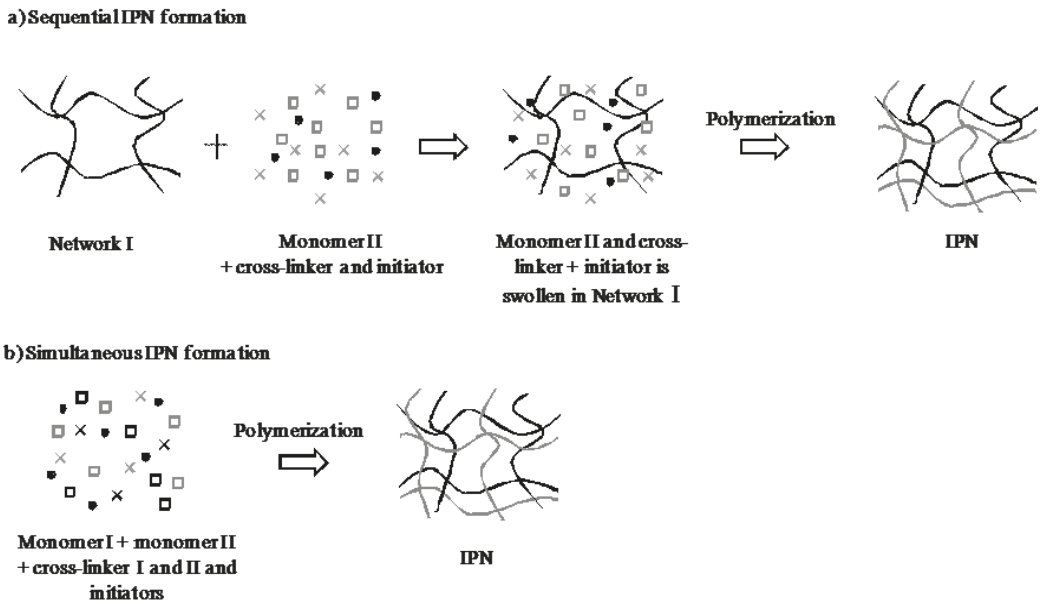

Figure 1: IPN synthesis routes: a) Sequential IPN; b) Simultaneous IPN. Monomer I and II could also consist of a prepolymer I and II

Other types of IPNs include: Latex IPN, gradient IPN, thermoplastic IPN and semi-IPN. Latex IPNs are prepared in the form of latexes, typically with a core and shell structure. Gradient IPNs have compositions or cross-linking densities that vary depending on location in the sample. Thermoplastic IPNs are hybrids between IPNs and polymer blends and have physical rather than chemical cross-links and semi-IPNs consist of one or more polymers being cross-linked into networks and one or more polymers being linear or branched.[16]

For many years the main focus of IPNs as DE actuators was on highly pre-strained acrylic 3M VHB tape due to this materials high electric breakdown field and large strains. The VHB IPN is created via a sequential approach by treating the pre-strained acrylic VHB film with cross-linkable monomer and initiator and then allowing the monomer and initiator to diffuse into the film. The monomer, upon thermal curing, forms a second polymer network, interlaced with the acrylic network. The formed IPN is allowed to relax to zero stress which makes the acrylic network contract and the second network to be compressed. [8,13,17] A schematic representation can be seen in Figure 2.

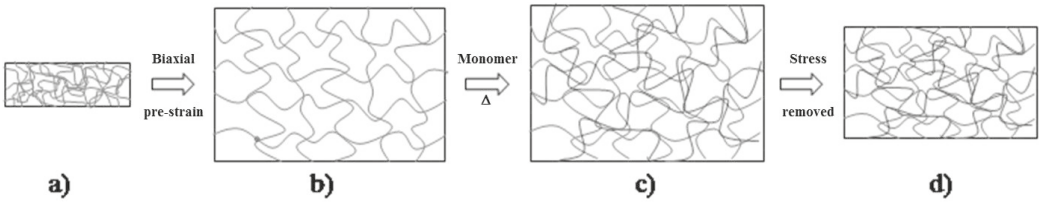

Figure 2: Schematic illustration of IPN formation based on 3M VHB tape: a) VHB acrylic tape before pre-strain; b) VHB acrylic tape after biaxial pre-strain; c) cross-linkable monomer is cured and interlaced with the acrylic network forming an IPN; d) stress is removed and the film retains most of the pre-strain

The two interpenetrating networks are now in equilibrium with one network highly stressed and the other highly compressed. The formed IPN is able to withstand strains up to 300 % which is comparable to the untreated pre-strained VHB tape.[8]

A lot of work has been conducted within the area of VHB acrylic based IPNs with curable multifunctional monomers such as bifunctional 1,6-hexandiol diacrylate (HDDA)[13,18] and trifunctional trimethylolpropane trimethacrylate (TMPTMA) monomers.[8,17,19] Literature has also been published regarding VHB acrylic elastomers combined with a PDMS. The PDMS chains were swollen with a co-solvent into the acrylic film and subsequently cross-linked. The resultant IPN material was shown to possess properties between the properties of the homonetworks thus eliminating some of the disadvantages that acrylic networks experience.[20] Limited literature has however been published regarding the use of non-acrylic based IPNs as dielectric elastomers; however several articles have been published regarding poly(3,4-ethylenedioxythiophene) (PEDOT) used in three-component IPNs where PEDOT acts as a electronically conducting polymer embedded in an elastic polymer electrolyte network to form solid polymer electrolytes (SPEs).[21] Several studies have used poly(ethylene oxide) and poly(butadiene) IPNs as the polymer electrolyte network with the PEDOT conducting polymer. The combination of poly(ethylene oxide) and poly(butadiene) in IPNs was shown to have suitable properties for actuator applications.[19,22,23] IPNs have also been prepared combining cellulose and chitosan as electroactive paper actuators.[24] These IPNs were synthesised by dissolving cellulose and chitosan in a co-solvent followed by treatment with glutaraldehyde and cross-linking. The resulting films showed good bending displacement but experienced severe degradation at high humidity due to electrode damage. As limited research has been published regarding the use of non-acrylic based IPNs as actuators, there is clearly a need for the development of new materials within this area.

The aim of this work is to prepare IPNs with improved properties compared to what is generally observed. This work focuses on the use of two types of polypropylene glycols (PPGs) as IPNs due to the low elastic modulus of this polymer. The difference between the two polymers is the molecular weight and the functional end-groups. The term PPG-OH is used to describe the low molecular weight polymer which contains hydroxyl end-groups and the term PPG-V is used to describe the higher molecular weight polymer which is vinyl terminated. The generation of the IPN is carried out by a simultaneous approach using two non-interfering chemical reactions (orthogonal reactions). PPG-OH is cross-linked using an isocyanate type cross-linker via a tin-catalyzed reaction and PPG-V is cross-linked with the use of pentaerythritol tetrakis(3-mercaptopropionate), a tetra-functional thiol. Thiol-ene reactions are a type of “click” reactions

that are characterised by being mild, having high yields and being orthogonal with other common organic synthesis reactions,[25] which makes this type of reaction ideal for simultaneous IPN formation. In this approach the thiol-ene "click" reaction is used as a cross-linking reaction in a new type of system with the PPG-V polymer. The reaction is carried out by free radical addition which is promoted by UV light.[26] As the PPG-OH tin-catalysed cross-linking reaction is facilitated by heat the two cross-linking reactions will be non-interfering, forming two independent networks. A schematic representation of the IPN formation can be seen in Figure 3.

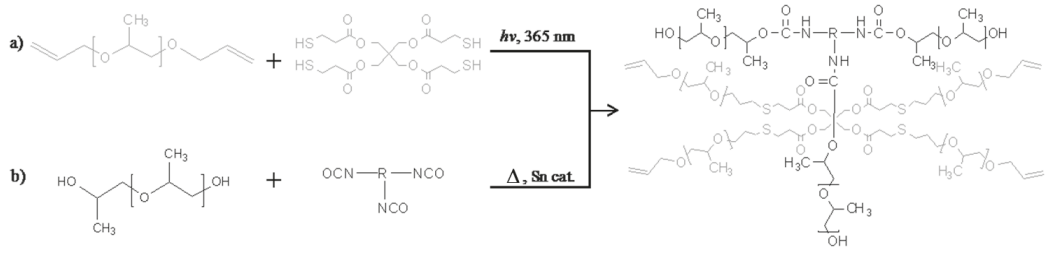

Figure 3: Schematic illustration of IPN formation based on PPG-V and PPG-OH: a) PPG-V is cross-linked via a tetra-functional thiol cross-linker using thiol-ene "click" chemistry and UV light; b) PPG-OH is cross-linked with heat, a tin catalyst and an isocyanate crosslinker with an average functionality of 3.4

This combination is envisioned as an alternative to the commonly used PDMS and acrylic elastomers. PDMS has been shown to have poor mechanical properties without added fillers, high permeability and low compatibility with other polymers which means that it tends to phase separate.[27] Acrylic elastomers have high viscous loss and poorer response speed, and tend to build up space charge which leads to enhanced localized electric fields and ultimately to electrical breakdown.[28],[29].The mechanical properties of the PPG based IPN will be greatly improved due to the morphological stability that these interlaced networks experience. By varying the compositions of the two networks it could be possible to achieve tuneable properties and high actuation without pre-stretching.

2. EXPERIMENTAL

2.1 Materials and Methods

Hydroxyl terminated poly (propylene glycol) (PPG-OH) of approximate molecular weight 4000 g/mol (Pluriol P 4000) was purchased from BASF, Germany and vinyl terminated poly (propylene glycol) (PPG-V) of molecular weight of 13500 g/mol from Kaneka Corp. The 3.4-functional crosslinker for PPG-OH DESMODUR N3300 was purchased from BAYER, Germany. All other chemicals were acquired from Sigma-Aldrich.

Rheological tests were performed in AR2000 stress controlled rheometer at 25°C with parallel plate geometry. Frequency sweep experiments were performed from 0.001Hz to 100Hz with 1mm thick samples at a fixed strain of 1% (the linear viscoelastic region was determined from initial strain sweeps).

Glass transition temperature (Tg) of both homo network and IPN was measured by differential scanning calorimetry (DSC) using TA Instruments Q1000 differential scanning calorimeter under nitrogen flow rate of 50ml/min. Measurements were performed from -85°C to 60°C at a heating rate of 10°C/min.

Thermal degradation behaviour was studied by thermogravimetric analysis (TGA). The apparatus used was TA instrument's Q500 TGA analyser from room temperature to 600°C at a heating rate of 20°C/min in air flow rate of 90ml/min.

Dielectric Relaxation Spectroscopy (DRS) was performed on a Novocontrol Alpha-A high performance frequency analyser from 1Hz to 10^6Hz.

2.1.1 Preparation of networks

2.1.1.1 Preparation of PPG-V homo network

Pentaerythritol tetrakis (3-mercaptopropionate) (crosslinker, 0.244 g, 0.5 mmol) and 2, 2-dimethyl-2-phenylacetophenone (photo initiator, 0.128 g, 0.5 mmol) were dissolved in minimum volume of toluene. PPO [10 g (0.74 mmol of reactive group) M_n= 13,500 g/mol)] was added to the toluene solution and the solution was mixed in a SpeedMixer™ at 2000 rpm for 3 minutes. The mixture was poured into an 8 cm × 10 cm steel mould placed over a glass plate lined with Parafilm® M. This setup was kept in a well-ventilated place for 30 minutes and subsequently transferred to the UV chamber (λ= 365nm) and irradiated for 45 minutes.

2.1.1.2 Preparation of PPG-OH homo network

The PPG-OH homo networks were prepared at room temperature by mixing DESMODUR N3300 (crosslinker, 1.21 g, 1.84 mmol), dibutyltin dilaurate (catalyst, 0.016 g, 0.026 mmol) with 10 g (2.5 mmol of reactive group) of PPG-OH (Mn= 4000g/mol) and the mixture was poured into the mould and left for 24 hours at room temperature.

2.1.1.3 Preparation of IPN

IPN of PPG-V and PPG-OH was prepared by mixing all of the above mentioned components together and keeping the stoichiometric imbalance ('r'-value) fixed for both PPG-V and PPG-OH. The mixture was poured into the mould and placed in the UV chamber for 45minutes and then stored at room temperature for 24 hours to ensure complete curing.

3. RESULTS AND DISCUSSION

Homo networks are pure PPG-V and PPG-OH networks and IPNs consist of both PPG-V and PPG-OH with varying weight ratio and both the homo networks and IPNs were prepared with this fixed stoichiometric imbalance ('r'-value), which is defined as [30],

$$r = \frac{f\left[-SH / -NCO\right]_0}{2\left[Vinyl / Hydroxyl\right]_0} \tag{1}$$

where f is the average functionality of the crosslinker used and $[...]_0$ is the initial concentration of the reactive group present in the crosslinker (*-SH/-NCO*) and in the polymer (*Vinyl/Hydroxyl*). The compositions are listed in Table 1.

Table 1: Composition of homo and interpenetrating networks

Sample name	PPG-V(Wt%)	PPG-OH(Wt%)
PPG-V	100	-
I-95/5	95	5
I-90/10	90	10
I-85/15	85	15
I-80/10	80	20
I-75/25	75	25
I-70/30	70	30
PPG-OH	-	100

In order to obtain mechanically strongest crosslinked network the 'r'-value is determined to be 1.35 for the PPG-V and 1.25 for the PPG-OH systems. Any further small increase in the 'r'-value results in a decrease in G' value which is consistent with the results obtained by Larsen et.al [30] in a vinyl terminated PDMS network.

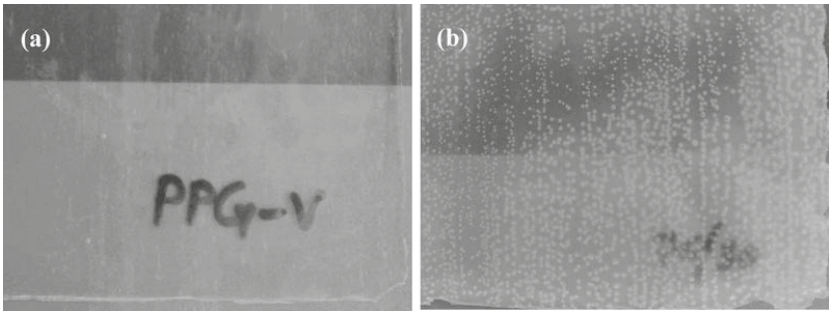

Figure 4: Digital image of a part of 8 cm × 10 cm prepared networks (a) PPG-V (b) I-70/30

Samples I-70/30 (Figure 4b) and I-75/25 have numerous bubbles inside and as this bubble formation is repeatable, they are rejected from further testing.

The linear viscoelastic (LVE) properties of the PPG networks have been measured to obtain the elastic modulus (G or Young's modulus Y=3G) and to investigate the elastomer performance in the low-strain limit. Figure 5 shows the LVE diagrams for the prepared networks.

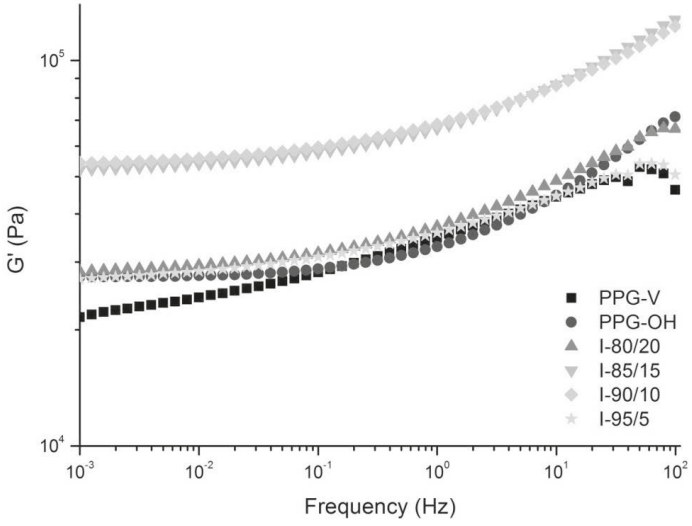

Figure 5: Storage modulus versus frequency for homo networks and IPNs at 25°C

As can be seen from Figure 5 the two components in the IPN system are fairly similar in their rheological properties. However, in the IPN materials the combination results in a system with improved shear storage moduli. In Table 2 the shear storage moduli as well as tan delta values (see figure 6) at low frequencies are extracted for comparison.

Table 2: LVE data for homo networks and IPNs

Sample name	Storage modulus (kPa) at 0.001Hz	tan delta at 0.001Hz
PPG-V	22	0.05
I-95/5	27	0.03
I-90/10	54	0.02
I-85/15	52	0.02
I-80/20	28	0.02
PPG-OH	27	0.02

As evident from Table 2 the value of the storage modulus (G') at the plateau terminal region (0.001Hz) is approximately 22 and 27 kPa, respectively, for PPG-V and PPG-OH homo networks which is very low compared to commercially available PDMS elastomers as well as non-filled silicone elastomers[30]. Reported G' for Elastosil RT 625 is 77kPa[31] in very thin films. In IPN compositions I-85/15 and I-90/10 the shear storage modulus value increases abruptly indicating additional chain restriction imposed by the PPG-OH networks. The shorter chains in PPG-OH results in higher crosslink density and behave as hard phase acting as anchor points hindering chain movements. No such increase in modulus is observed at the two extremes of the IPN compositions.

The tan delta plots (Figure 6) and the values reported in Table 2 can also give some insight into the molecular motion and damping behaviour of the polymers.

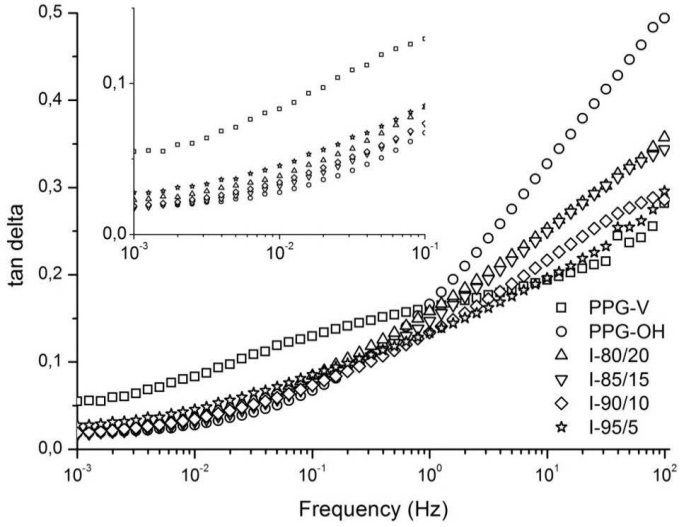

Figure 6: Damping (tan delta) versus frequency curve for homo networks and IPNs at 25°C. The inset shows the tan delta curves of homo networks and IPNs at the terminal region

The frequency dependency of tan delta at the terminal frequency region is not significant for homo network and IPNs which is typical of crosslinked elastomers. Moreover the dissipative nature of the homo and interpenetrating networks is evident from the increasing trend in the tan delta curves at frequencies above 1Hz. A close inspection of the curves at the terminal region reveals that I-85/15 and I-90/10 have very low tan delta similar to PPG-OH, indicating low loss while PPG-V remains well above any of the IPNs and PPG-OH.

The glass transition temperature of the homo networks and IPNs is studied by DSC and reported in Table 3.

Table 3: DSC results of homo networks and IPNs

Sample name	Tg(°C)
PPG-V	-64.0
I-95/5	-64.0
I-90/10	-65.1
I-85/15	-64.6
I-80/20	-64.8
PPG-OH	-64.9

Few polymers are completely miscible, which often results in gelation and phase separation during IPN formation. Both phenomena influence the stability of the IPN produced. If gelation occurs first then the phase domains remain small in contrast to when phase separation occurs before gelation where domains are larger [16]. Since the backbone structures of both polymers are identical in this study, phase separation is expected to be limited. Both networks are formed simultaneously, which ensures good mixing until the gelation point of one of the networks. This is evident from the T_g values, which are comparative for both the homopolymers and the IPNs.

Thermal degradation of IPNs can be best understood when compared to the thermal behaviour of the homo networks as shown in Figure 7 where the Thermo Gravimetric Analysis (TGA) of homo networks and IPNs are compared.

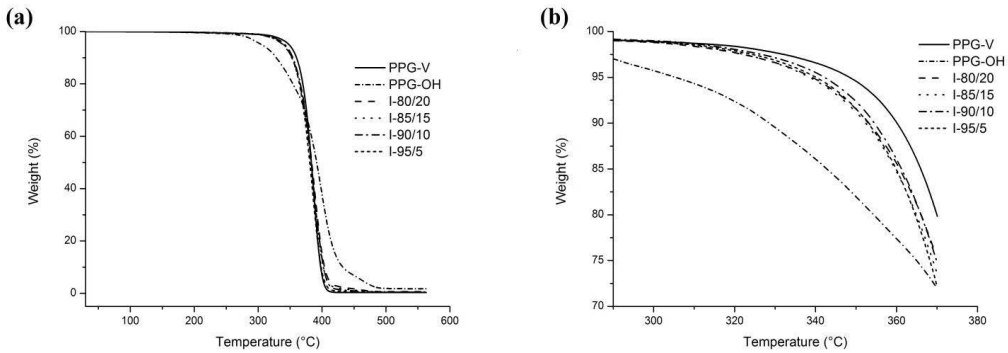

Figure 7: (a) TGA of homo networks and IPNs (b) magnified view of T_5

As seen from Figure 7, both the homo network and IPNs show single step degradation process corresponding to complete decomposition of polymer backbone. Different temperatures attributed to various levels of thermal stability of a polymer can be identified from the TGA curve, namely T_5, T_{50}, and T_{95}, defined as the temperature where 5, 50 and 95% mass loss of the polymer occurs. In this case there is an improvement in the onset of degradation, which is illustrated from Figure 7 (b).

The T_5 values of homo networks and IPNs are extracted from Figure 7 (b) and listed in Table 4 for easy comparison.

Table 4: T_5 temperature for homo networks and IPNs

Sample name	T_5(°C)
PPG-V	344
I-95/5	340
I-90/10	342
I-85/15	339
I-80/20	339
PPG-OH	306

The T5 degradation temperatures from Table 4 clearly show only a minor reduction in thermal stability of the IPN as the PPO-OH content is increased. This corroborates the DSC results indicating a completely miscible polymer system with a homogeneous distribution of the two components in the IPN.

For applications in DEAP materials the permittivity and the dielectric damping are important design parameters and all the materials have been investigated by dielectric relaxation spectroscopy (DRS) as shown in Figure 8.

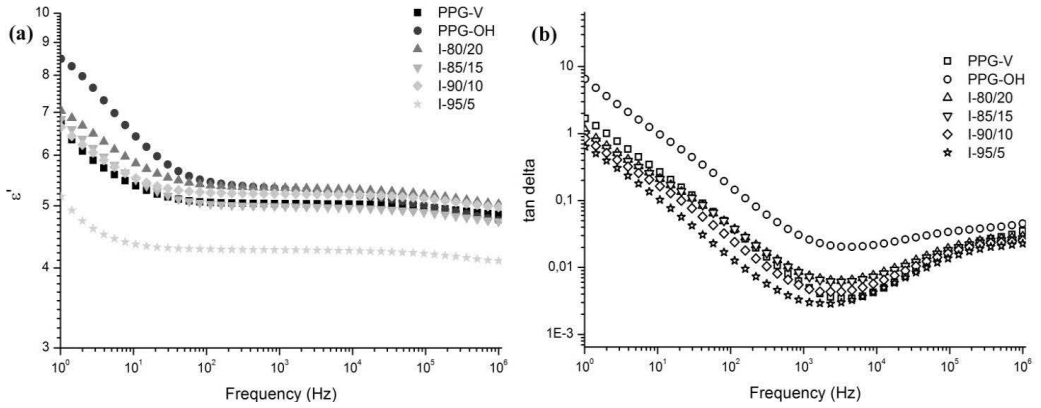

Figure 8: (a) Real part of permittivity and (b) dielectric damping (tan delta) vs. frequency for homo networks and IPNs obtained from DRS.

From Figure 8 it is apparent that the system is homogeneous resulting in no dielectric transitions from interfacial polarizations in the IPNs. In the medium to high frequency range (10^2-10^6Hz) where the dielectric property depends on the bulk polarization process[32], the ε' for the homo and interpenetrating networks are almost constant. The value of relative permittivity for homo networks and IPNs, except for I-95/5, is calculated to be 5.0-5.2 at 10^4Hz, which is about 67% higher than pure or fumed silica reinforced PDMS[31].

All compositions have same trend in damping behaviour as seen from Figure 8(b). The tan delta values for PPG-V and IPNs start from 1 at 1Hz and gradually decrease as the frequency is increased with the minimum in tan delta at ~10^3Hz. PPG-OH although follows the same trend as the rest, shows a much higher damping in the entire frequency range, which is a result of a higher loss.

For evaluation of the proposed PPG material for DEAP applications some of the essential properties of PPG-V are compared to a PDMS for DEAP applications (Elastosil RT625) in Table 5.

Table 5: Comparison of different properties of Elastosil RT625 and PPG-V

Property	Elastosil RT625	PPG-V
Permittivity (ε')	3.0	5.0
Breakdown strength(BD) (V/μm)[31]	60	60[a]
Young's modulus (Y) (kPa)[31]	227	66
Figure of merit ($F_{om} = \frac{\varepsilon'(BD)^2}{Y}$) [33]	48	273

[a]Breakdown strength of fumed silica filled PPG-V system.

It is clear from Table 5 that the PPG material has superior properties in some of the critical design parameters for a efficient DEAP material. The PPG has a substantially improved permittivity as well as a low Young's modulus, which both look very promising for the further testing of the electromechanical properties of PPG based systems.

4. CONCLUSION

Interpenetrating polymer networks (IPNs) are promising materials for new dielectric elastomer (DE) transducers. The main focus of IPNs as DE transducers have previously been based on pre-strained acrylic 3M VHB tape due to the large achievable strain of this material. Acrylic elastomers have, however, large viscous loss and a tendency to accumulate space charge which can potentially lead to premature electrical breakdown. Therefore, this work was focused on developing a new type of non-acrylic based IPN that exhibit improved properties compared to what is generally observed. A new type of IPN elastomer based on polypropylene glycols (PPGs) has been developed and prepared. The initial tests of the system presented here, show a good thermal stability and good mechanical properties, resulting in a low elastic modulus (Young's modulus Y=66 kPa). In addition to this, the one pot procedure for the preparation of the IPN resulted in a homogenous distribution of the two networks illustrated by several different techniques. The DRS investigations revealed a high dielectric permittivity (ε'= 5.0) in the medium to high frequency range. The properties of the PPG system have been found promising for further studies of the application of these materials for DE transducers.

ACKNOWLEDGMENT

The authors wish to acknowledge the Danish National Advanced Technology Foundation for financial support.

REFERENCES

[1] Ahnert, K., Abel, M., Kollosche, M., Jørgensen, P.J., and Kofod, G., "Soft capacitors for wave energy harvesting," Journal of Materials Chemistry 21(38), 14492–14497 (2011).

[2] Heydt, R., Kornbluh, R., Eckerle, J., and Pelrine, R., "Sound radiation properties of dielectric elastomer electroactive polymer loudspeakers," in Proceedings of SPIE 6168, Y. Bar-Cohen, Ed., 61681M–61681M–8 (2006).

[3] Brochu, P., and Pei, Q., "Advances in dielectric elastomers for actuators and artificial muscles.," Macromolecular rapid communications 31(1), 10–36 (2010).

[4] Madden, J.D.W., [Dielectric elastomers as high-performance electroactive polymers] , in Dielectric Elastomers as Electromechanical Transducers, F. Carpi, D. De Rossi, R. Kornbluh, R. Pelrine, and P. Sommer-larsen, Eds., Elsevier, Amsterdam, 13–21 (2008).

[5] Pelrine, R., Kornbluh, R., and Kofod, G., "High-Strain Actuator Materials Based on Dielectric Elastomers," Advanced Materials 12(16), 1223–1225 (2000).

[6] Skov, A.L., and Sommer-Larsen, P., [Physical and chemical properties of dielectric elastomers] , in Dielectric Elastomers as Electromechanical Transducers, F. Carpi, D. De Rossi, R. Kornbluh, R. Pelrine, and P. Sommer-larsen, Eds., Elsevier, Amsterdam, 23–32 (2008).

[7] Kofod, G., "Dielectric elastomer actuators," The Technical University of Denmark, Ph. D. thesis(September), (2001).

[8] Ha, S.M., Yuan, W., Pei, Q., Pelrine, R., and Stanford, S., "Interpenetrating networks of elastomers exhibiting 300% electrically-induced area strain," Smart Materials and Structures 16(2), S280–S287 (2007).

[9] Pelrine, R., "High-Speed Electrically Actuated Elastomers with Strain Greater Than 100%," Science 287(5454), 836–839 (2000).

[10] Kofod, G., Sommer-Larsen, P., Kornbluh, R., and Pelrine, R., "Actuation Response of Polyacrylate Dielectric Elastomers," Journal of Intelligent Materials Systems and Structures 14(12), 787–793 (2003).

[11] Pei, Q., Pelrine, R., Rosenthal, M.A., Stanford, S., Prahlad, H., and Kornbluh, R.D., "Recent progress on electroelastomer artificial muscles and their application for biomimetic robots," in Proceedings of SPIE 5385, Y. Bar-Cohen, Ed., 41–50 (2004).

[12] Palakodeti, R., and Kessler, M.R., "Influence of frequency and prestrain on the mechanical efficiency of dielectric electroactive polymer actuators," Materials Letters 60(29-30), 3437–3440 (2006).

[13] Ha, S.M., Yuan, W., Pei, Q., Pelrine, R., and Stanford, S., "Interpenetrating Polymer Networks for High-Performance Electroelastomer Artificial Muscles," Advanced Materials 18(7), 887–891 (2006).

[14] Sommer-Larsen, P., Kofod, G., Shridhar, M.H., Benslimane, M., and Gravesen, P., "Performance of dielectric elastomer actuators and materials," in Proceedings of SPIE 4695, Y. Bar-Cohen, Ed., 158–166 (2002).

[15] Madsen, F.B., Dimitrov, I., Daugaard, A.E., Hvilsted, S.S., and Skov, A.L., "Novel cross-linkers for PDMS networks for controlled and well distributed grafting of functionalities by click chemistry," Polymer Chemistry 4(5), 1700–1707 (2013).

[16] Sperling, L.H., [Interpenetrating Polymer Networks: An Overview] , in Interpenetrating Polymer Networks, D. Klempner, L. H. Sperling, and L. A. Utracki, Eds., American Chemical Society, Washington, DC, 3–38 (1994).

[17] Ha, S.M., Park, I.S., Wissler, M., Pelrine, R., Stanford, S., Kim, K.J., Kovacs, G., and Pei, Q., "High Electromechanical Performance of Electroelastomers Based on Interpenetrating Polymer Networks," in Proceedings of SPIE 6927, Y. Bar-Cohen, Ed., 69272C–69272C–9 (2008).

[18] Ha, S.M., Yuan, W., Pei, Q., Pelrine, R., and Stanford, S., "New high-performance electroelastomer based on interpenetrating polymer networks," in Proceedings of SPIE 6168, Y. Bar-Cohen, Ed., 616808–616808–12 (2006).

[19] Brandell, D., Kasemägi, H., and Aabloo, A., "Poly(ethylene oxide)–poly(butadiene) interpenetrated networks as electroactive polymers for actuators: A molecular dynamics study," Electrochimica Acta 55(4), 1333–1337 (2010).

[20] Mathew, G., Rhee, J., Nah, C., and Leo, D., "Effects of silicone rubber on properties of dielectric acrylate elastomer actuator," Polymer Engineering & Science 46(10), 1455–1460 (2006).

[21] Plesse, C., Khaldi, A., Wang, Q., Cattan, E., Teyssié, D., Chevrot, C., and Vidal, F., "Polyethylene oxide–polytetrahydrofurane–PEDOT conducting interpenetrating polymer networks for high speed actuators," Smart Materials and Structures 20(12), 124002 (2011).

[22] Plesse, C., Vidal, F., Randriamahazaka, H., Teyssié, D., and Chevrot, C., "Synthesis and characterization of conducting interpenetrating polymer networks for new actuators," Polymer 46(18), 7771–7778 (2005).

[23] Plesse, C., Vidal, F., Gauthier, C., Pelletier, J.-M., Chevrot, C., and Teyssié, D., "Poly(ethylene oxide)/polybutadiene based IPNs synthesis and characterization," Polymer 48(3), 696–703 (2007).

[24] Cai, Z., and Kim, J., "Cellulose-chitosan interpenetrating polymer network for electro-active paper actuator," Journal of Applied Polymer Science 114(1), 288–297 (2009).

[25] Hoyle, C.E., and Bowman, C.N., "Thiol-ene click chemistry.," Angewandte Chemie (International ed. in English) 49(9), 1540–73 (2010).

[26] Lowe, A.B., "Thiol-ene 'click' reactions and recent applications in polymer and materials synthesis," Polymer Chemistry 1(1), 17–36 (2010).

[27] Yin, W., and Gu, T., "Silicon secondary crosslinked IPN based on poly (methyl acrylate-co-hydroxylethyl acrylate) and SiO2," Polymer 38(20), 5173–5178 (1997).

[28] Tanaka, T., "Peculiar space charge characteristics in some elastomers," in 2008 International Symposium on Electrical Insulating Materials (ISEIM 2008), 187–190 (2008).

[29] Sarathi, R., Danikas, M., Chen, Y., and Tanaka, T., "Understanding Charge Dynamics in Elastomers Adopting Pulsed Electro Acoustic (PEA) Technique," International Journal of Electrical and Electronics Engineering 4(5), 335–340 (2010).

[30] Larsen, A.L., Hansen, K., Sommer-Larsen, P., Hassager, O., Bach, A., Ndoni, S., and Jørgensen, M., "Elastic Properties of Nonstoichiometric Reacted PDMS Networks," Macromolecules 36(26), 10063–10070 (2003).

[31] Skov, A.L., Bejenariu, A., Bøgelund, J., Benslimane, M., and Egede, A.D., "Influence of micro- and nanofillers on electro-mechanical performance of silicone EAPs," in Proceedings of SPIE 8340, Y. Bar-Cohen, Ed., 83400M–83400M–10 (2012).

[32] Carpi, F., Gallone, G., Galantini, F., and Rossi, D. De, [Enhancing the dielectric permittivity of elastomers] , in Dielectric Elastomers as Electromechanical Transducers, F. Carpi, D. De Rossi, R. Kornbluh, R. Pelrine, and P. Sommer-Larsen, Eds., Elsevier, Amsterdam, 51–68 (2008).

[33] Sommer-Larsen, P., and Larsen, A.L., "Materials for dielectric elastomer actuators," in Proceedings of SPIE 5385, Y. Bar-Cohen, Ed., 68–77 (2004).

Article B2: *Reinforced poly(propylene oxide): a very soft and extensible dielectric electroactive polymer*

Goswami, K., Galantini, F., Mazurek, P. S., Daugaard, A. E., Gallone, G. & Skov, A. L. 2013 *Smart Materials and Structures* Vol. 22, 115011-1-7

Reinforced poly(propylene oxide): a very soft and extensible dielectric electroactive polymer

2013 Smart Mater. Struct. 22 115011

(http://iopscience.iop.org/0964-1726/22/11/115011)

Smart Mater. Struct. **22** (2013) 115011 (7pp) doi:10.1088/0964-1726/22/11/115011

Reinforced poly(propylene oxide): a very soft and extensible dielectric electroactive polymer

K Goswami[1], F Galantini[2], P Mazurek[1], A E Daugaard[1], G Gallone[2,3] and A L Skov[1]

[1] DTU, The Danish Polymer Centre, Department of Chemical and Biochemical Engineering, Kongens Lyngby, Denmark
[2] 'E Piaggio' Research Centre, University of Pisa, Largo Lucio Lazzarino 2, I-56122, Pisa, Italy
[3] Department of Civil and Industrial Engineering, University of Pisa, Largo Lucio Lazzarino 2, I-56122, Pisa, Italy

E-mail: al@kt.dtu.dk

Received 28 June 2013, in final form 30 August 2013
Published 3 October 2013
Online at stacks.iop.org/SMS/22/115011

Abstract
Poly(propylene oxide) (PPO), a novel soft elastomeric material, and its composites were investigated as a new dielectric electroactive polymer (EAP). The PPO networks were obtained from thiol-ene chemistry by photochemical crosslinking of α,ω-diallyl PPO with a tetra-functional thiol. The elastomer was reinforced with hexamethylenedisilazane treated fumed silica to improve the mechanical properties of PPO. The mechanical properties of PPO and composites thereof were investigated by shear rheology and stress–strain measurements. It was found that incorporation of silica particles improved the stability of the otherwise mechanically weak pure PPO network. Dielectric spectroscopy revealed high relative dielectric permittivity of PPO at 10^3 Hz of 5.6. The relative permittivity was decreased slightly upon addition of fillers, but remained higher than the commonly used acrylic EAP material VHB4910. The electromechanical actuation performance of both PPO and its composites showed properties as good as VHB4910 and a lower viscous loss.

S Online supplementary data available from stacks.iop.org/SMS/22/115011/mmedia

1. Introduction

The interest in using elastomers for electromechanical transducers has increased during the last decade due to their large strains, frequency responses of the order of milliseconds, work densities higher than human muscle, and a high degree of electromechanical coupling [1, 2]. A special class of elastomers known as dielectric electroactive polymers (DEAPs) has emerged as a strong candidate in this field due to their low density, fast response time, low cost of production, low energy consumption and low heat generation. It has been found that these DEAPs possess mechanical properties very similar to human muscle and can mimic human muscular function, and thus they are commonly nicknamed 'artificial muscle' [3].

In a typical configuration for DEAP transducers, a thin film of dielectric elastomer is sandwiched between very thin layers of compliant electrodes, which are connected to the power supply for transduction. The equation governing the actuation of a DEAP actuator is given as [4]

$$p = \varepsilon_0 \varepsilon_r E^2 = \varepsilon_0 \varepsilon_r \left(\frac{V}{d}\right)^2 \quad (1)$$

where p is the electrostatic pressure acting on the dielectric elastomer due to an applied electric field E, V is the applied voltage, d is the thickness of the dielectric elastomer, ε_0 is the vacuum dielectric permittivity (8.85×10^{-12} F m^{-1}) and ε_r is the relative permittivity of the elastomer. At equilibrium, the electrostatic pressure equals the internal stress in the material so that the strain produced on the elastomer (S) can be written

as

$$S = \frac{\varepsilon_0 \varepsilon_r}{Y} \left(\frac{V}{d}\right)^2 \quad (2)$$

where Y is the elastic modulus of the elastomer. Widely used DEAPs include poly(dimethyl siloxane) (PDMS), acrylics and polyurethane (PU), but each of them suffers from one or more drawbacks such as low dielectric permittivity, long response time or high elastic modulus etc. As a fact, none of the elastomers available on the market today are designed specifically for transduction, and this leaves room for further development of the materials. One downside of the currently used materials is the high voltage required for transduction, which adds cost to the transducer device due to expensive electronic components. From equation (2), it is seen that to lower the required voltage for a given strain of DEAP, we can decrease either the film thickness or the elastic modulus or alternatively increase the relative permittivity of the elastomer. The influence of material properties and processing parameters such as elastic modulus, dielectric constant and film thickness on the electromechanical properties for commercially available PDMS has already been discussed by Skov *et al* [5]. For large scale processing a thickness of 40 μm is currently the threshold value for thin films with corrugations prepared from commercially available silicone so it is not regarded as a possible optimization parameter here [6].

A decrease of the elastic modulus is not easily achieved since filler particles are required in most systems to improve the mechanical properties, such as maximum elongation and tear strength. Bejenariu *et al* [7] showed that by use of an advanced mixing sequence, so-called heterogeneous bimodal networks could be prepared. The heterogeneous bimodal networks possessed very small elastic moduli and simultaneously improved tear strength and maximum elongation compared to unfilled silicone.

The first elastomeric material to be used successfully as a dielectric elastomer was the acrylic VHB tape from 3M. In an earlier article on dielectric elastomers, it was reported that this material showed extraordinarily high strain and high electrostatic pressure. It was also shown in the same article that the performance could be increased manifold by applying prestrain in the planar direction [8]. But the long response time and need for prestrain of VHB are the reasons for the decreasing trend of using VHB as DEAP material. On the other hand commercially available silicones do not require prestrain. However, prestrain of silicones is still favorable but not as necessary as for the acrylics, since the Young's modulus decreases after prestretch and the films become thinner [9]. Since the high operating voltage adds to the cost of the transducer, a great deal of research is focused on increasing the dielectric permittivity of the DEAP material in order to reduce the operating voltage. By blending two low dielectric constant elastomers, PDMS and PU, Gallone *et al* [10] obtained a new dielectric elastomer with improved transduction performance. Also, the use of a 0.5 wt% of properly functionalized carbon nanotubes as a filler for a polyurethane elastomer was demonstrated to be effective in increasing the ε_r/Y ratio, without worsening the dielectric losses, and doubled the transduction performance of the neat matrix [11]. Polyurethanes [12, 13] possess higher dielectric permittivity than PDMS, but suffer from higher dielectric loss and lower breakdown voltage compared to PDMS due to moisture absorption, and therefore they must be maintained under strict environmental conditions with respect to temperature and humidity.

As an alternative to both PDMS and PU, in this study PPO has been investigated as a new DEAP material against commercially available acrylic (VHB4910). The aim was to develop a new DEAP material with enhanced electromechanical response, compared to VHB. In addition, a thorough electrical breakdown measurement of this system could also be made in the future in order to investigate the effect of filler addition on the electrical breakdown strength, as it is known that such a particulate filled system could suffer from low breakdown strength. Jensen *et al* [14, 15] investigated the networks from PPO as materials for very soft skin adhesives. They applied silicone hydride functional crosslinkers to crosslink the end-linked vinyl functional PPO, which was found to be inefficient. In the work presented here, novel, fast and efficient UV photo-crosslinking was employed to crosslink PPO and its composites with treated fumed silica. Mechanical, dielectric, rheological and electromechanical characterization was performed on the new material and its composites in order to evaluate the potential of PPO as a new electroactive polymer.

2. Experimental details

2.1. Materials

Allyl terminated PPO of approximate molecular weight 16 500 g mol^{-1} (Kaneka Silyl ACS 003) was obtained from Kaneka Corp., Japan. 2,4,6-trimethylbenzoyl-phenylphosphinic acid ethyl ester (Lucirin TPO-L) was purchased from BASF. VHB 4910 was obtained as 1 and 0.5 mm thick films with polyethylene backing material from 3M. The filler used for the elastomeric composites was hexamethyldisilazane (HMDS) treated fumed silica AEROSIL® R812, from Evonik Industries. The reported Brunauer, Emmett and Teller (BET) surface area of AEROSIL® R812 was 260±30 m^2 g^{-1}. All the other chemicals used in this work were purchased from Sigma-Aldrich.

2.2. Methods

Rheological tests were performed in a stress controlled rheometer (AR2000) from TA Instruments, with 25 mm parallel plate geometry. Measurement conditions were set to controlled strain mode at 1% strain, which was ensured to be within the linear viscoelastic region as determined from initial strain sweeps. Frequency sweep experiments were performed from 100 to 0.001 Hz at 25 °C. Broadband dielectric spectroscopy was carried out on disk-shaped samples of both the pure matrix and the composites (diameter of 25 mm and thickness 1 mm) at 25 °C in the frequency range 20 Hz–2 MHz by means of an ARES G2 rheometer

equipped with DETA accessory including an inductance (*L*)—capacitance (*C*)—resistance (*R*) (*LCR*) meter (Agilent E4980A). The electromechanical response of the PPO films, shaped in rectangular material strips of dimension 20 × 25 mm^2 and thickness varying between 80 and 226 μm, was studied after they were provided with opposed compliant electrodes by smearing a carbon based conductive grease (Nyogel 755G, Tecnolube Seal, USA) on both their major surfaces. For each sample a vertical prestrain of 100% and a dc high voltage with stepwise increment of 250 V were applied across the elastomer by means of a power supply (HV-DC 205A-30P, Bertan, USA). At each voltage level isotonic transverse strains were measured by a displacement transducer, waiting until a constant deformation was obtained. One sample for each composition was measured. A two-column ultimate testing machine (5500R, Instron, UK) was used to perform uniaxial elongation tests for PPO and the composites at a constant deformation rate of 25 mm min^{-1} with a 10 N load cell. Molecular weights and polydispersity index (PDI) were estimated by size exclusion chromatography (SEC) using Viscotek GPCmax VE-2001. The machine was equipped with Viscotek TriSEC Model 302 triple detector array (refractive index detector, viscometer detector, and laser light scattering detector with the light wavelength of 670 nm, and measuring angles of 90° and 7°) and a Knauer K-2501 UV detector using two PLgel mixed-D columns from Polymer Laboratories (PL). The samples were run in tetrahydrofuran (THF) at 30 °C (1 ml min^{-1}). Molecular weights were calculated using polystyrene (PS) standards from PL. Nuclear magnetic resonance (NMR) spectroscopy was performed on a 300 MHz cryomagnet from Spectrospin and Bruker, in $CDCl_3$ at room temperature. Fourier transform infrared spectroscopy (ATR-FTIR) was performed on a Nicolet iS50 from Thermo Fischer Scientific with a universal attenuated total reflection sampling accessory on a diamond crystal.

2.2.1. Standard procedure for preparation of PPO networks. Pentaerythritol tetrakis (3-mercaptopropionate) (4 functional crosslinker, 0.244 g, 0.5 mmol) and 2,4,6-trimethylbenzoyl-phenylphosphinic acid ethyl ester (Lucirin TPO-L) (photoinitiator, 0.192 g, 0.6 mmol) were added to α, ω-diallyl PPO (10 g (0.6 mmol of allyl groups) $M_n = 16\,500$ g mol^{-1}) and mixed in a SpeedMixer™ (DAC 150 FVZ, Hauschild Co., Germany) at 3500 rpm for 5 min. The mixture was poured into an 8 cm × 10 cm steel mold placed over a glass plate lined with Parafilm® M. This setup was kept in a well-ventilated place for 45–60 min and subsequently transferred to the UV chamber ($\lambda = 365$ nm, 4.5 mW cm^{-2}) and irradiated for 45 min in ambient atmosphere.

2.2.2. Standard procedure for filled PPO systems. The system was prepared as above for PPO networks. The filler was added with 40–60 wt% toluene directly into the PPO–crosslinker mixture prior to speed mixing; otherwise, the procedure was unchanged. The resulting films were studied by scanning electron microscopy (SEM) to ensure proper mixing of the fillers into the elastomer.

Table 1. Storage modulus (G') of networks at different crosslinker contents at 10^{-3} Hz. (Note: the complete data series has been included in SI-figure 1 (available at stacks.iop.org/SMS/22/115011/mmedia).)

Stoichiometry (r)	0.8	1.0	1.2	1.32	1.65	1.85
G' (kPa)	0.49	0.30	0.43	25.2	34.7	27.9

3. Results and discussions

3.1. Sample preparation and characterization

In this study a novel network material for DEAP applications based on PPO was prepared. The network was prepared through highly efficient crosslinking of a commercially available α,ω-diallyl poly(propylene oxide) with pentaerythritol tetrakis(3-mercaptopropionate), a tetra-functional thiol. Thiol-ene reactions are a type of 'click' reactions that are characterized by being highly efficient and easy to perform in bulk processes [16, 17]. The reaction is tolerant to a large number of functional groups and can be initiated through both thermal and photochemical initiators, as shown in scheme 1 for the photochemical initiator (Lucirin) applied here.

The thiol-ene crosslinking reaction shown in scheme 1 relies on a high degree of end-group functionality in order to be efficient and produce a crosslinked network with a minimum of dangling chains. The presence of the end groups on the commercial α,ω-diallyl PPO base material has been confirmed by ^{1}H-NMR spectroscopy, where the presence of the allyl end group was confirmed with a characteristic set of doublets at 5.2 ppm and a multiplet at 5.9 ppm. The presence of the allyl end groups was also confirmed by FT-IR, where the double bond stretching was found at 1650 cm^{-1}.

The crosslinked PPO networks were prepared with a controlled stoichiometric imbalance (r) [18], which is defined as $r = \frac{f[\text{thiol}]_0}{2[\text{vinyl}]_0}$, where f is the average functionality of the crosslinker used and $[\cdots]_0$ is the initial molar concentration of the reactive groups present in the crosslinker (thiol) and in the polymer (vinyl).

In order to obtain the mechanically strongest network, rheological tests were performed on PPO networks by monitoring the storage modulus (G') in the linear viscoelastic region for different compositions. The storage moduli at 10^{-3} Hz are summarized in table 1.

From table 1, it can be seen that the mechanically strongest network was obtained at approximately $r = 1.65$ corresponding to the highest G' among other pure PPO networks and this stoichiometry was thereafter kept constant throughout the study for the pure PPO network and PPO composites.

The pure PPO network was prepared as shown in scheme 1. Particle composites were prepared as for the pure PPO network, with the addition of different amounts of filler before mixing and UV crosslinking. In the compositions, the non-rubber ingredients (such as fillers in this case) are expressed as parts per hundred rubber (phr). In this convention, the filler amount is taken as the ratio against 100

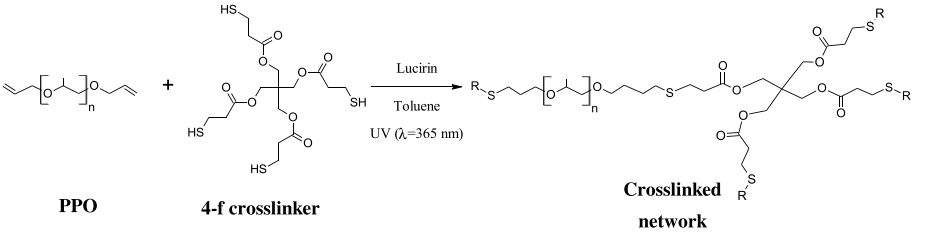

Scheme 1. Photoinitiated crosslinking of α, ω-diallyl PPO by thiol-ene chemistry, where *R* signifies the network.

parts (by weight) of rubber. In a typical composition, PPO_10 indicates 10 phr (1 g) treated fumed silica was mixed with 10 g pure PPO.

3.2. Rheological measurement

The linear viscoelastic (LVE) properties of pure and composite PPO networks were measured in order to characterize the material response in the low strain limit. Figure 1(a) shows the storage modulus (G') and figure 1(b) shows the loss tangent (tan delta) of the materials. Tan delta is also known as the damping of the material. It is obvious that, with respect to the viscous loss in the investigated frequency regime, all PPO networks are superior to VHB (see inset in figure 1(b) for comparison).

From figure 1(a) it can be seen that the storage modulus (G') at the plateau (terminal) region (10^{-3} Hz) is approximately 35 kPa for pure PPO which is very low compared to VHB as well as non-filled silicone elastomers [18]. On the addition of treated fumed silica into the soft PPO network, the storage modulus (G') at low frequencies gradually increases from 35 to 106 kPa due to the hindrance in chain movement imposed by the filler.

The tan delta plots (figure 1(b)) also give some insight into the molecular motion and damping behavior of the polymers. At 5 phr treated fumed silica loading, the viscous loss of pure PPO is reduced significantly in the entire frequency range, and it continues to decrease as the filler content is raised up to 10 phr. However, upon addition of 15 and 30 phr treated fumed silica the composites show increased tan delta, indicating prominent damping behavior of the composites and hence a possible destruction of the network properties [18]. Moreover, at low frequencies the samples containing treated fumed silica exhibit an almost stable tan delta, as is typical for a loaded crosslinked rubber in which chain movements are further restricted due to the presence of filler particles. Compared to PPO, VHB remains a material with a significant loss, a higher tan delta and showing a much more dispersive behavior than PPO and any of the composites (figure 1(b)).

3.3. Dielectric spectroscopy

One interesting aspect of this study is the measurement of the effect of incorporating treated fumed silica as a reinforcing

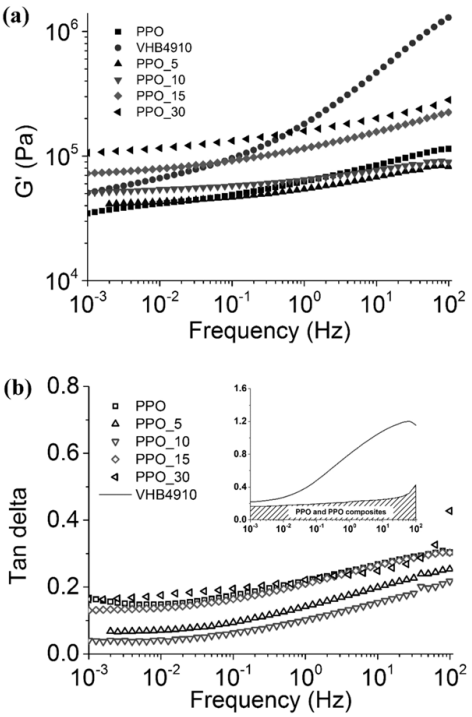

Figure 1. (a) Storage modulus and (b) tan delta versus frequency for pure PPO and filled PPO networks at 25 °C. Inset shows the difference in tan delta between the PPO formulations (shaded region) and VHB.

agent on dielectric permittivity of PPO. Figures 2(a) and (b) show dielectric spectra for PPO and its composites.

At low frequencies, an increase in the dielectric constant of both PPO and its composites is observed as frequency is progressively lowered from about 10^2 down to 20 Hz (figure 2(a)), which is accompanied by a parallel increase of tan delta (figure 2(b)). Such an increase, which shows up as a low frequency dispersion in all dielectric spectra, can be ascribed to Maxwell–Wagner polarization, which is caused by a limited displacement of charges induced by the electric field in corresponding interfaces between different phases. While in the case of pure PPO such dispersion could

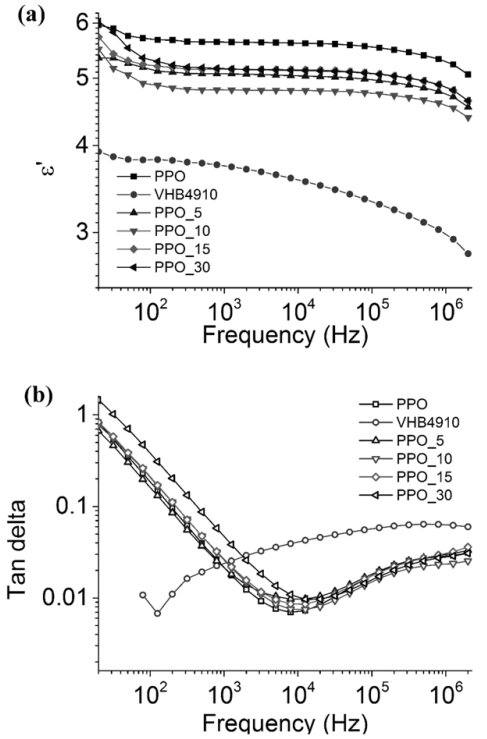

Figure 2. Dielectric spectroscopy plot (a) real part of permittivity versus frequency and (b) imaginary part of permittivity versus frequency for PPO and the composites.

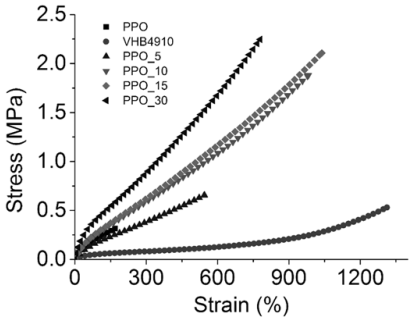

Figure 3. Tensile testing of PPO and reinforced composites.

Table 2. Local elastic modulus of PPO and its composites at different strains.

Sample	Modulus at 25% strain (kPa)	Modulus at 50% strain (kPa)	Modulus at 100% strain (kPa)
PPO	264	205	143
VHB4910	78	31	19
PPO_5	200	160	119
PPO_10	327	241	176
PPO_15	338	240	178
PPO_30	474	344	239

arise only from a polarization contribution at the level of the sample/electrode interface, in the composites it could be indicative of the presence of further interfaces. Indeed, the fact that in the composites such polarization effects are more significant than in pure PPO is likely due to the presence of interfaces between the PPO matrix and the filler. Coherently, it is also found that as the filler amount is increased, the interface polarization effect increases. In the region of medium–high frequencies (10^2–10^6 Hz), where the dielectric response mainly depends on the bulk polarization processes [19], there are no significant changes in the ε' (figure 2(a)) for all the materials. However, the dielectric constant varies with the composites compared to that of the pure matrix. From figure 2(a) the relative dielectric constant for pure PPO at 1 kHz can be determined to be 5.6, which is higher than the value reported for VHB4910 (3.21 at 1 kHz) [20, 21]. Treated fumed silica was used as a filler for reinforcement, and since it is a low dielectric constant filler ($\varepsilon_r = 3.9$) it gives a minor decrease in the dielectric permittivity, as predicted by common mixing rules [22]. Although, at higher treated fumed silica content the bulk permittivity of PPO_15 and PPO_30 becomes higher than PPO_5 and PPO_10, it remains lower than the pure matrix. This change in the behavior of the dielectric properties at higher filler loading factors could be the result of a larger contribution from interfaces at filler/matrix boundaries as the filler volume fraction is increased. Some studies have already revealed that the presence of such boundary layers inside a material increases the dielectric permittivity. For instance, at the interface between matrix and filler in a particulate composite or between two immiscible phases in a polymer blend, intermediate interaction regions can provide additional polarization properties, which can play a major role in determining the final permittivity of such material [10, 23–25].

3.4. Mechanical analysis

The mechanical properties of PPO and reinforced composites were investigated by tensile testing as shown in figure 3.

Each test was stopped either at sample break, which occurred for all samples except PPO_30, or when the load cell reached maximum limit (10 N). Observed elongation at break of pure PPO is 170% while all the composites show maximum elongation exceeding 500%. Thus, filler incorporation in PPO network increases the extensibility of the networks, clearly showing the desired improvement in mechanical stability of the prepared composites.

Table 2 summarizes the local elastic moduli (tangent slope) at different strains of PPO and the composites.

From the table, it is clear that for PPO composites the local elastic modulus steadily decreases as the strain is increased up to about 100%, which is a common feature of elastomeric behavior. At higher elongations the situation

Table 3. Material data comparison between PPO, PPO_5 and VHB4910.

Sample	Shear modulus (kPa) at 10^{-3} Hz	Tan delta from rheology at 10^{-3} Hz	Storage permittivity at 1 kHz	Tensile modulus (kPa) at 100% strain	Electrically induced strain (%) at ∼14 V μm^{-1}
PPO	34.7	0.16	5.6	143	1.2
PPO_5	41.2	0.07	5.1	119	1.6
VHB4910	50.7	0.2	3.7	19	1.8

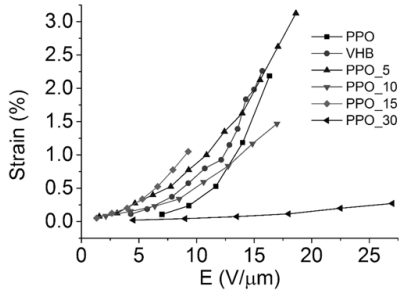

Figure 4. Electromechanical response of PPO and the composites.

changes and a steeper monotonic increase in the stress curves is observed (except for pure PPO as the sample failed at about 170% strain), recognizable as an up-swing after a flex point above 100% strain, which is due to the preferred orientation of the polymer chains in the direction of extension. When the filler amount is increased, the respective curves shift to higher stresses at corresponding strains (figure 3) with the exception of PPO_5, for which the response remains below that of the pure matrix. One plausible reason might be that in the case of PPO_5 the reduction of crosslink density dominates induced mechanical improvement due to filler addition thereby making the sample softer than PPO. A markedly different stress–strain behavior is observed for VHB, where a very low modulus at strains below 600% is observed (which is advantageous for electromechanical actuation) followed by a moderate increase at strains beyond 900%.

3.5. Actuation study

Electromechanical tests were performed on 100% pre-stretched samples of both PPO and its composites, and the results are presented in figure 4. The electromechanical response of prestretched VHB4910 is included in figure 4 for easy comparison. Due to the detection of partial electrical conduction at fields over 20 V μm^{-1} in samples containing treated fumed silica, the effective electric field acting on these samples was not considered reliable beyond this threshold value. Therefore, data have been reported only for reliable values below 20 V μm^{-1} (with the exception of PPO_30, which showed reliable actuation at an electric field as high as 27 V μm^{-1}). For pure PPO the sample failed at fields around 17 V μm^{-1}, while VHB4910 did not show any such failure.

As seen in figure 4, the electromechanical response of pure PPO is very close to that of VHB4910. Addition of filler significantly reduces the stickiness of PPO and improves its mechanical performance manifold (figures 1 and 3). The decrease in Young's modulus at low filler loading, followed by an increase as filler amount is increased, directly reflects on the electromechanical response of PPO composites. From figure 4, it can be seen that PPO_5 shows the maximum actuation strain among the studied PPO composites, followed by PPO_10 and PPO_15. The relatively low actuation strain of PPO_10 and PPO_15 is due to the higher modulus and lower dielectric permittivity compared to pure PPO and PPO_5. At higher content of treated fumed silica the strain induced by the electrostatic pressure becomes very small as can be seen for PPO_30. These observations are in good agreement with equation (2) and all measurements agree well at low voltages whereas the different losses start to play an important role at higher voltages for all types of materials investigated here. Considering the results obtained from electromechanical tests, PPO filled with small amounts of filler has very good actuation behavior and good mechanical properties. Higher filler content gave better mechanical property, but severely hindered the electromechanical performance of the material. Therefore a convenient tradeoff between the required mechanical reinforcement of PPO composites and the electromechanical response opens a pathway into the development of stacked actuators [26, 27]. The PPO samples possess natural adhesiveness, which would be beneficial for sandwiching several actuators on top of each other. Future development of this material would be to strike a balance between improving mechanical properties and electromechanical response by either employing chemical modification of the base polymer or using novel filler materials. However, the filler selection is limited to fillers with little UV absorption.

Table 3 summarizes and compares all the material data for PPO, PPO_5 and VHB4910 obtained in this study.

From table 3 it is seen that pure PPO is a relatively soft material; however, it shows high viscous loss owing to high tan delta. When treated fumed silica is added, the shear modulus increases, indicating reinforcement effect of the PPO matrix with a parallel decrease in viscous loss. The storage permittivity of pure PPO is about 1.5 times higher than VHB4910 although a slight decrease in permittivity can be seen in the case of PPO_5 as predicted by the mixing rule mentioned earlier. PPO_5 and VHB4910 show similar electromechanical behavior which is an improvement over pure PPO.

4. Conclusions

This study reveals the potential of PPO reinforced with treated fumed silica filler as a new dielectric electroactive polymer actuator. A novel PPO elastomer and its composites

were developed by a simple and easily manageable processing scheme. Shear rheology showed enhancement in the mechanical stability of PPO composites over the mechanically weak pure PPO network, and additionally, both PPO and its composites showed significantly less viscous loss as compared to the widely used VHB elastomer. The reinforcement effect was also reflected in mechanical tests, where the composites showed elongations of more than 500% compared to the 150% for the pure network. The relative permittivity of pure PPO at 10^3 Hz was found to be 5.6, and all the PPO composites showed permittivities above 4.8, which is significantly higher than VHB4910. The electromechanical test showed that PPO composites with small amounts of filler (5–10 phr) have the best electromechanical behavior. The observed performance, combined with their intrinsic stickiness, suggests that these materials have a great potential in the application area of stacked actuators. PPO composites were also found to be similar to VHB4910 in their electromechanical response with the added advantage of possessing very low viscous dissipation. Furthermore, PPO presents another advantage over VHB4910 since further optimization of PPO networks is allowed due to the reactive handles resulting from an excess of thiol groups. This will be studied in the future.

Acknowledgments

The authors acknowledge financial support for this research from both Danish Agency for Science, Technology and Innovation and the Danish National Advanced Technology Foundation.

The STSM (Short-Term Scientific Missions) program in the framework of ESNAM (European Scientific Network for Artificial Muscles)—COST (European Cooperation in Science and Technology) Action MP1003, is also gratefully acknowledged.

References

[1] Madden J D W 2008 Dielectric elastomers as high-performance electroactive polymers *Dielectric Elastomers as Electromechanical Transducers* ed F Carpi, D De Rossi, R Kornbluh, R Pelrine and P Sommer-larsen (Amsterdam: Elsevier) pp 13–21

[2] Pelrine R, Kornbluh R and Kofod G 2000 High-strain actuator materials based on dielectric elastomers *Adv. Mater.* **12** 1223–5

[3] Shankar R, Ghosh T K and Spontak R J 2007 Dielectric elastomers as next-generation polymeric actuators *Soft Matter* **3** 1116–29

[4] Pelrine R E, Kornbluh R D and Joseph J P 1998 Electrostriction of polymer dielectrics with compliant electrodes as a means of actuation *Sensors Actuators* A **64** 77–85

[5] Skov A L, Bejenariu A, Bøgelund J, Benslimane M and Egede A D 2012 Influence of micro- and nanofillers on electro-mechanical performance of silicone EAPs *Proc. SPIE* **8340** 83400M

[6] Vudayagiri S, Junker M D and Skov A L 2013 Factors affecting the surface and release properties of thin polydimethylsiloxane films *Polym. J.* **45** 871–8

[7] Bejenariu A G, Yu L and Skov A L 2012 Low moduli elastomers with low viscous dissipation *Soft Matter* **8** 3917–23

[8] Pelrine R 2000 High-speed electrically actuated elastomers with strain greater than 100% *Science* **287** 836–9

[9] Akbari S, Rosset S and Shea H R 2013 More than 10-fold increase in the actuation strain of silicone dielectric elastomer actuators by applying prestrain *Proc. SPIE* **8687** 86871P

[10] Gallone G, Galantini F and Carpi F 2010 Perspectives for new dielectric elastomers with improved electromechanical actuation performance: composites versus blends *Polym. Int.* **59** 400–6

[11] Galantini F, Bianchi S, Castelvetro V and Gallone G 2013 Functionalized carbon nanotubes as a filler for dielectric elastomer composites with improved actuation performance *Smart Mater. Struct.* **22** 055025

[12] Ueda T, Kasazaki T, Kunitake N, Hirai T, Kyokane J and Yoshino K 1997 Polyurethane elastomer actuator *Synth. Met.* **85** 1415–6

[13] Jo N-J, Lim D-H, Bark G-M, Chun H-H, Lee I-W and Park H 2010 Polyurethane-based actuators with various polyols *J. Mater. Sci. Technol.* **26** 763–8

[14] Jensen M K, Bach A, Hassager O and Skov A L 2009 Linear rheology of cross-linked polypropylene oxide as a pressure sensitive adhesive *Int. J. Adhes. Adhes.* **29** 687–93

[15] Jensen M K, Hassager O, Rasmussen H K, Skov A L, Bach A and Koldbech H 2009 Planar elongation of soft polymeric networks *Rheol. Acta* **49** 1–13

[16] Lowe A B 2010 Thiol-ene click reactions and recent applications in polymer and materials synthesis *Polym. Chem.* **1** 17–36

[17] Hoyle C E and Bowman C N 2010 Thiol-ene click chemistry *Angew. Chem. Int. Edn* **49** 1540–73

[18] Frankær S M G, Jensen M K, Bejenariu A G and Skov A L 2012 Investigation of the properties of fully reacted unstoichiometric polydimethylsiloxane networks and their extracted network fractions *Rheol. Acta* **51** 559–67

[19] Carpi F, Gallone G, Galantini F and De Rossi D 2008 Enhancing the dielectric permittivity of elastomers *Dielectric Elastomers as Electromechanical Transducers* ed F Carpi, D De Rossi, R Kornbluh, R Pelrine and P Sommer-Larsen (Amsterdam: Elsevier) pp 51–68

[20] www.3m.com

[21] Molberg M, Leterrier Y, Plummer C J G, Walder C, Löwe C, Opris D M, Nüesch F A, Bauer S and Månson J-A E 2009 Frequency dependent dielectric and mechanical behavior of elastomers for actuator applications *J. Appl. Phys.* **106** 054112

[22] Gallone G, Carpi F, De Rossi D, Levita G and Marchetti A 2007 Dielectric constant enhancement in a silicone elastomer filled with lead magnesium niobate–lead titanate *Mater. Sci. Eng.* C **27** 110–6

[23] Ozmusul M S and Picu R C 2002 Elastic moduli of particulate composites with graded filler–matrix interfaces *Polym. Compos.* **23** 110–9

[24] Todd M G and Shi F G 2003 Characterizing the interphase dielectric constant of polymer composite materials: effect of chemical coupling agents *J. Appl. Phys.* **94** 4551–7

[25] Todd M G and Shi F G 2005 Complex permittivity of composite systems: a comprehensive interphase approach *IEEE Trans. Dielectr. Electr. Insul.* **12** 601–11

[26] Kovacs G, Düring L, Michel S and Terrasi G 2009 Stacked dielectric elastomer actuator for tensile force transmission *Sensors Actuators* A **155** 299–307

[27] Bar-Cohen Y 2009 Electroactive polymer (EAP) actuators for future humanlike robots *Proc. SPIE* **7287** 728703

Article B3: *UV-Cured, Platinum-Free, Soft Poly(dimethylsiloxane) Networks*

Goswami, K., Skov, A. L. & Daugaard, A. E. 2014 *Chemistry: A European Journal* Vol. 20, 9230-9233

ChemPubSoc Europe
DOI: 10.1002/chem.201402871
CHEMISTRY A European Journal Communication

Silicon Polymers

UV-Cured, Platinum-Free, Soft Poly(dimethylsiloxane) Networks

K. Goswami, A. L Skov, and A. E. Daugaard*[a]

Abstract: To overcome the drawbacks exhibited by platinum-catalyzed curing of silicones, photoinitiated thiol–ene cross-linking of high-molecular-weight poly(dimethylsiloxane) (PDMS) prepolymers has been investigated as a pathway to novel soft PDMS networks, based on commercially available starting materials was developed. Through a fast and efficient two-step cross-linking reaction highly flexible PDMS elastomers were prepared.

In recent years, UV chemistry has gained importance in curing of elastomers, as it allows for rapid reaction at ambient temperature and thereby saves energy. Moreover, since little or no solvent is involved in the UV curing it can be considered an environmentally friendly process.[1] Depending on the types of photoinitiators used, UV curing follows either free-radical, cationic, or photoacid mechanisms. In the free-radical mechanism, the photoinitiator absorbs UV light and generates free radicals, which react with unsaturated bonds and initiate the cross-linking process. Free-radical-initiated reactions are generally very fast and have been applied for especially acrylate-based systems as they are efficient and fast enough to take place at ambient conditions.[2] However, the cross-linking requires an inert atmosphere, which puts substantial limitations to the broader application of such systems.[3] Recently, increased attention has been drawn to the use of thiol–ene chemistry as an alternative reaction, since it does not require an inert atmosphere and benefits from the presence of oxygen for inhibition of side reactions.[4] Thiol–ene reactions generally take place under ambient conditions and have been used for preparation of a large range of systems, including side-chain functionalization of polymers as well as for cross-linking of bulk systems.[5]

In the silicone industry, the majority of vinyl-terminated silicones that are cured at low temperatures use platinum-catalyzed addition reactions. Only a few silicone formulations can be cured through UV curing, and most of these UV-curable silicones still use platinum for additional addition cross-linking reactions.[6] The major drawbacks of platinum-catalyzed cross-linking of silicones are the highly priced noble metal catalyst used in the cross-linking reaction as well as poisoning of the catalyst by compounds containing nitrogen, sulfur, phosphorus, and tin. Studies have been done extensively on UV curing of acrylic silicones[7] or classical condensation curing by UV light,[8] but very few examples on vinyl-terminated silicones are available in the literature.[9] Previously prepared UV-curable PDMS systems rely on low-molecular-weight linear PDMS, which results in heavily cross-linked hard networks.[9b,c] To overcome the drawbacks exhibited by platinum-catalyzed curing of silicones, photoinitiated thiol–ene cross-linking of high-molecular-weight PDMS prepolymers have been investigated as a pathway to novel soft PDMS networks.

The possibility of performing a simple, direct, cross-linking of a commercially available α,ω-terminated vinyl PDMS by photoinitiated thiol–ene chemistry as shown in Scheme 1was initially investigated.

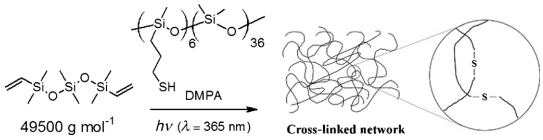

Scheme 1. UV-initiated thiol–ene cross-linking of α,ω-vinyl PDMS with poly(3-mercaptopropylmethylsiloxane)-*co*-dimethylsiloxane) by employing 2,2-dimethoxy-2-phenylacetophenone (DMPA) as photoinitiator.

The direct cross-linking of high-molecular-weight PDMS prepolymers ($M_w = 49500\ g\,mol^{-1}$) resulted in networks with a very long curing time of up to 5–7 days. Such slow curing kinetics is believed to be due to slow diffusion of the cross-linker molecule, which in turn slows down the cross-linking reaction. Silicones that contain vinyl groups as the reactive group are either cross-linked at low temperatures by addition reactions, or at elevated temperatures by peroxides. Peroxide-cured silicones are known to be more prone to slow curing kinetics due to the formation of volatiles during the cross-linking reaction compared to addition-cured silicones.[10] Shama et al. showed similar effects in UV-cured urethane/acrylate and vinyl ether/urethane systems.[11] Compared to the acrylate systems and the classical hydrosilylation reactions, the thiol–ene system is not as fast, which is believed to result in the reaction being heavily influenced by diffusion and thereby the viscosity of the reaction medium and the molecular weight of the prepolymers.

The high-molecular-weight PDMS is a requirement in order to prepare soft networks with a sufficiently low cross-linking

[a] *K. Goswami, Prof. A. L. Skov, Prof. A. E. Daugaard*
Danish Polymer Centre
Department of Chemical and Biochemical Engineering
Technical University of Denmark, DTU
Søltofts Plads, Building 229, 2800, Kgs. Lyngby (Denmark)
Fax: (+45) 4588-2161
E-mail: adt@kt.dtu.dk

Supporting information for this article is available on the WWW under http://dx.doi.org/10.1002/chem.201402871.

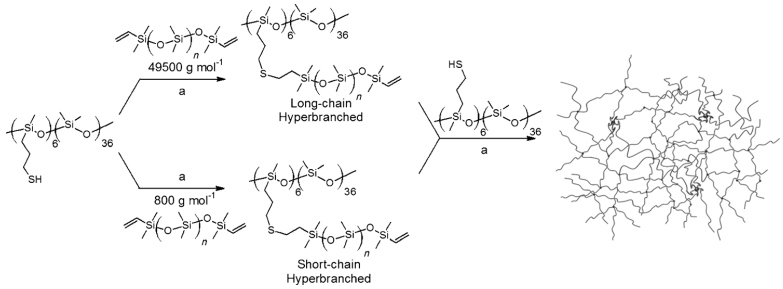

Scheme 2. Preparation of hyperbranched intermediates based on high- and low-molecular-weight PDMS from poly(3-mercaptopropylmethylsiloxane)-*co*-dimethylsiloxane) reacted with excess of α,ω-vinyl-PDMS (49 500 and 800 g mol^{-1}, respectively); a) DMPA, $h\nu$, $\lambda = 365$ nm. Combination of the hyperbranched intermediates and following photocross-linking resulted in a fast and efficient network formation.

density. Heterogeneous bimodal networks have been advocated as a pathway to mechanically improved systems without the requirement of reinforcing fillers.[12] Another advantage of such systems is that they show superior efficiency in mixing due to lower viscosity of the reactive mixture before cross-linking. This reduced viscosity of the bimodal systems were exploited here in order to increase the rate of reaction and prevent the viscosity limiting effect observed for direct mixing as shown in Scheme 2.

The hyperbranched intermediates were formed fast and efficiently through the UV-initiated thiol–ene reaction, since the prereactions are run at off-stoichiometric conditions ensuring that hyperbranching takes place below the gelation point. The theoretical fraction of unreacted polymer chains in the pre-reacted mixtures is calculated as $(1-r)^2 = 0.81$, in which r is the stoichiometry given by $r = n(\mathrm{SH})/n(\mathrm{enes})$, since an unreacted polymer chain requires that both chain ends are unreacted, that is, with a probability of $(1-r)^2$.[13] Similarly, the fraction of polymer chains reacted with the cross-linker at both ends (probability of r^2) and dangling polymer chains (probability of $2r\times(1-r)$) present in the pre-reacted mixtures are found to be 0.01 and 0.18, respectively. The intermediates were characterized by FT-IR spectroscopy and size-exclusion chromatography (SEC) (Figures 1–4 in the Supporting Information), as well as by ^{1}H NMR spectroscopy as shown in Figure 1, from which the full conversion of all the thiols from the cross-linker can be confirmed.

The mechanical properties (storage moduli: G') of the fully cured two-step network were investigated by low shear linear viscoelastic rheology (tan delta) as shown in Figure 2 compared to the one-step network as a function of frequency. Bi*xx-yy* refers to the two-step systems with a ratio of *xx* hyperbranched high-molecular-weight PDMS to *yy* hyperbranched low-molecular-weight PDMS. In the second step, the hyperbranched intermediates were combined and cross-linked, resulting in fully cured networks after exposure to UV-light. The combination of both high and low molecular weight PDMS is necessary in order to ensure a sufficiently low viscosity of the system until the gelation point is reached. Limiting the hyperbranching to the high-molecular-weight PDMS and subsequent cross-linking was inefficient and resulted in long curing times as observed for direct cross-linking.

As can be seen from Figure 2, the procedure results in the targeted soft PDMS networks with storage moduli (G') as low as 20 kPa. In addition to this, the combination of high- and low-molecular-weight PDMS in the two-step networks can be seen to reflect in a gradual increase in G', as the amount of short chain PDMS is increased. This can be compared to a storage modulus of 135 kPa for a similar molecular weight PDMS network obtained from a classical platinum-catalyzed cross-linking.[10a] In the two-step networks, the short-chain hyperbranched domains act as apparent cross-linkers of the hyperbranched long-chain domains and the network remains soft until the point at which the stress becomes sufficiently large to initiate deformations of the short chain clusters which can be seen from the low G' exhibited by Bi90-10 and Bi85-15 with low short-chain content.[10] Since the molecular weight of the short chain PDMS (800 g mol^{-1}) used within this study is significantly lower than the entanglement molecular weight (M_e) of PDMS (ca. 12 000 g mol^{-1}),[14] the elastic modulus of the short-chain cluster within the two-step networks will be dominated by cross-links rather than entanglements. Therefore, at higher loadings of short-chain PDMS (more than 15%), the short-chain clusters act as reinforcing domains and restrict chain movements significantly thereby increasing the modulus of Bi80-20, Bi75-25, and Bi70-30, respectively.

The tan delta plots (Figure 2b) also give some insight into the molecular motion and damping behavior of the polymers.

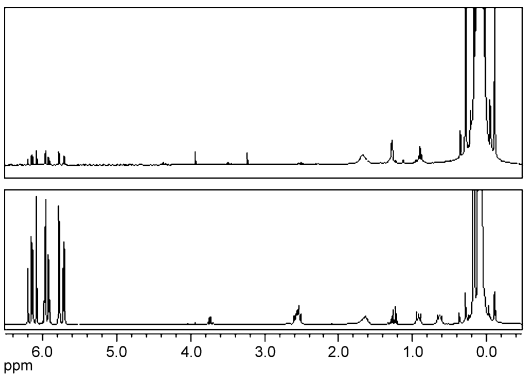

Figure 1. ^{1}H NMR spectra of the two hyperbranched structures (top: hyperbranched high-molecular-weight PDMS; bottom: hyperbranched low-molecular-weight PDMS), showing full conversion of the thiol cross-linker as well as the excess vinyl groups from the PDMS.

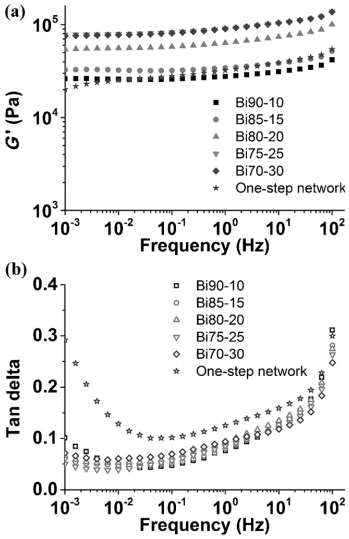

Figure 2. a) Storage moduli (G') and b) tan delta of the fully cured two-step networks compared to the one-step network as a function of frequency. See text for an explanation of the Bi*xx-yy* nomenclature. Measurements are performed at room temperature.

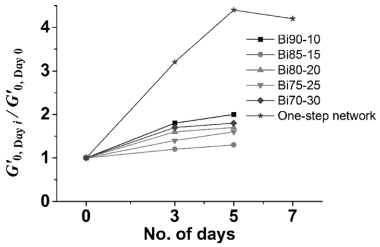

Figure 3. Development in storage moduli (G') for the respective networks relative to the initially observed storage modulus measured immediately after the curing reaction and after storage at RT in the dark for up to 5 or 7 days.

From the figure, it is seen that the one-step network shows higher tan delta values than the two-step networks at all frequencies. The sharp increase in tan delta of the one-step network at lower frequencies is due to long relaxation times exhibited by the long dangling chains. However, in the two-step networks no such relaxations were present at these frequencies. Moreover the low tan delta values for the two-step networks at frequencies lower than 10^{-1} Hz indicates that the prepared two-step networks have significantly less dangling chains and lower viscous losses compared to the one-step network.

The development of storage moduli throughout the curing is related to the kinetics of the network formation. Storage moduli of one and two-step networks were measured for several days after UV exposure until the difference between two successive measurements became 10% or less. The obtained storage moduli were normalized to illustrate the differences in curing kinetics as shown in Figure 3 (the full data set can be seen in the supporting information Figures 5 and 6 in the Supporting Information).

The effect of the earlier mentioned curing time can clearly be seen from Figure 3, in which the one-step network requires five days to reach a stable storage modulus, indicating slow and inefficient curing compared to the two-step networks. All the two-step networks show very limited developments in storage moduli as a function of time due to the step-wise mixing procedure. This would in all practical applications be an insignificant change in the material.

In summary, the two-step procedure clearly enables a fast and efficient UV curing process of α,ω-vinyl-PDMS by thiol–ene chemistry without the use of the expensive platinum catalyst. Rheological studies reveal that the prepared UV-cured PDMS networks are softer than the classical platinum-catalyzed addition cured network. In addition to this, the two-step networks show very low viscous losses. Due to the formation of pre-reacted structures before the final cross-linking, two-step networks show stable mechanical properties compared to the one-step network even several days after the UV exposure due to faster curing kinetics.

Acknowledgements

The authors would like to acknowledge the financial support from Danish Agency for Science, Technology and Innovation and the Danish National Advanced Technology Foundation.

Keywords: cross-linking · curing · photochemistry · poly(dimethylsiloxane) · silicon

[1] C. Decker, *Macromol. Rapid Commun.* **2002**, *23*, 1067 – 1093.
[2] a) Z. Yang, D. A. Wicks, J. Yuan, H. Pu, Y. Liu, *Polymer* **2010**, *51*, 1572 – 1577; b) K. Studer, C. Decker, E. Beck, R. Schwalm, *Prog. Org. Coat.* **2003**, *48*, 92 – 100.
[3] K. Studer, C. Decker, E. Beck, R. Schwalm, *Prog. Org. Coat.* **2003**, *48*, 101 – 111.
[4] M. J. Kade, D. J. Burke, C. J. Hawker, *J. Polym. Sci. Part A* **2010**, *48*, 743 – 750.
[5] a) A. B. Lowe, *Polym. Chem.* **2010**, *1*, 17 – 36; b) C. E. Hoyle, C. N. Bowman, *Angew. Chem.* **2010**, *122*, 1584 – 1617; *Angew. Chem. Int. Ed.* **2010**, *49*, 1540 – 1573; c) K. Gross, W. Schultz, US Patent 6605692, **2003**.
[6] a) T. J. Drahnak, US Patent 4510094, **1985**; b) F. Lewis, G. Salvi, *Inorg. Chem.* **1995**, *34*, 3182 – 3189; c) J. Oxman, L. Boardman US Patent 6376569, **2002**.
[7] a) F. Masson, C. Decker, S. Andre, X. Andrieu, *Prog. Org. Coat.* **2004**, *49*, 1 – 12; b) H. K. Kim, H. T. Ju, J. W. Hong, *Eur. Polym. J.* **2003**, *39*, 2235 – 2241; c) U. Müller, H.-J. Timpe, J. Neuenfeld, *Eur. Polym. J.* **1991**, *27*, 621 – 625.
[8] A. Chemtob, H. De Paz-Simon, C. Croutxé-Barghorn, S. Rigolet, *J. Appl. Polym. Sci.* **2014**, *131*, 39875.
[9] a) G.-B. Zhang, X.-D. Fan, J. Kong, Y.-Y. Liu, *Polym. Bull.* **2008**, *60*, 863 – 874; b) U. Müller, A. Kunze, C. Herzig, J. Weis, *J. Macromol. Sci. Part A* **1996**, *33*, 439 – 457; c) Y. Zuo, H. Lu, L. Xue, X. Wang, L. Ning, S. Feng, *J. Mater. Chem. C* **2014**, *2*, 2724.
[10] S. Braley, *J. Macromol. Sci. Chem.* **1970**, *4*, 529 – 544.

[11] S. A. Shama, *J. Photopolym. Sci. Technol.* **1991**, *4*, 9 – 22.
[12] a) A. G. Bejenariu, L. Yu, A. L. Skov, *Soft Matter* **2012**, *8*, 3917 – 3923; b) F. B. Madsen, A. E. Daugaard, C. Fleury, S. Hvilsted, A. L. Skov, *RSC Adv.* **2014**, *4*, 6939 – 6945.
[13] S. M. G. Frankær, M. K. Jensen, A. G. Bejenariu, A. L. Skov, *Rheol. Acta* **2012**, *51*, 559 – 567.
[14] L. Fetters, D. Lohse, D. Richter, *Macromolecules* **1994**, *27*, 4639 – 4647.

Received: March 31, 2014
Published online on July 7, 2014

The Danish Polymer Centre
Department of Chemical and Biochemical Engineering
Technical University of Denmark
Søltofts Plads, Building 227
DK-2800 Kgs. Lyngby
Denmark

Phone: +45 4525 6801
Web: www.dpc.kt.dtu.dk

ISBN : 978-87-93054-47-9